The Hemodynamic Response and More: Advances and Prospects for fMRI

Peter A. Bandettini, Ph.D

Unit on Functional Imaging Methods
&
3T Neuroimaging Core Facility

Laboratory of Brain and Cognition
National Institute of Mental Health

Alternating Left and Right Finger Tapping

~ 1992

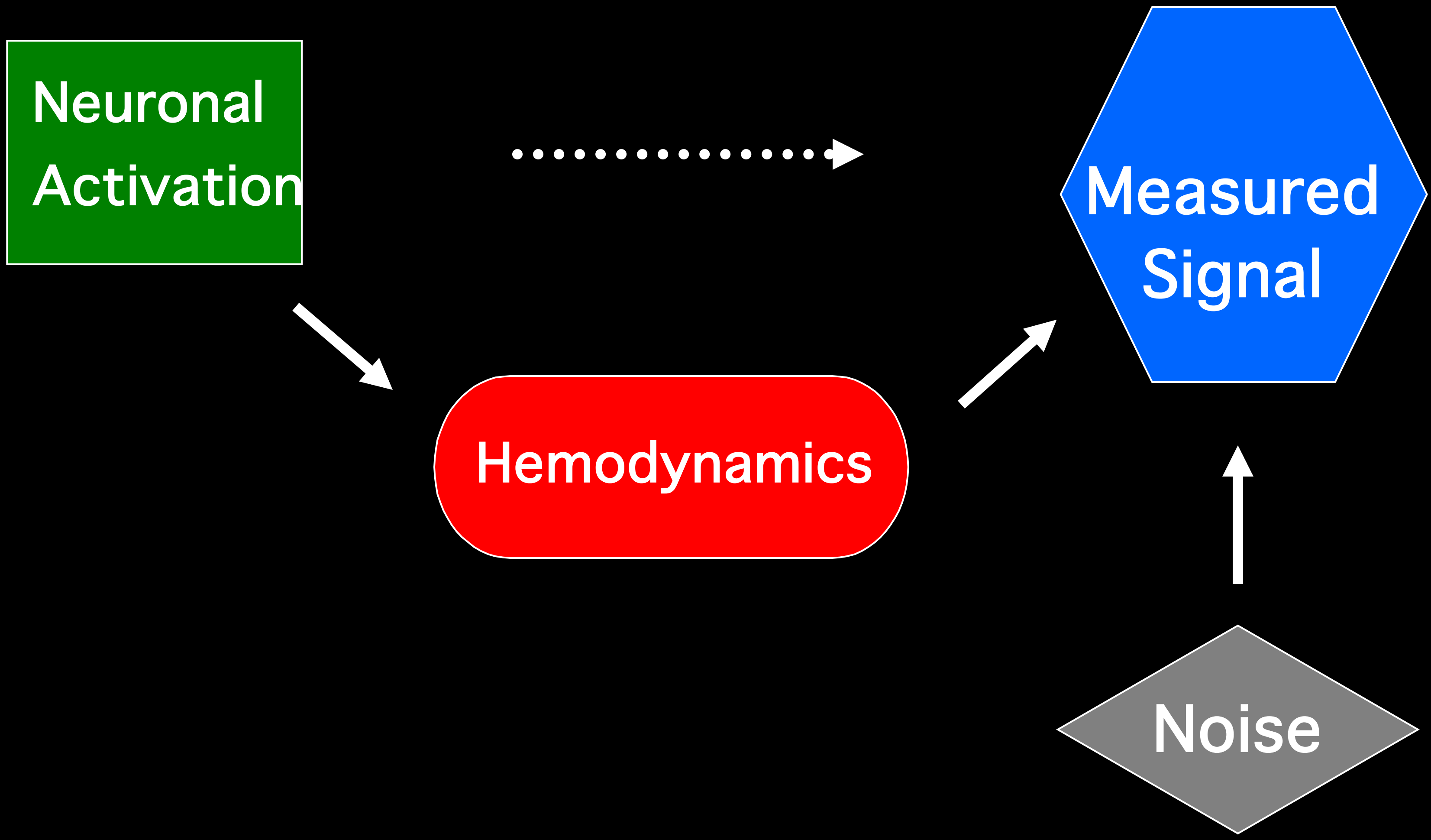
Neuronal Activation
Hemodynamics
Measured Signal
Noise

A Primary Challenge:

...to make progressively more precise inferences using fMRI without making too many assumptions about non-neuronal physiologic factors.

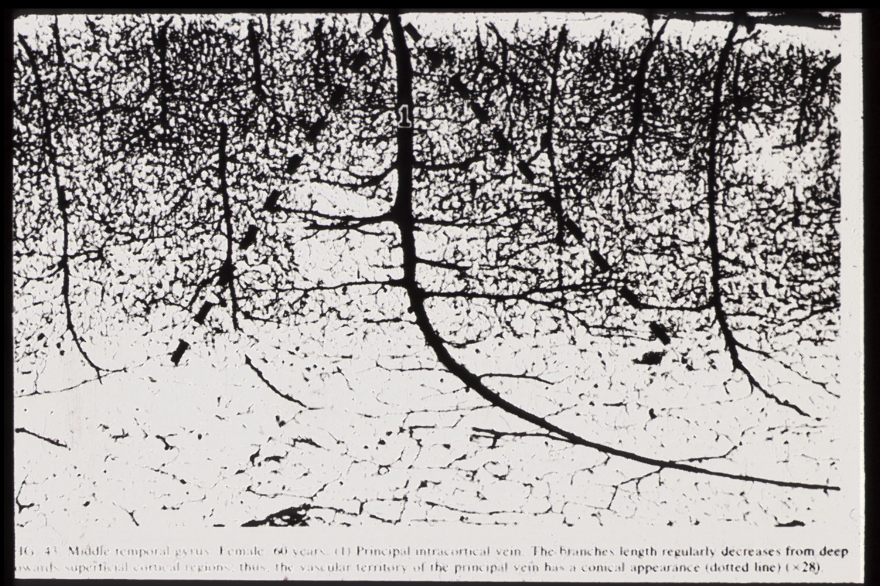

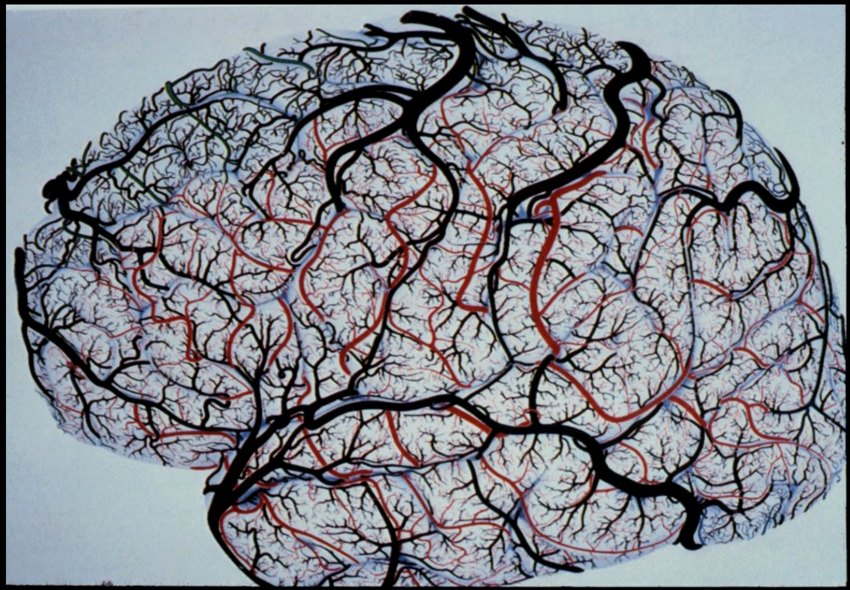

Rasmus Birn
Patrick Bellgowan
Hauke Heekeren
Ziad Saad
Marta Maieron
Sergio Casciaro
James Patterson

Natalia Petridou

Wen-Ming Luh
Sean Marrett
Jerzy Bodurka
Frank Ye

Dan Kelley
Elisa Kapler
Hannah Chang

Increased:

Spatial Resolution
Temporal Resolution
Interpretability
Sensitivity
Robustness

Karen Bove-Bettis
Adam Thomas
Kay Kuhns
Julie Frost

Linearity

Latency

Fluctuations and Sensitivity

“Current” Imaging

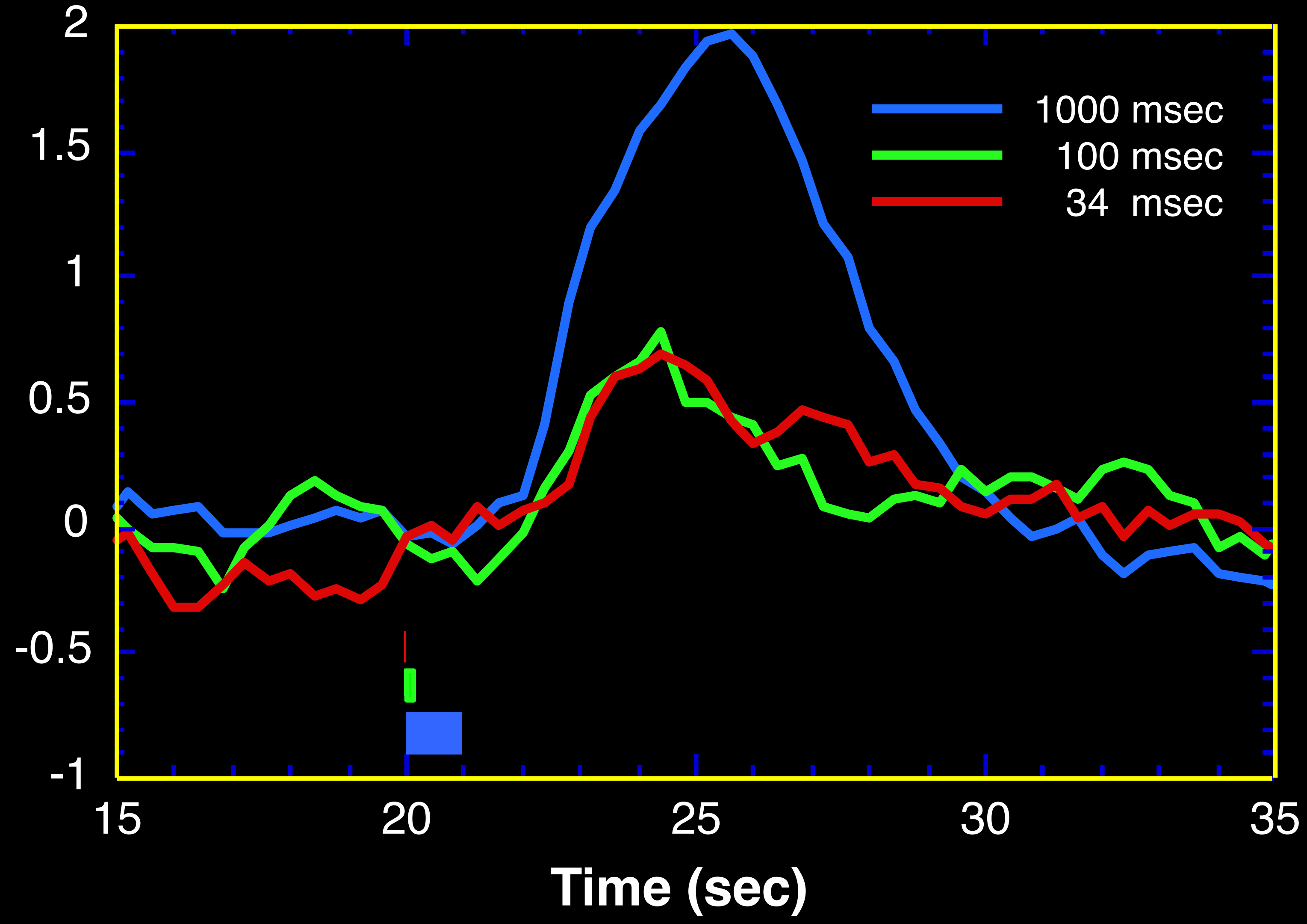

2
1.5
1
0.5
0
-0.5
-1
15
20
25
30
35
Time (sec)
1000 msec
100 msec
34 msec

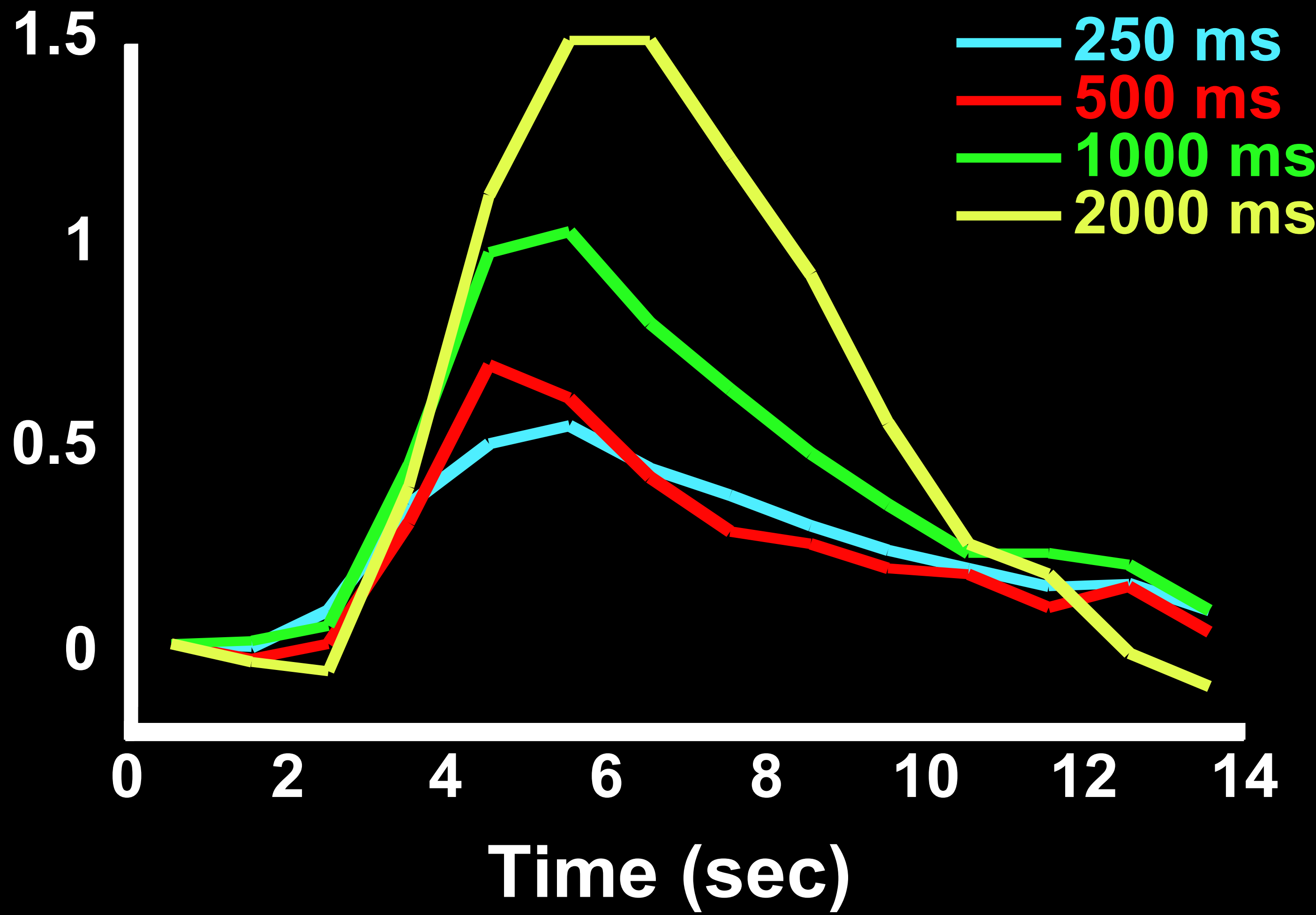

1.5
1
0.5
0
0
2
4
6
8
10
12
14
Time (sec)
250 ms
500 ms
1000 ms
2000 ms

Source of the Nonlinearity

Neuronal

Hemodynamic

Miller et al. 1998 – Flow is linear, BOLD is nonlinear

Friston et al. 2000 – hemodynamics can explain nonlinearity

If nonlinearity is hemodynamic in origin, a measure of this nonlinearity may reflect a spatial variation of the vasculature

Methods

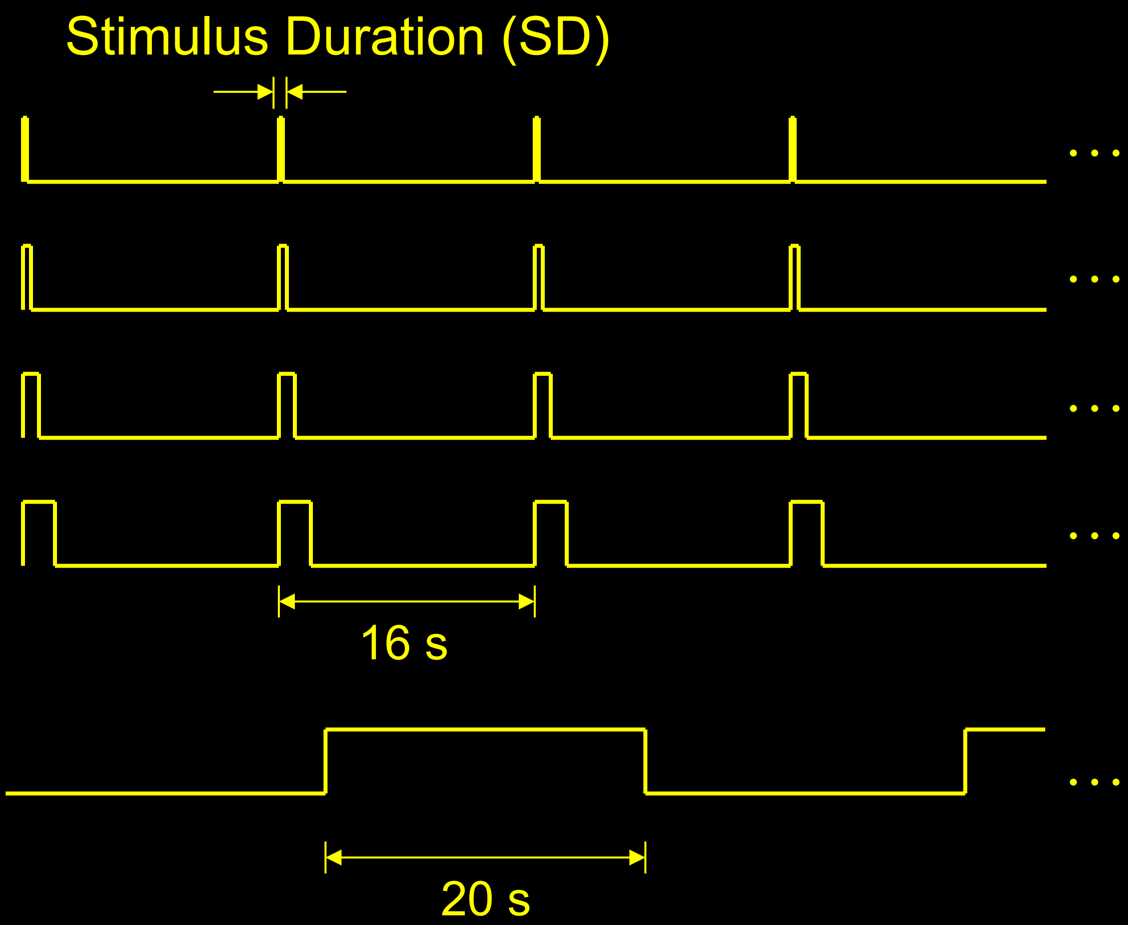

Visual	Motor
SD = 250 ms	SD = 500 ms
SD = 500 ms	SD = 1000 ms
SD = 1000 ms	SD = 2000 ms
SD = 2000 ms	SD = 4000 ms

Blocked Trial

Observed Responses

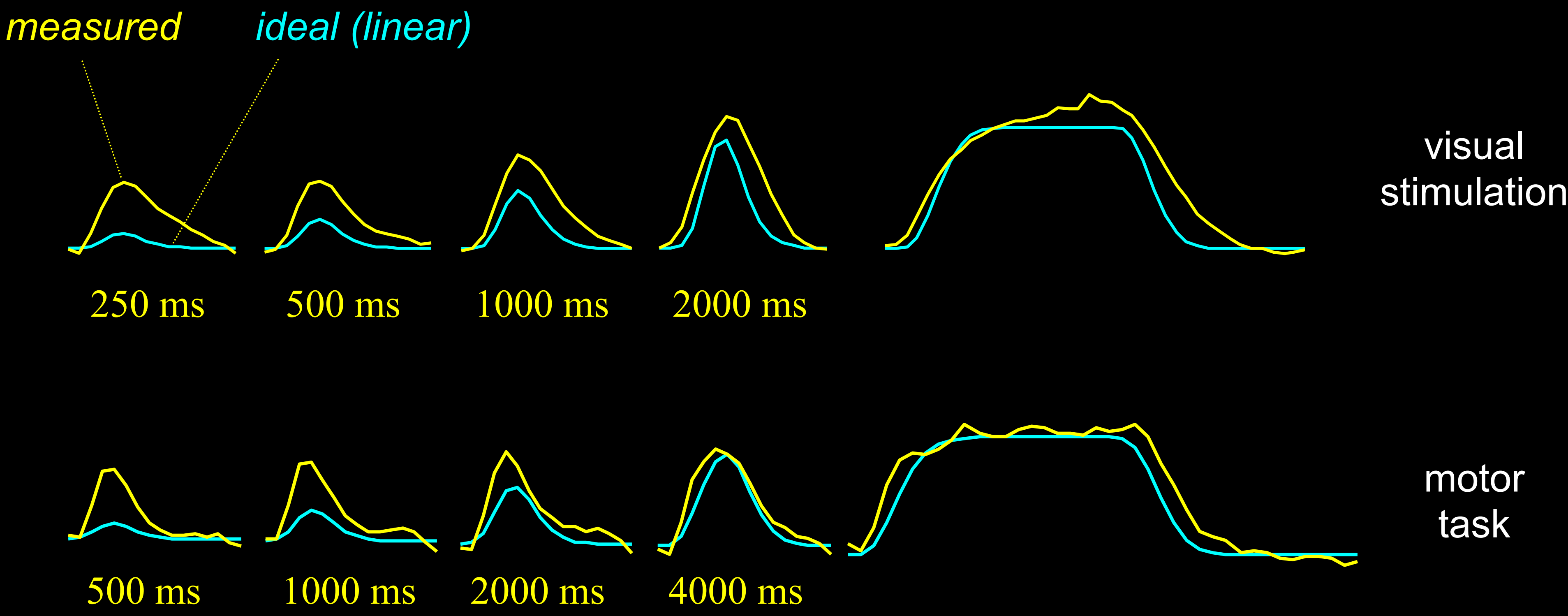

BOLD response is nonlinear

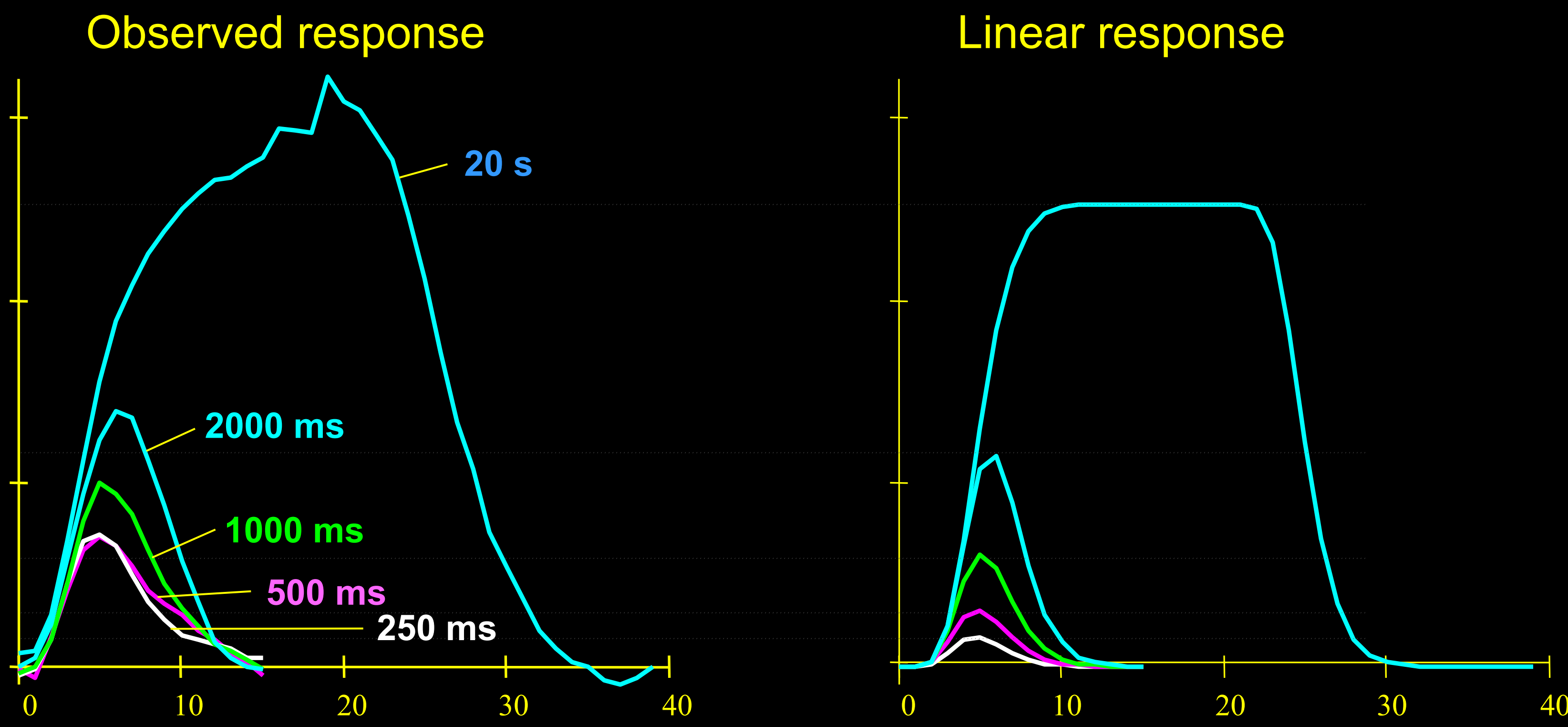

Short duration stimuli produce larger responses than expected

Compute nonlinearity *(for each voxel)*

- Area under response / Stimulus Duration

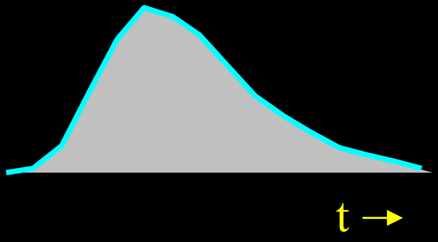

Output Area / Input Area

Nonlinearity

Visual

Motor

Magnitude

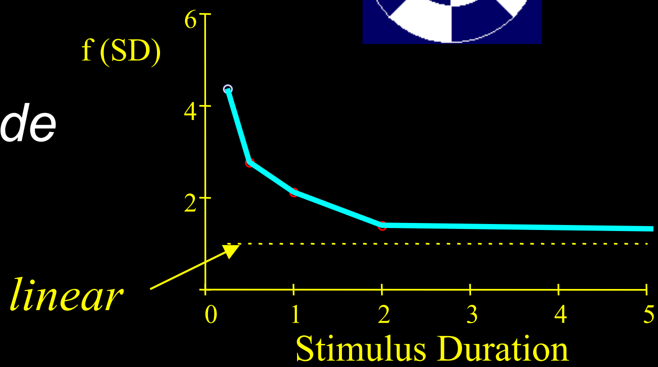

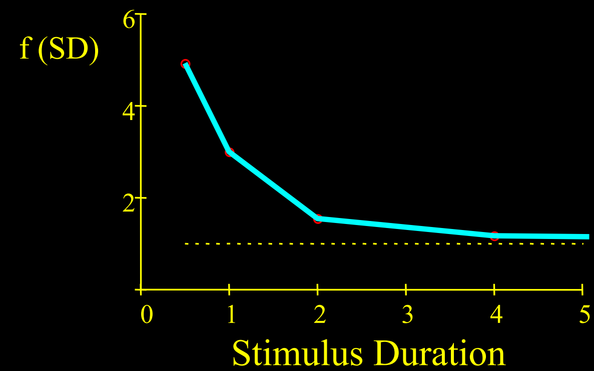

Area

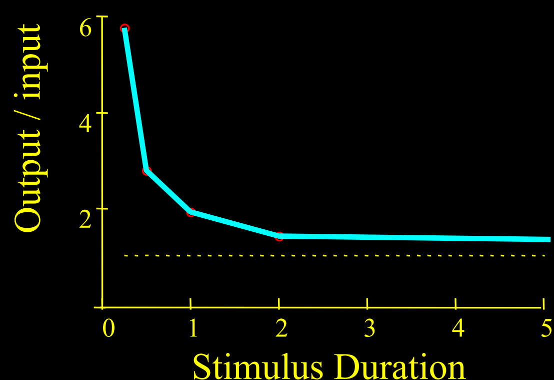

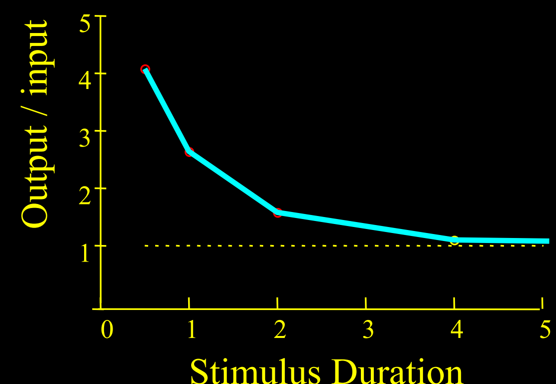

Results – visual task

response

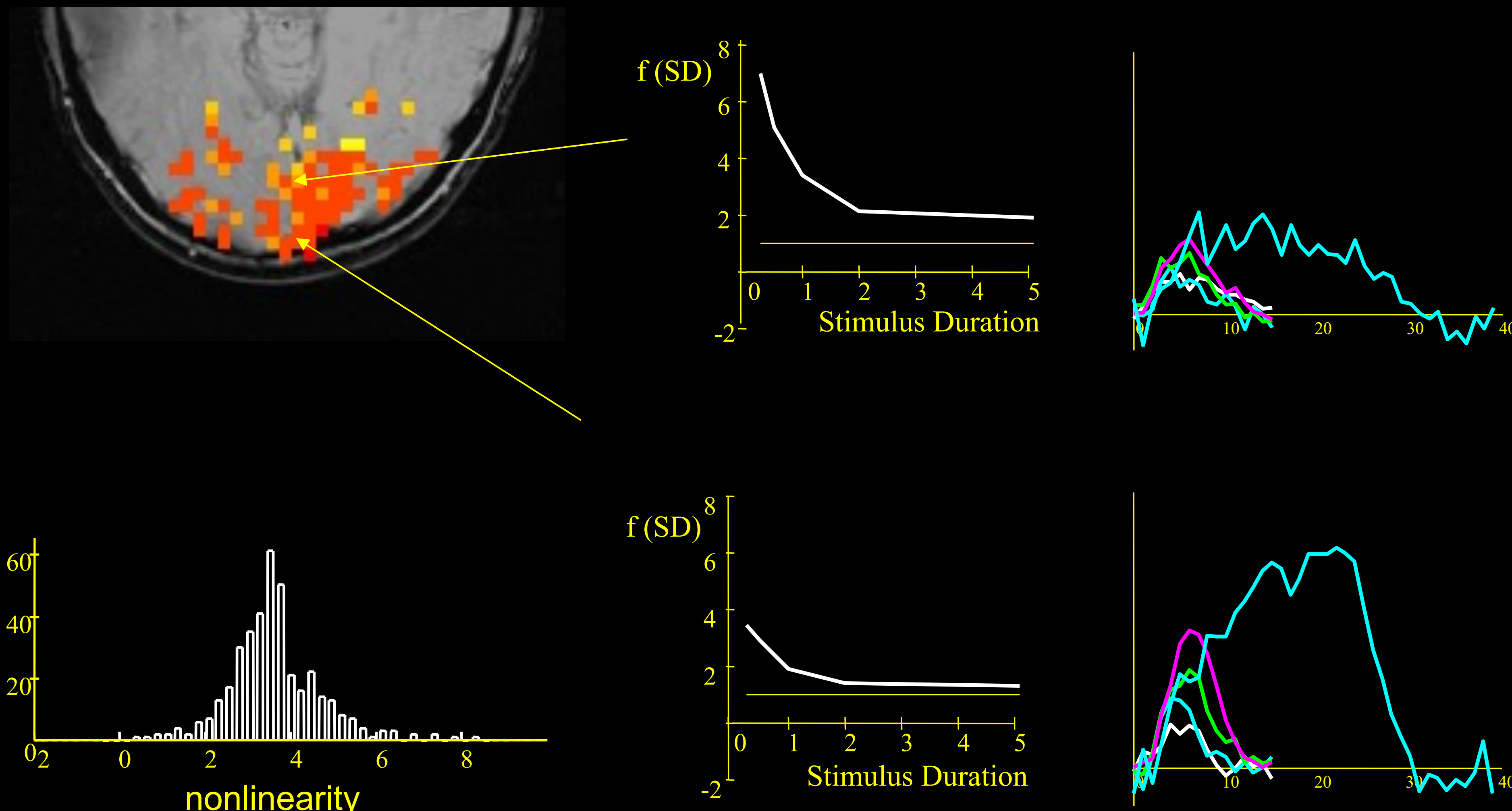

Results – visual task

Nonlinearity

Magnitude

Latency

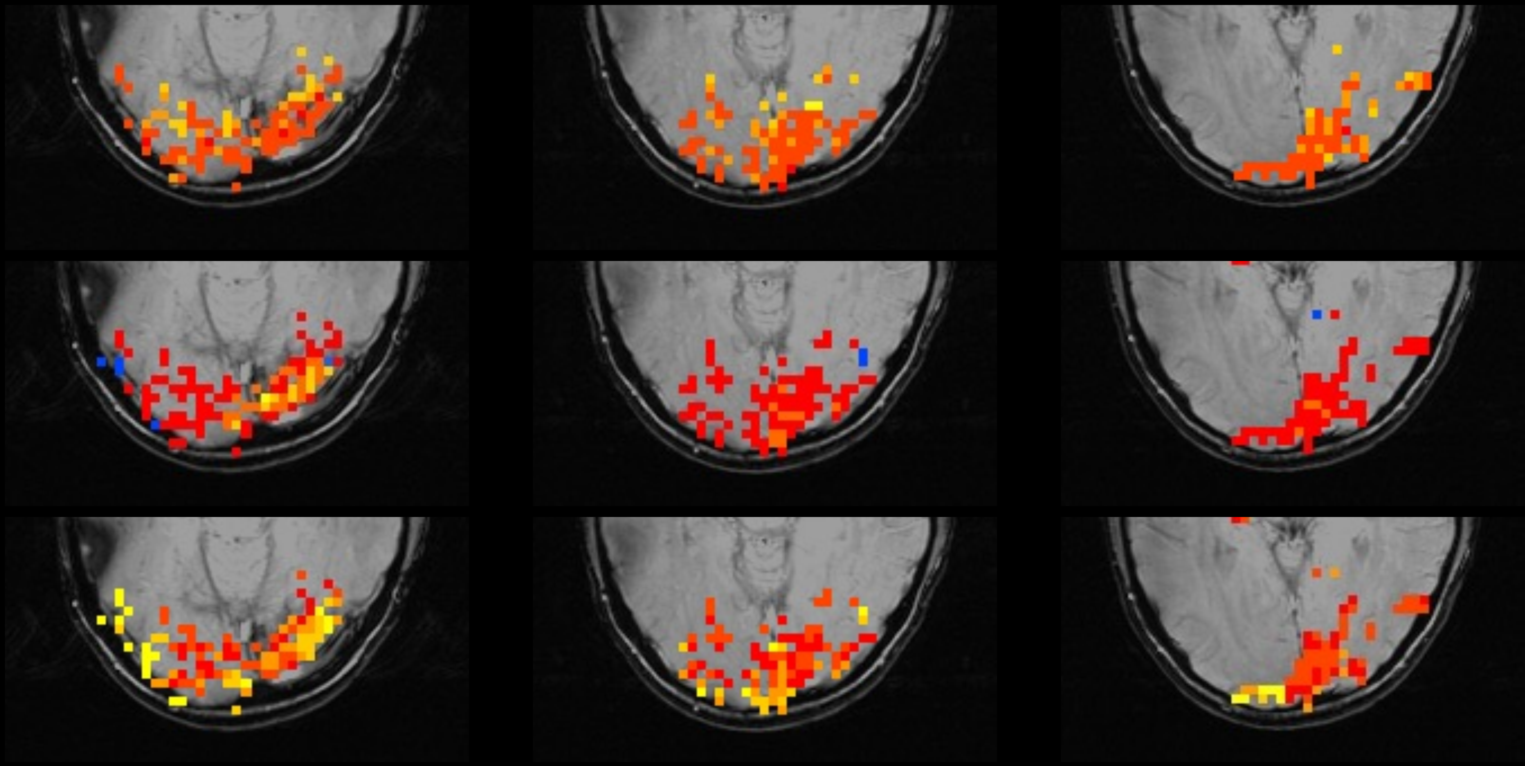

Results – motor task

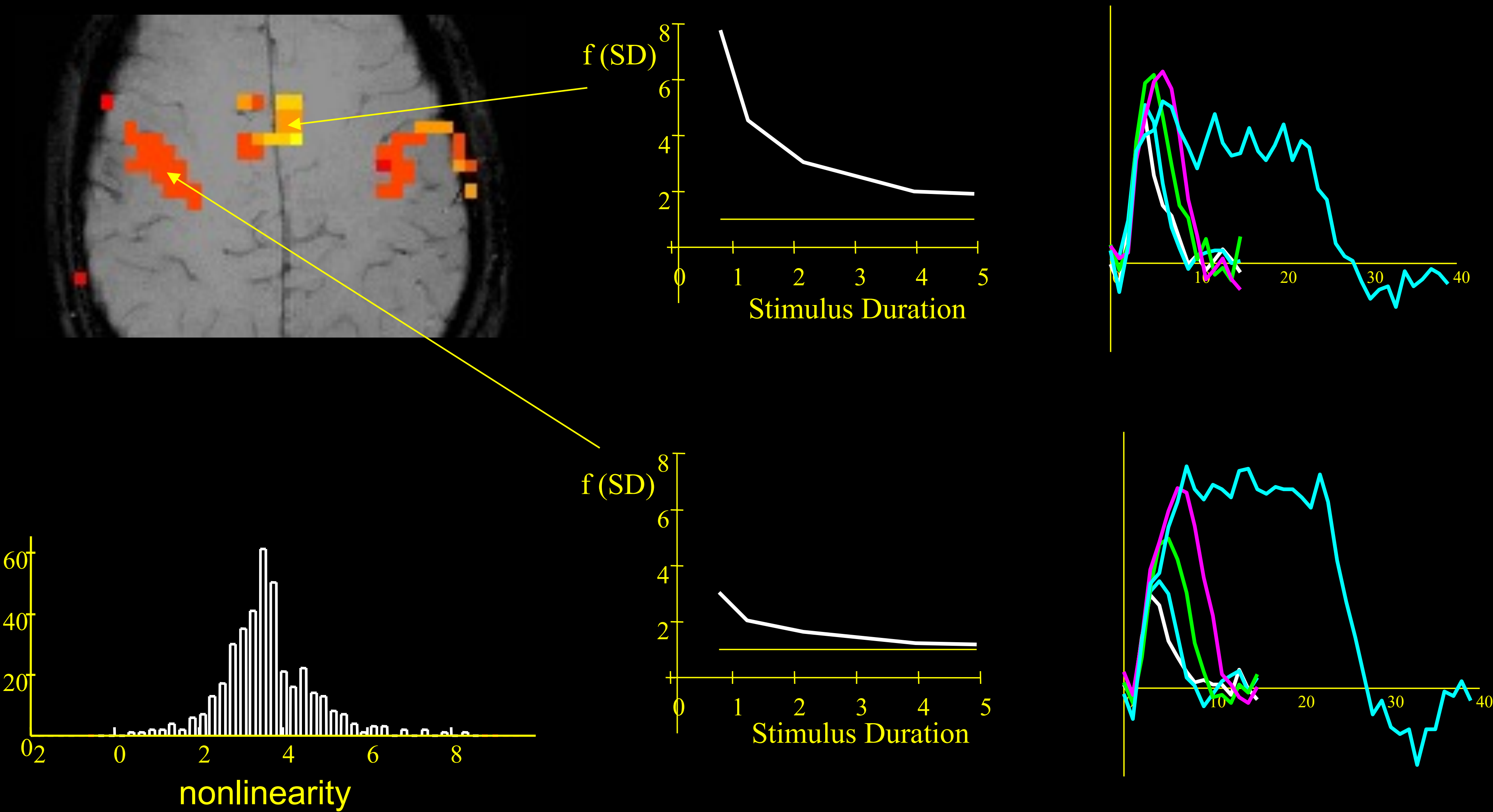

Results – motor task

Nonlinearity

Magnitude

Latency

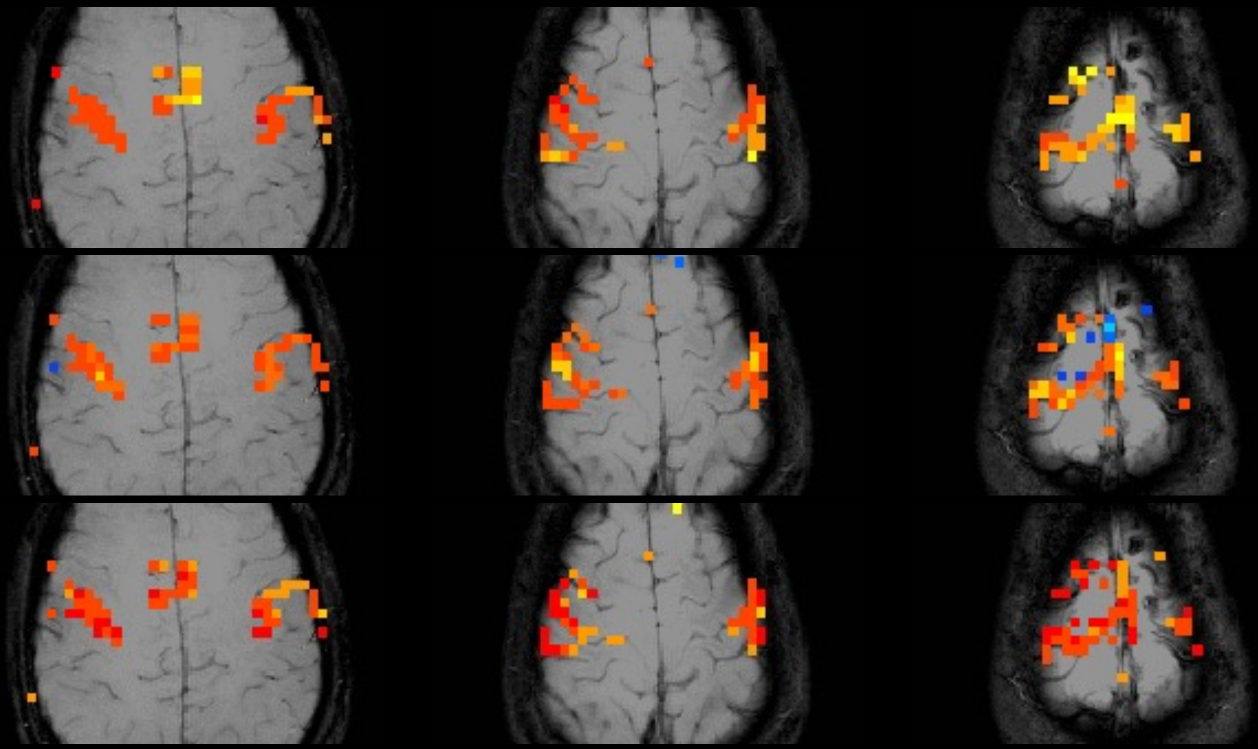

Reproducibility

Visual task

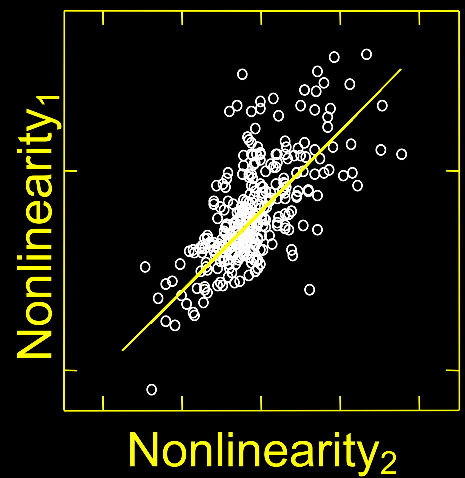

Motor task

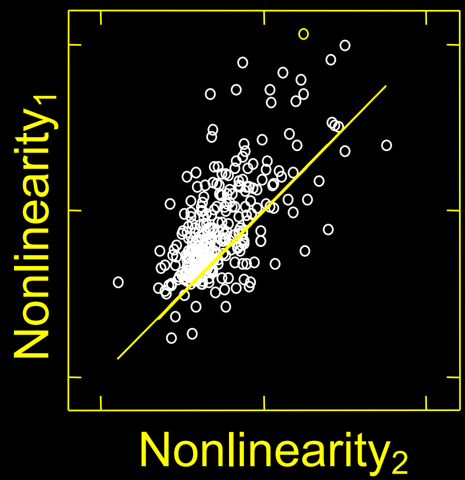

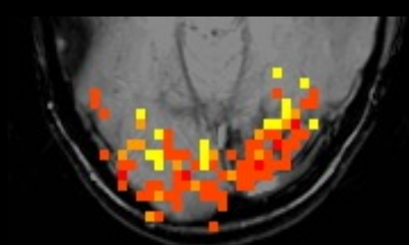

Experiment 1

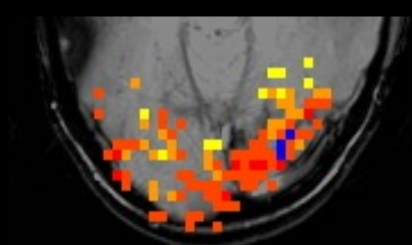

Experiment 2

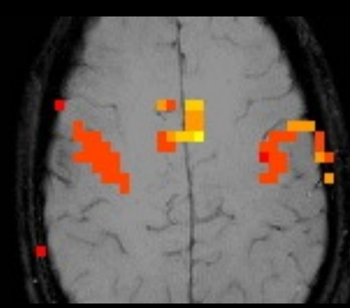

Experiment 1

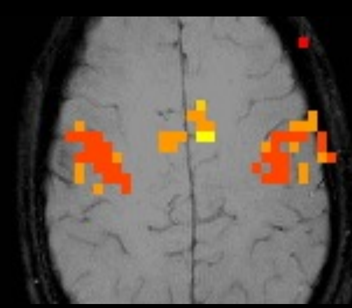

Experiment 2

Different stimulus "ON" periods

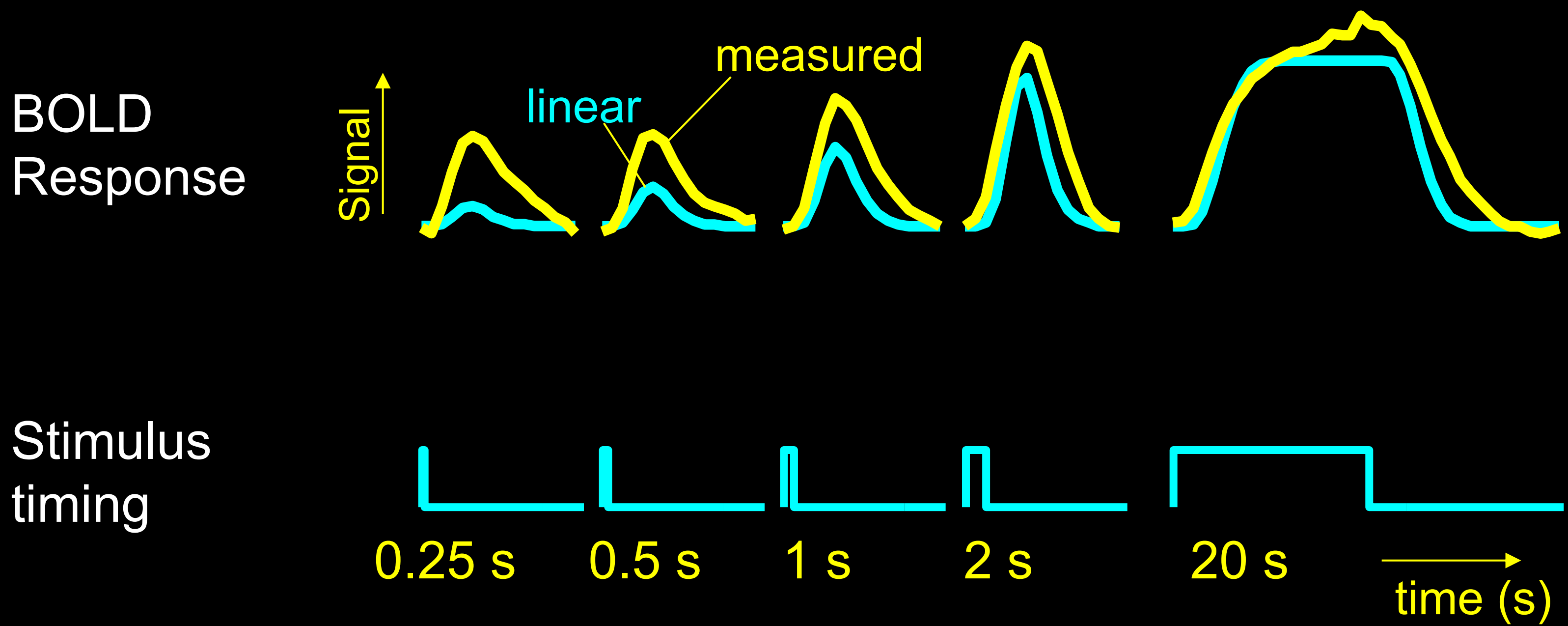

Brief stimuli produce larger responses than expected

Different stimulus "ON" periods

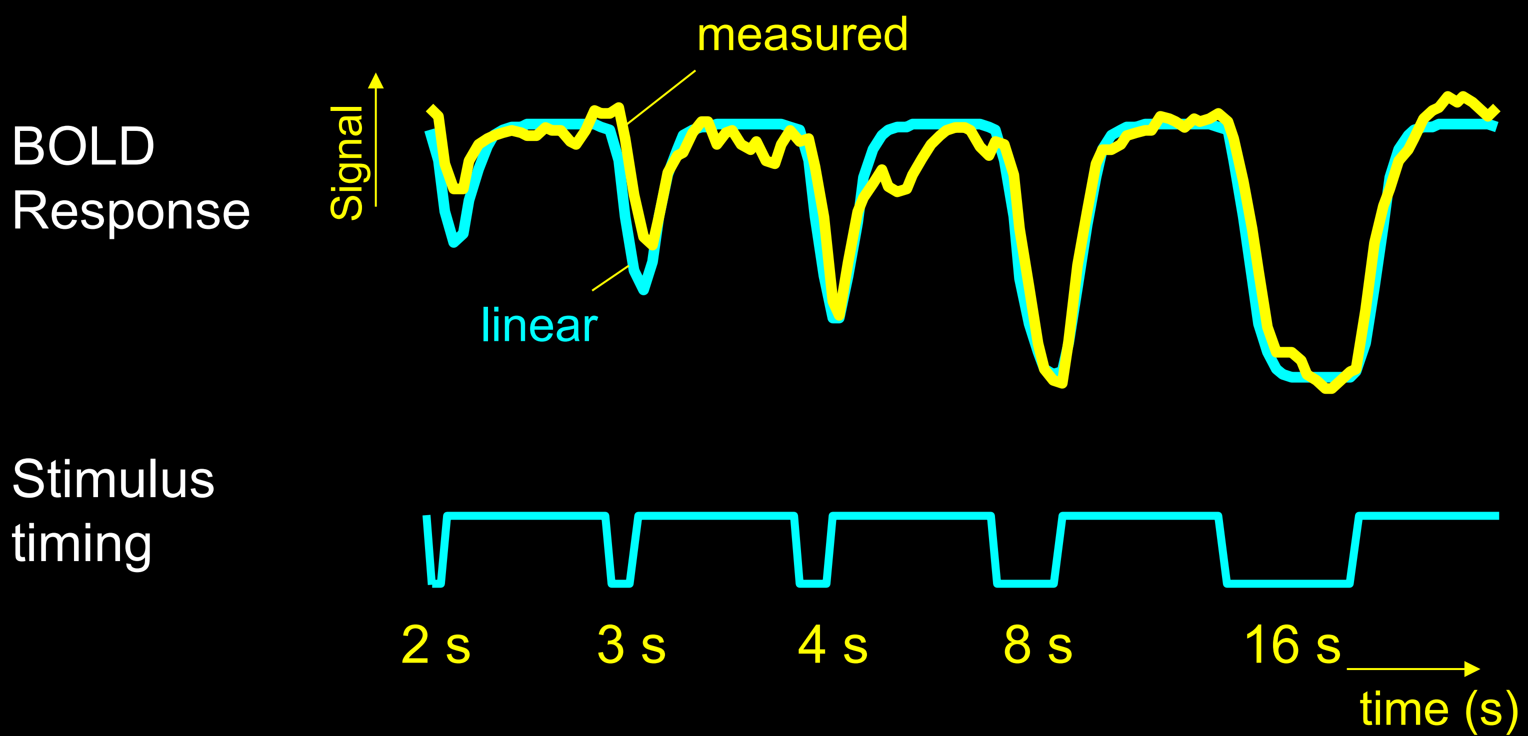

Brief stimulus OFF periods produce smaller decreases than expecte

Sources of this Nonlinearity

- Neuronal

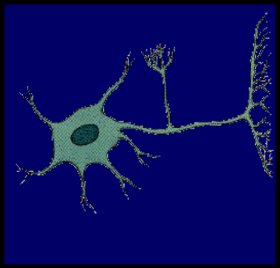

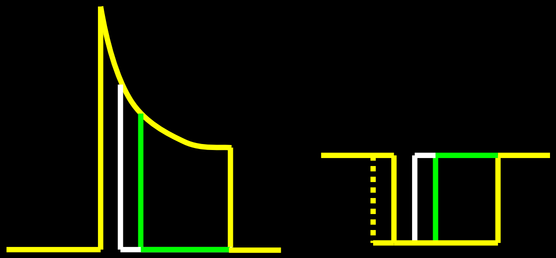

- Hemodynamic
  - Oxygen extraction
  - Blood volume dynamics

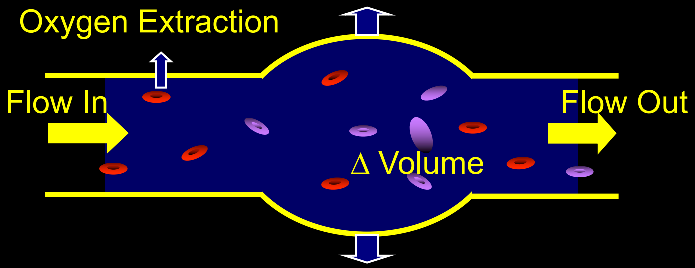

Balloon Model

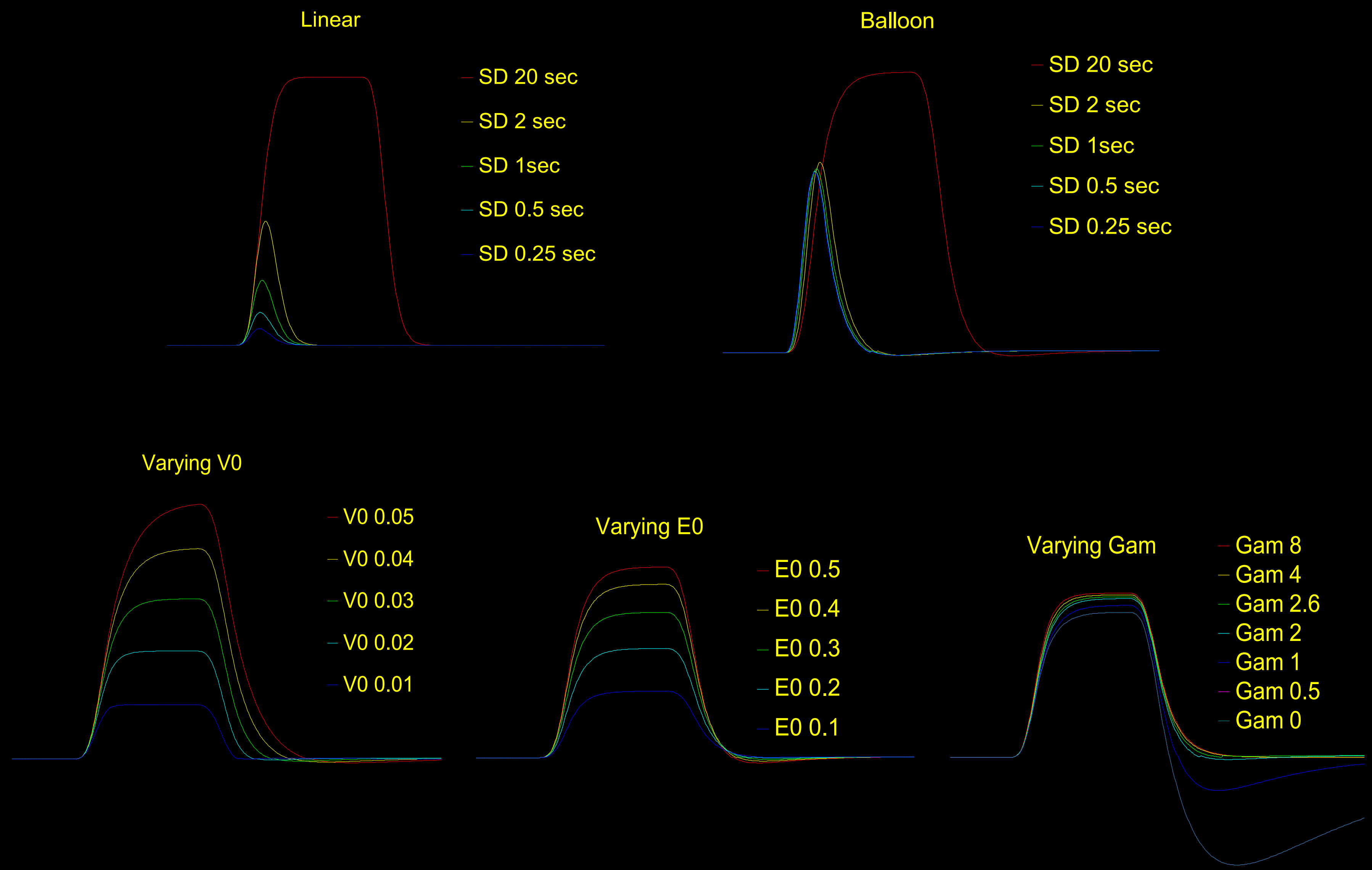

Overview

Balloon Input

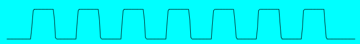

ShiftedFlowIn(t)

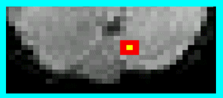

Functional Dataset

Balloon Model Equations

$$\frac{\Delta S}{S} = V_0\left[(k1+k2)(1-q(t)) - (k2+k3)(1-v(t)\right]$$

$$\mathrm{Exfrac}(t) = 1-(1-E_0)^{\frac{1}{\mathrm{ShiftedFlowIn}(t)}}$$

$$\mathrm{CMRO_2}(t) = \mathrm{ShiftedFlowIn}(t) * \frac{\mathrm{Exfrac}(t)}{E_0}$$

$$\mathrm{FlowOut}(t) = v(t)^{\mathrm{Gam}}; \quad \frac{df}{dv} = \mathrm{Gam}(v(t))^{(\mathrm{Gam}-1)}$$

$$\tau_0 = \frac{V_0}{\mathrm{FlowOut}(0)}$$

$$q(t) = \frac{Q(t)}{Q_0}; \quad \frac{dq}{dt} = \frac{1}{\tau_0}\left[\mathrm{ShiftedFlowIn}(t)\frac{\mathrm{Exfrac}(t)}{E_0} - \mathrm{FlowOut}(t)\frac{q(t)}{v(t)}\right]$$

$$v(t) = \frac{V(t)}{V_0}; \quad \frac{dv}{dt} = \frac{1}{\tau_0}\left[\frac{\mathrm{ShiftedFlowIn}(t) - \mathrm{FlowOut}(t)}{1+0.5\left(\frac{dt}{\tau_0}\right)\left(\frac{df}{dv}\right)+\left(\frac{\mathrm{viscos}}{\sqrt{v(t)}}\right)}\right]$$

Optimized Balloon Output

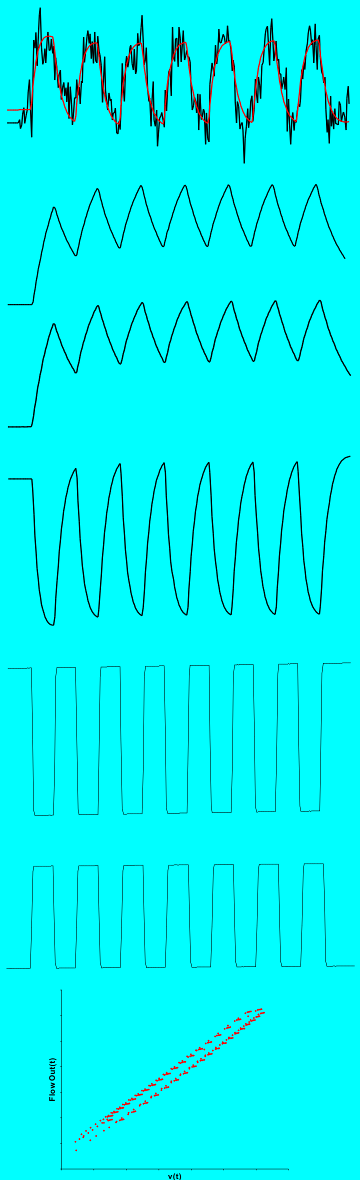

Balloon Fit to BOLD Signal

FlowOut(t)

v(t)

q(t)

Exfrac(t)

$CMRO_2$

FlowOut(t) versus v(t)

Voxelwise Analysis

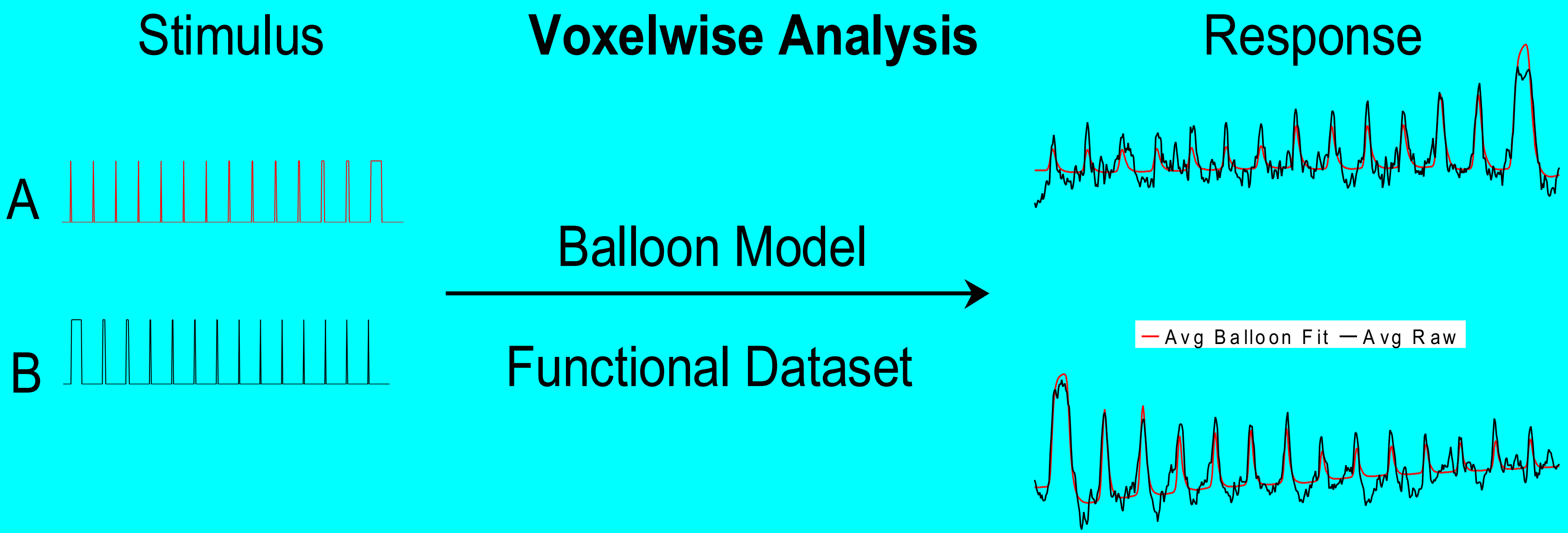

BOLD Correlation with Neuronal Activity

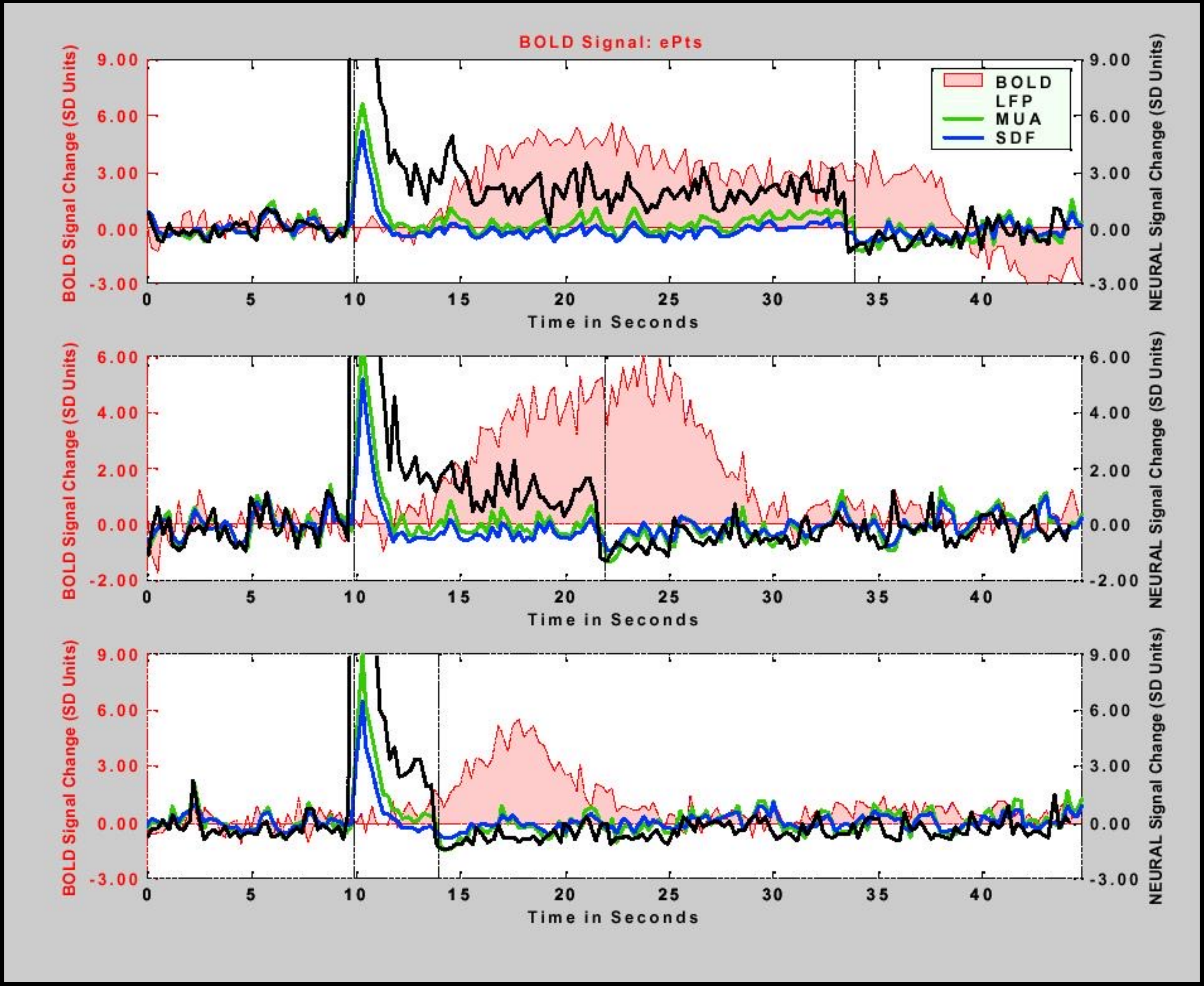

Logothetis et al. Nature, 412, 150-157

BOLD Correlation with Neuronal Activity

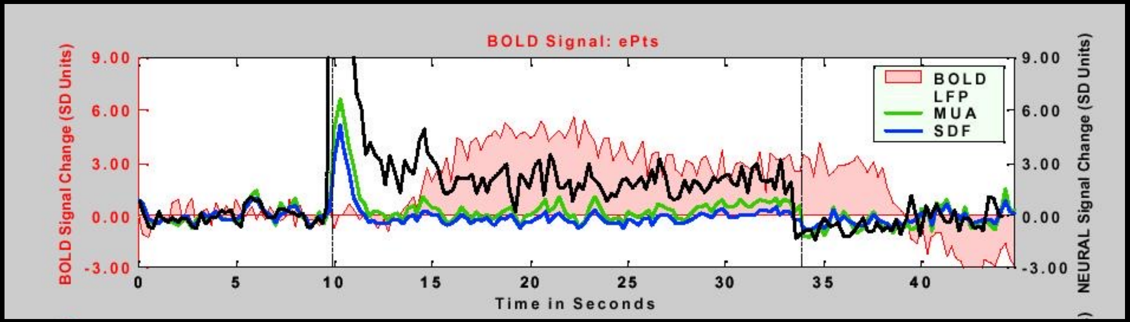

Logothetis et al. Nature, 412, 150-157

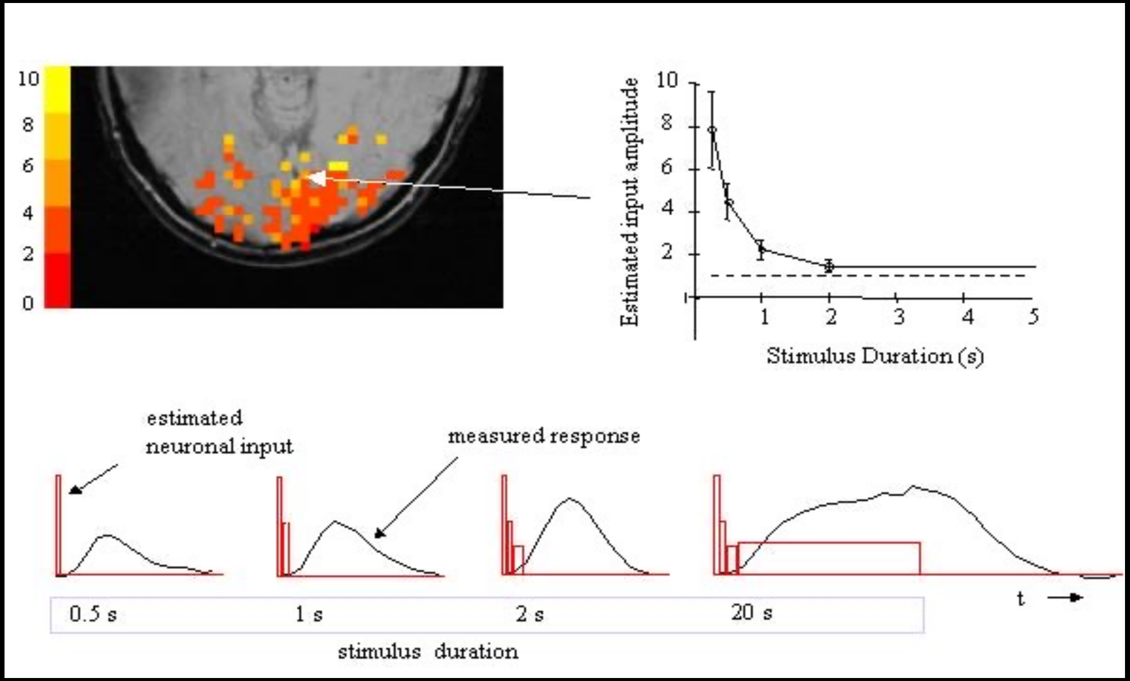

Bandettini and Ungerleider, Nature Neuroscience, 4, 864-866

Stationary grating

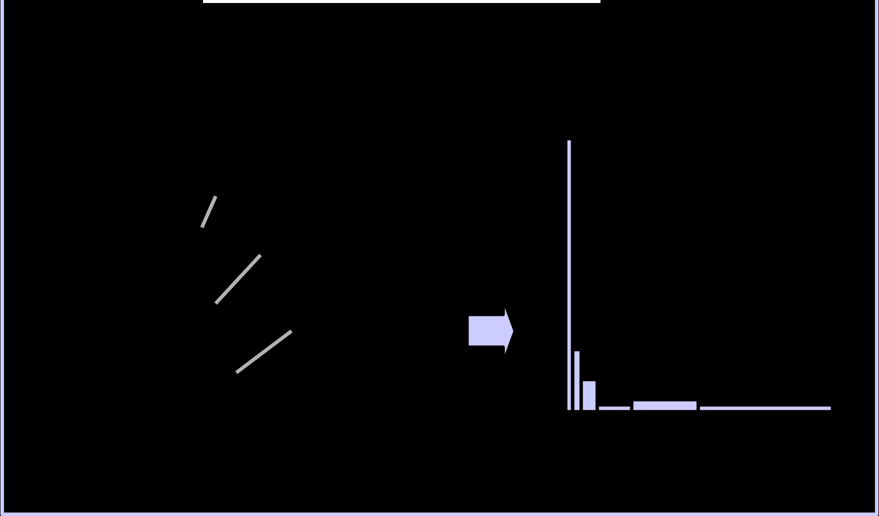

Contrast-reversing checkerboard

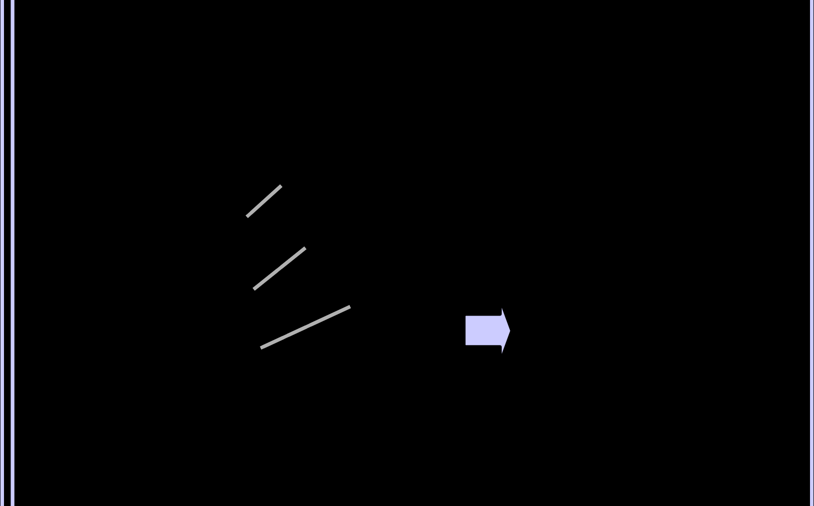

Motor Cortex

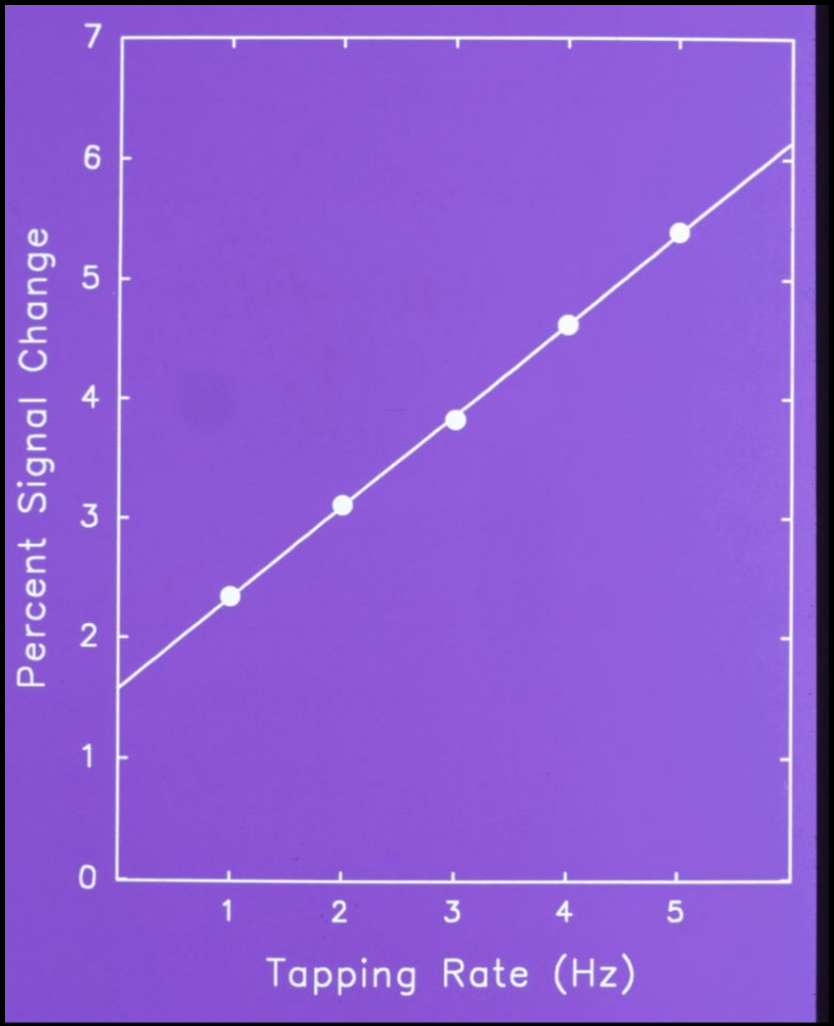

Auditory Cortex

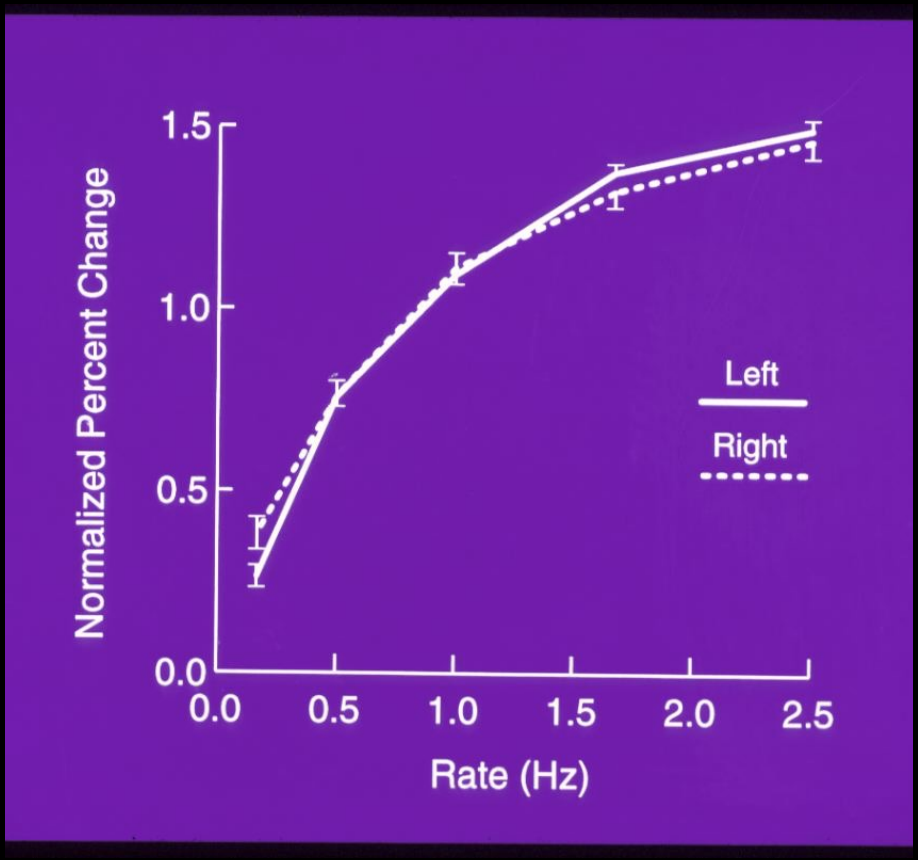

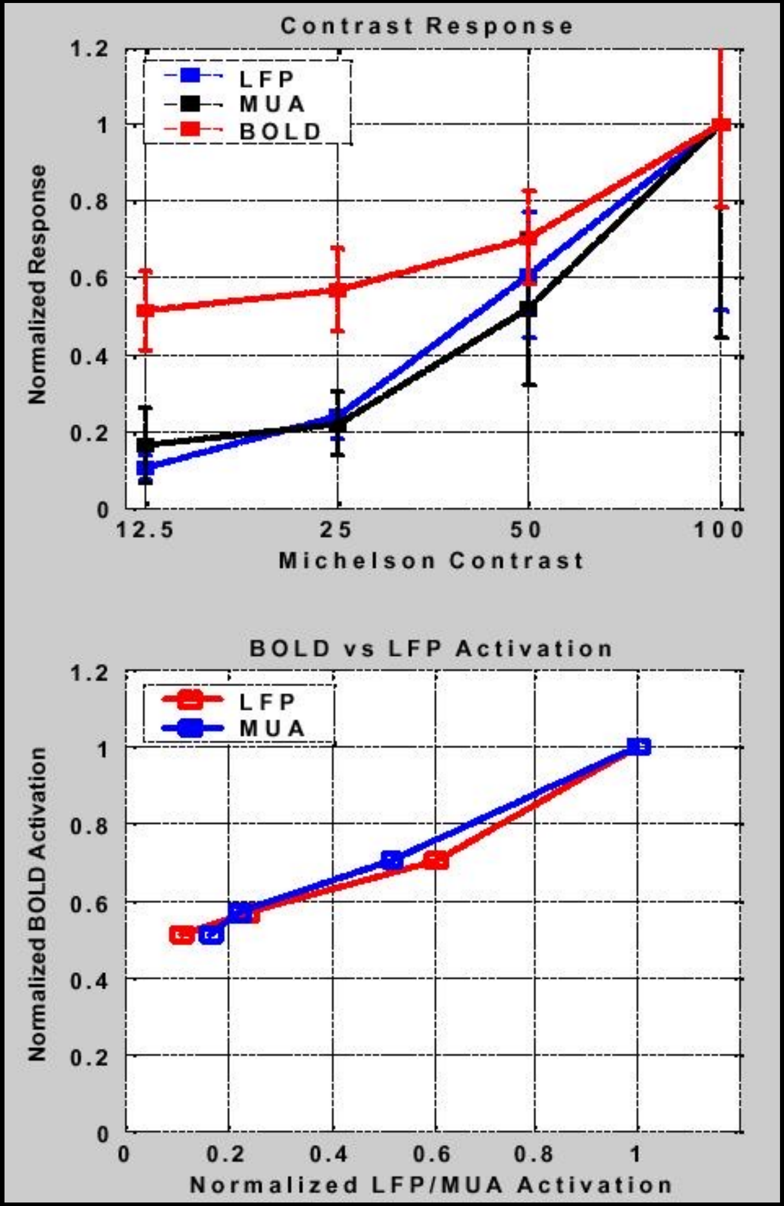

Logothetis et al. Nature, 412, 150-157

Functional Contrast

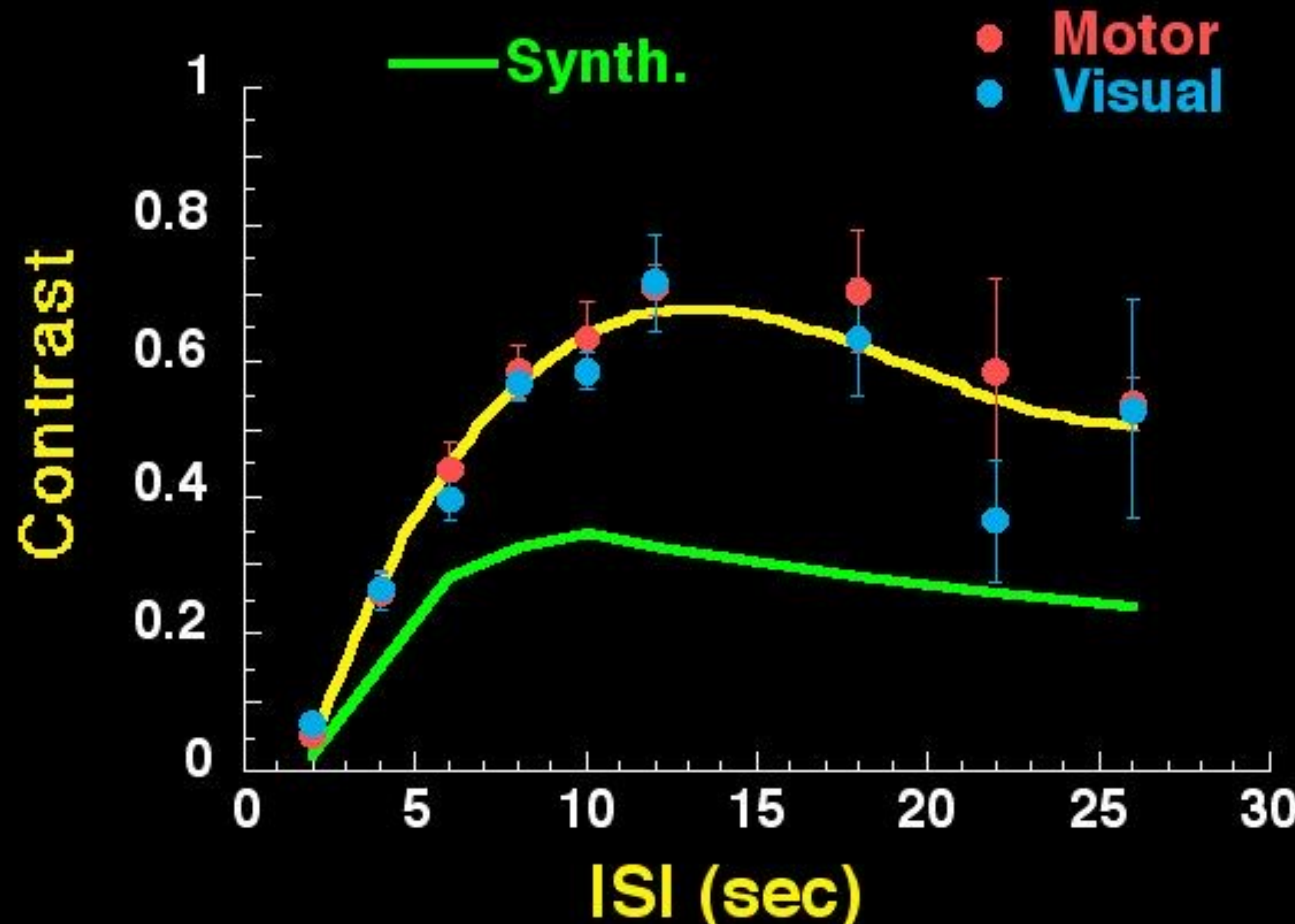

(Block design = 1)

Contrast to Noise Images

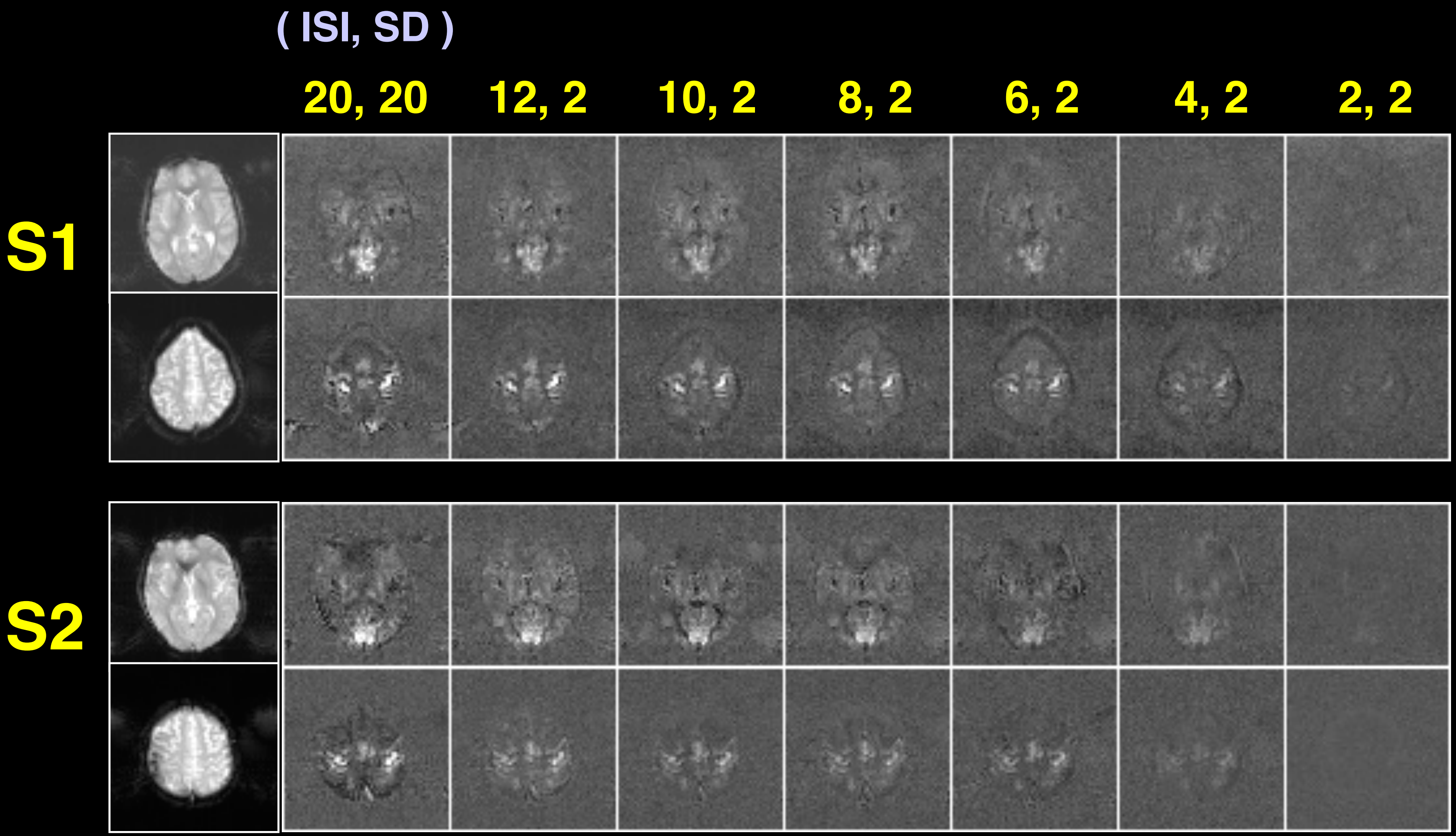

Detectability – constant ISI

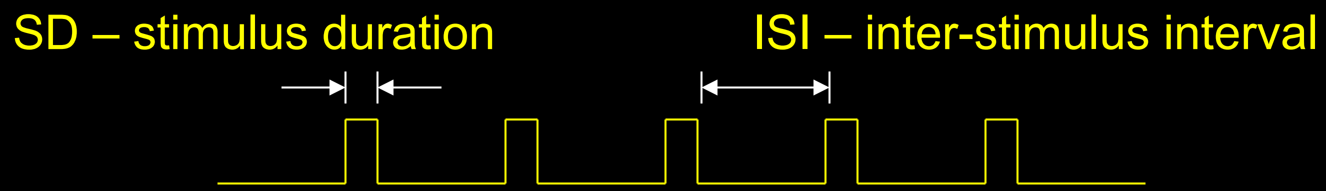

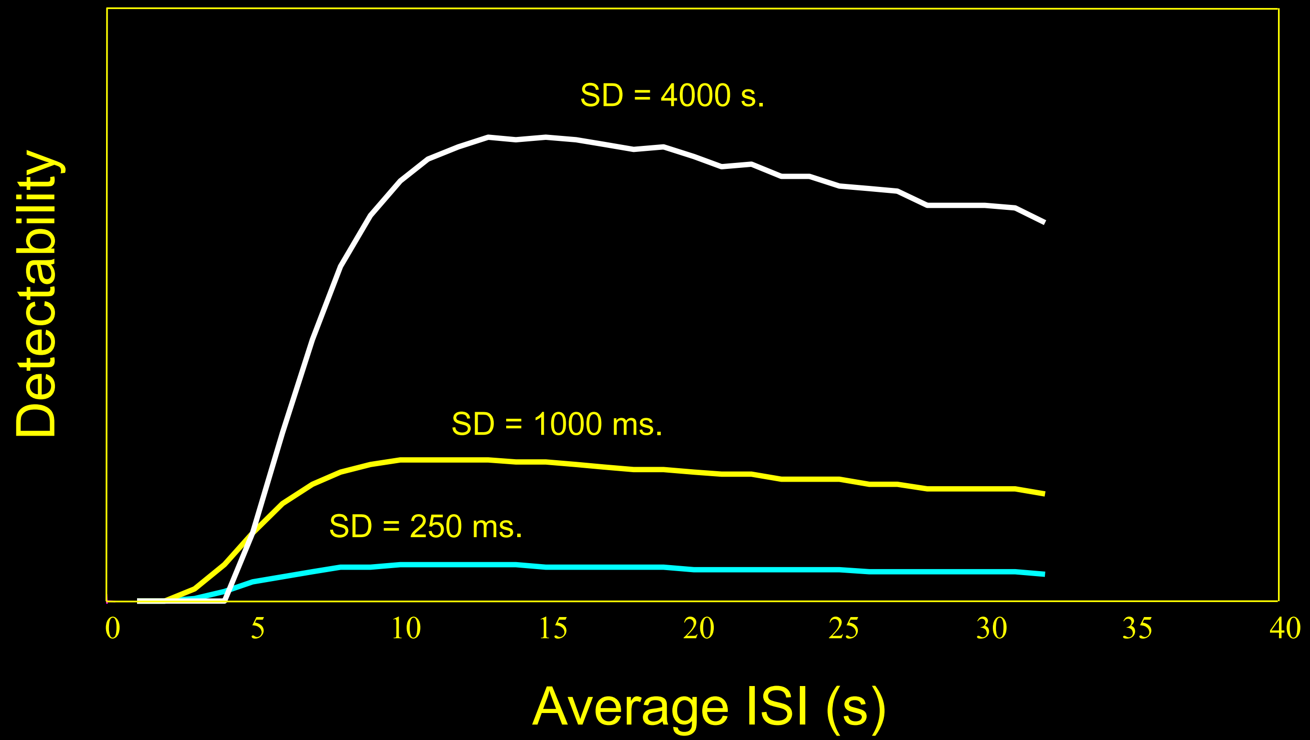

Visual Activation Paradigm: 1 , 2, & 3 Trials

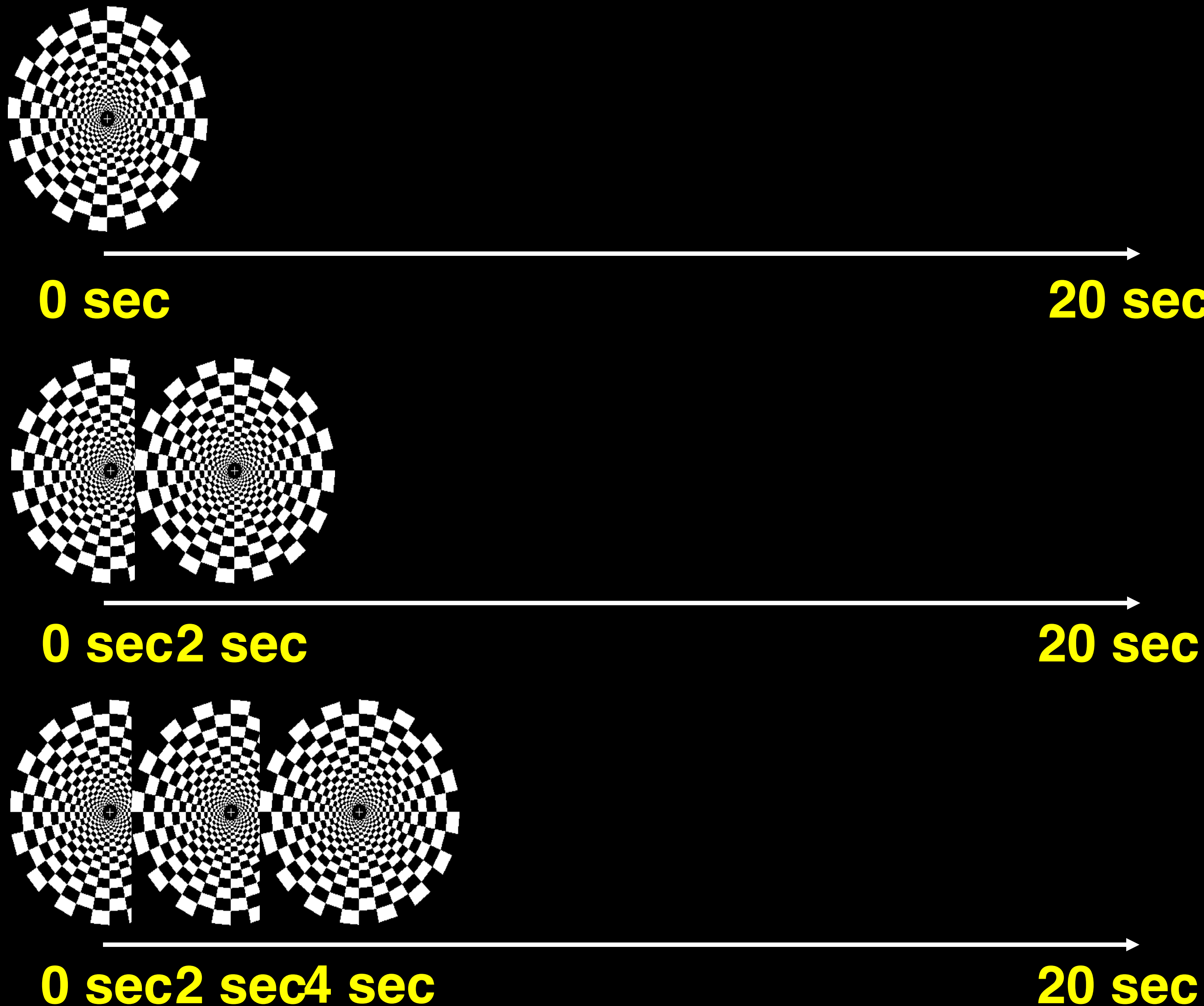

Response to Multiple Trials: Subject RW

RAW DATA

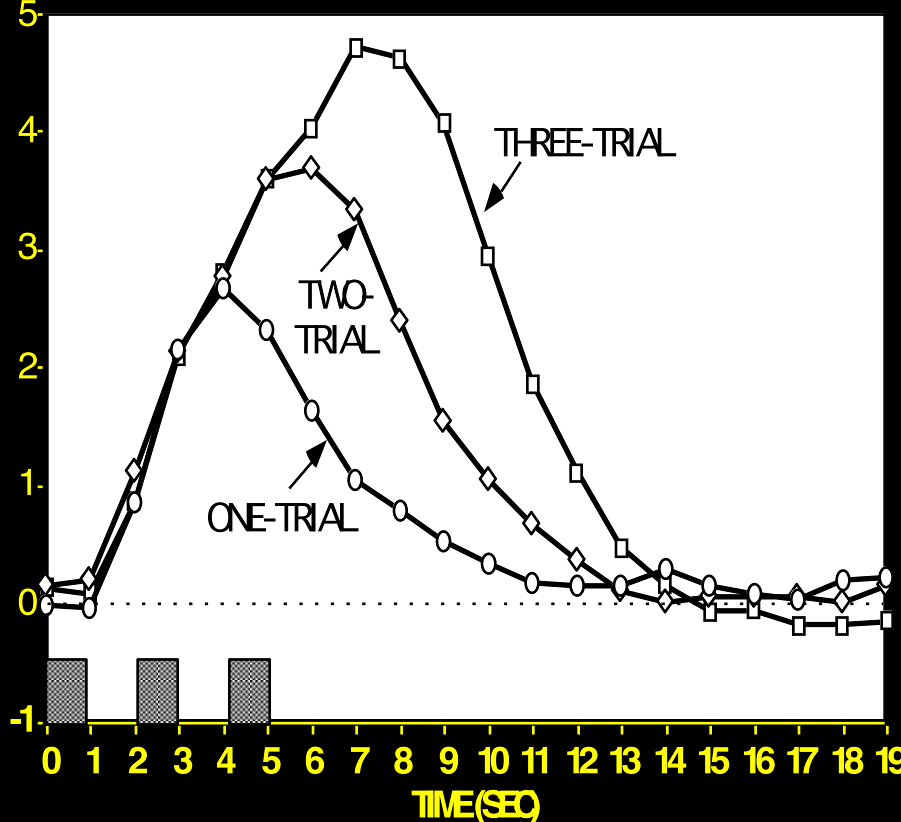

ESTIMATED RESPONSES

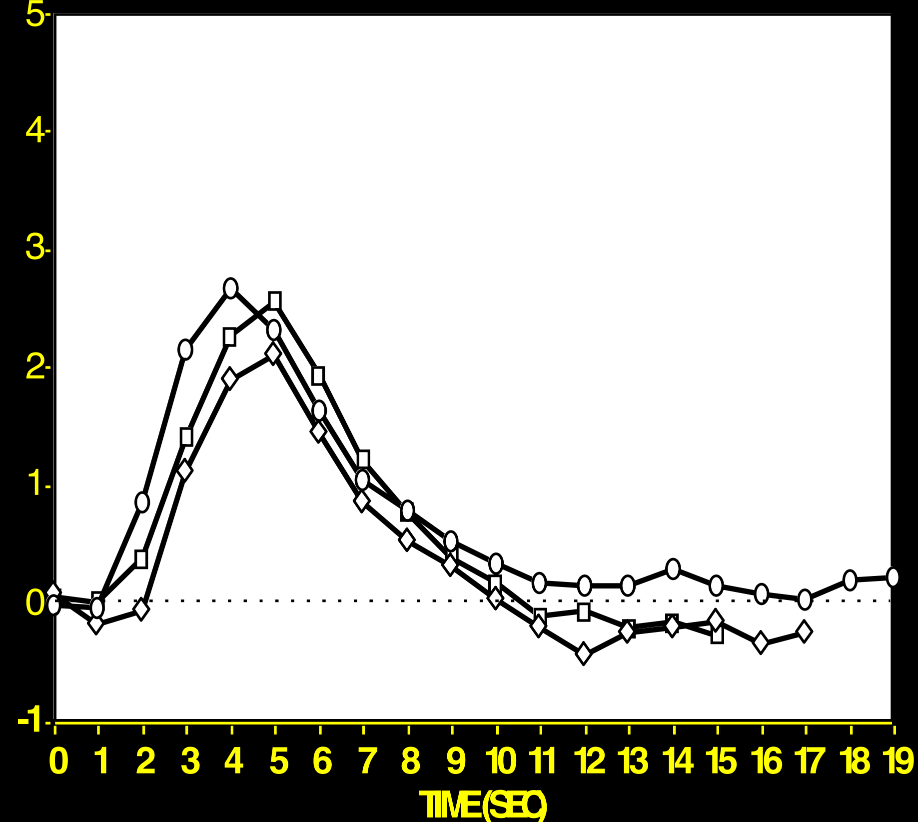

Detectability vs. Average ISI

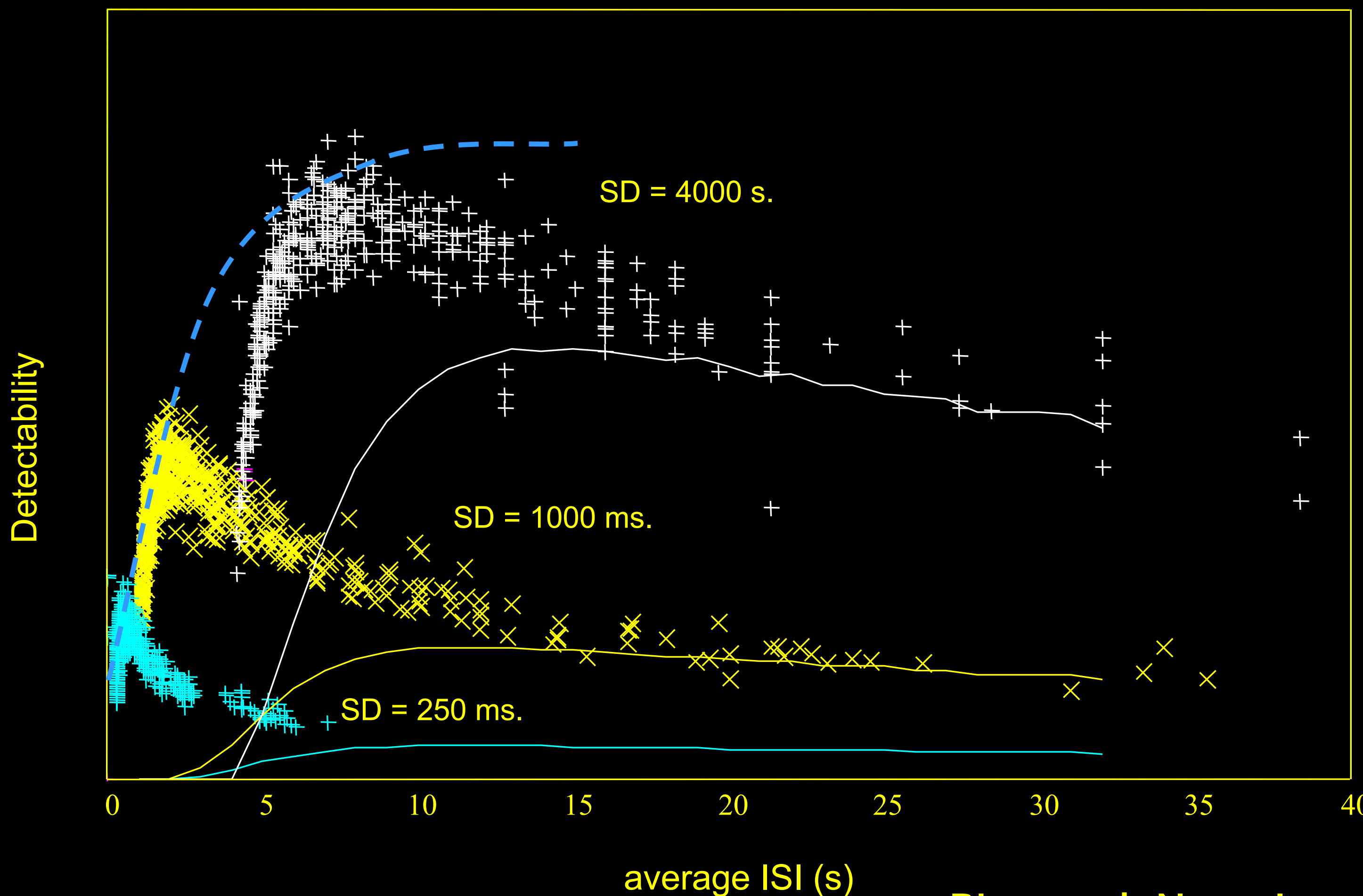

Birn et al. NeuroImage

Estimation accuracy vs. average ISI

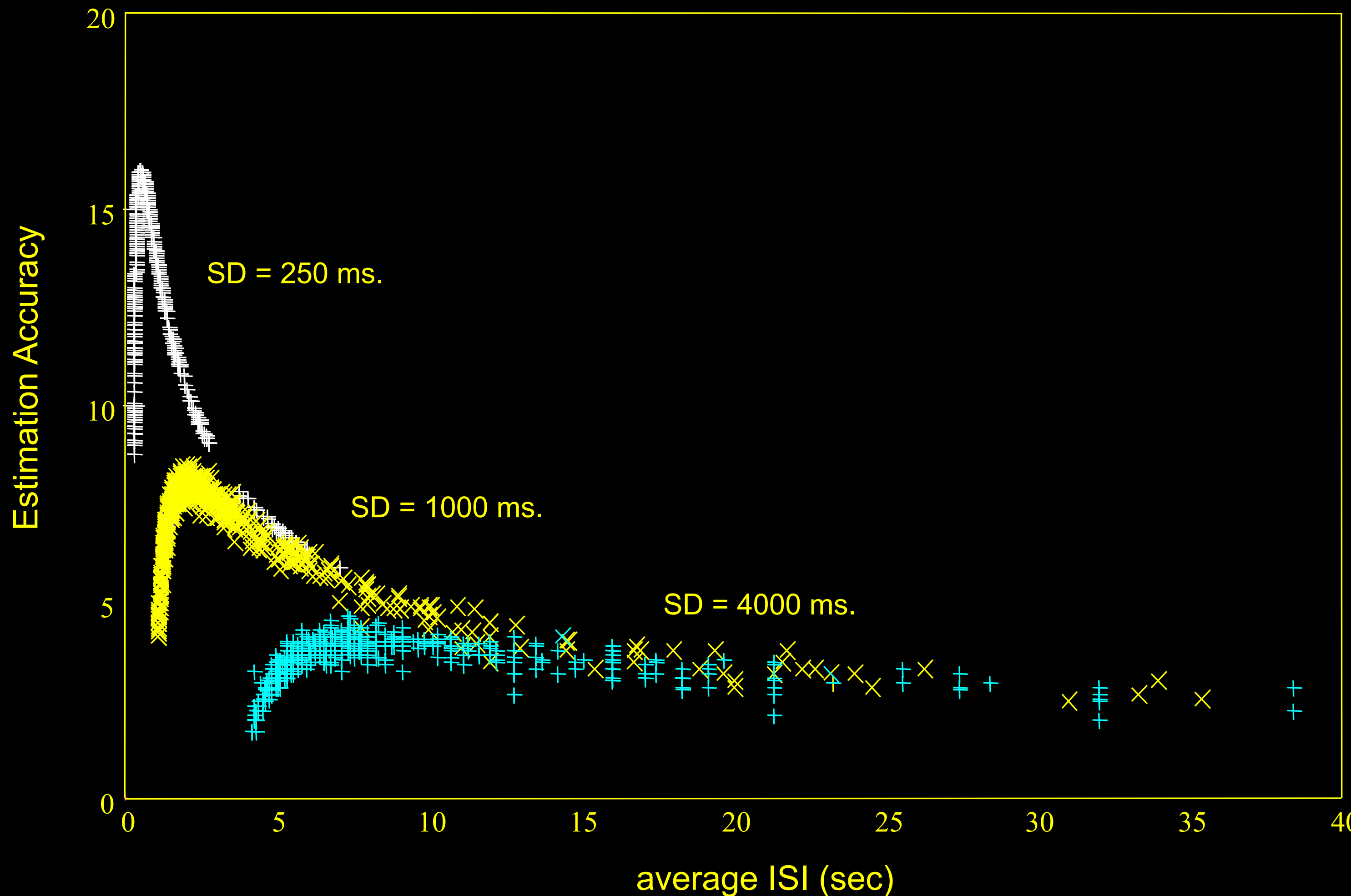

Birn et al. NeuroImage

Varying "ON" and "OFF" periods

- *Rapid event-related design with varying ISI*

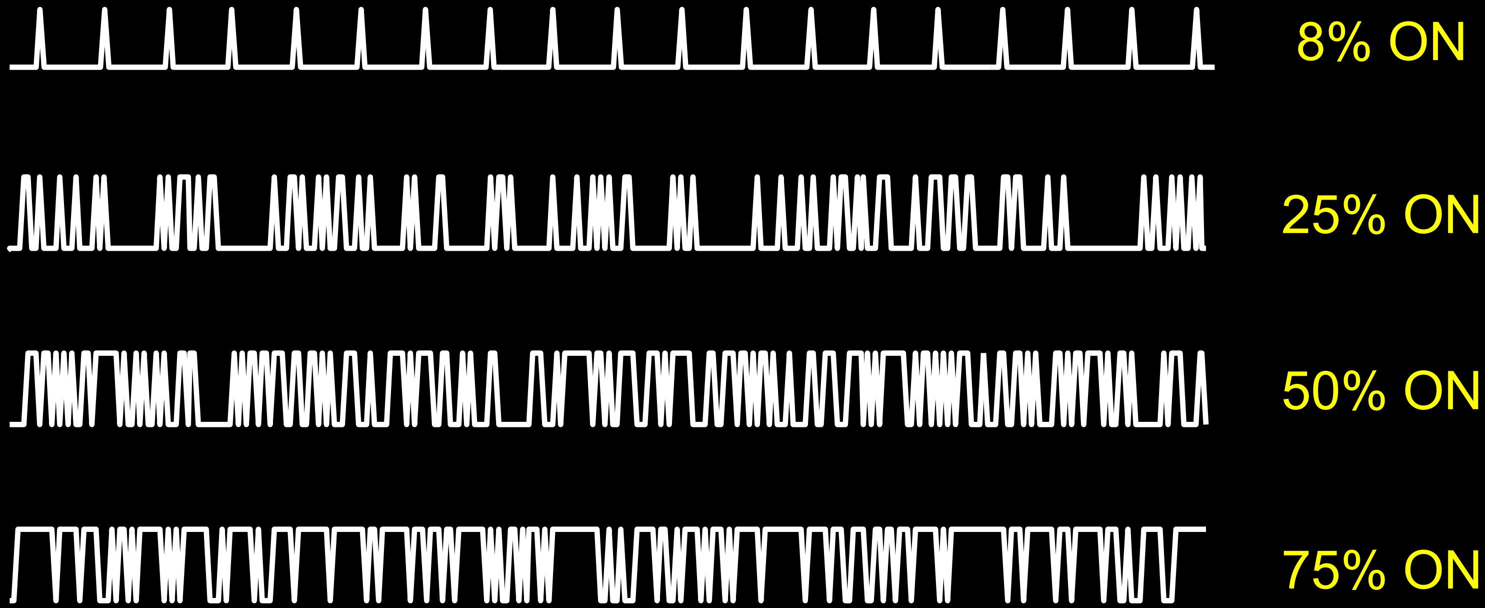

Varying "ON" and "OFF" periods

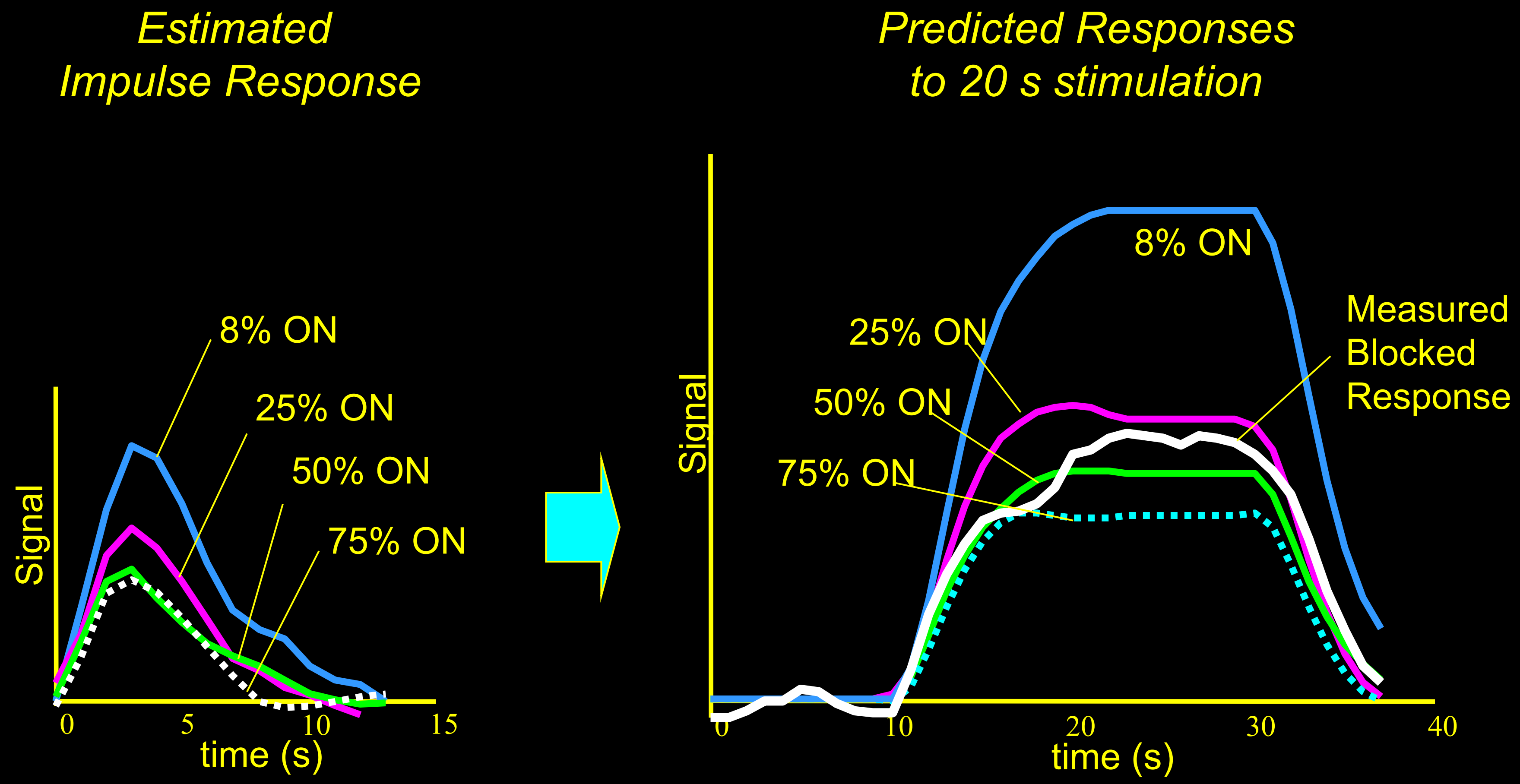

Linearity

Latency

Fluctuations and Sensitivity

“Current” Imaging

Time Course Comparison Across Brain Regions

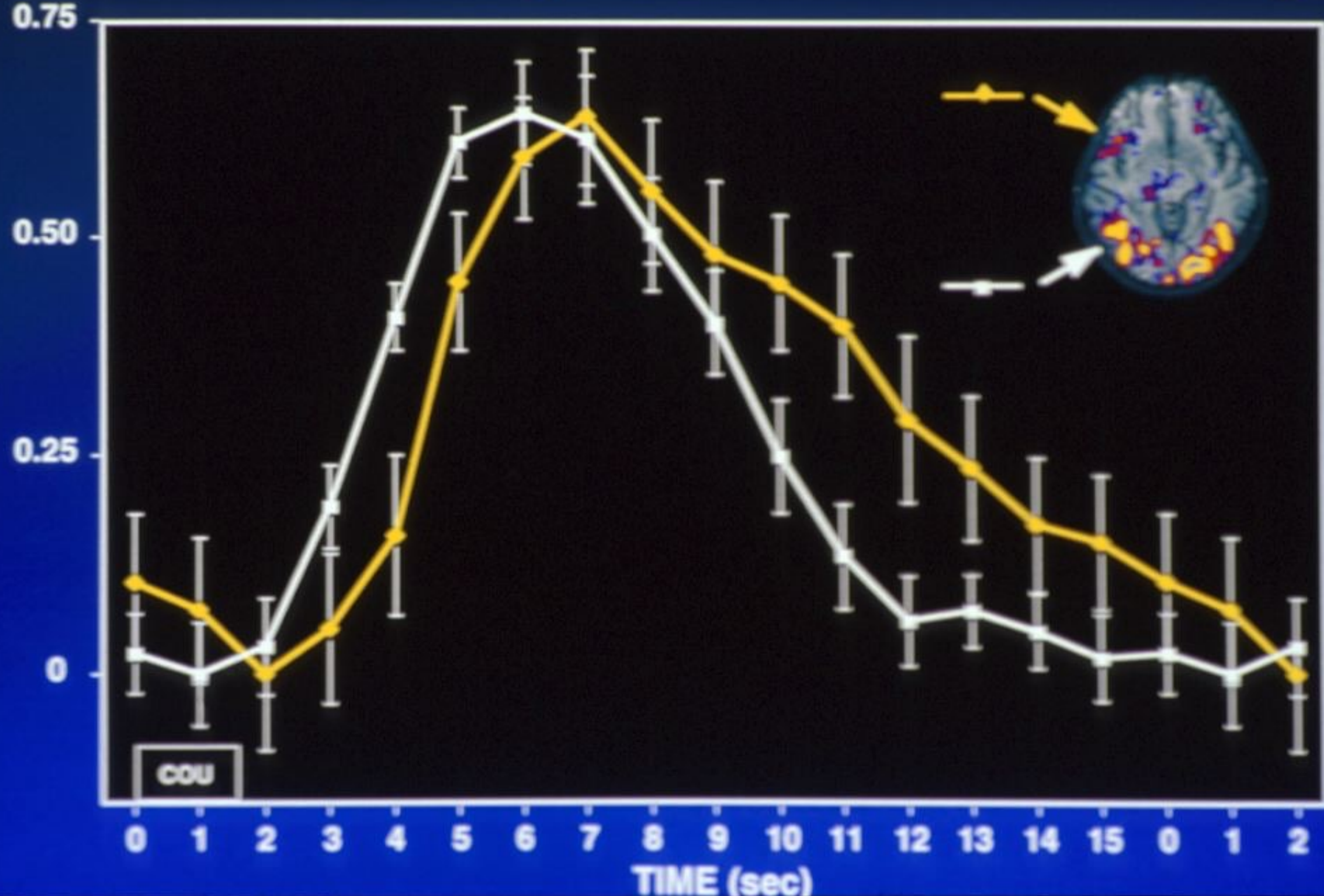

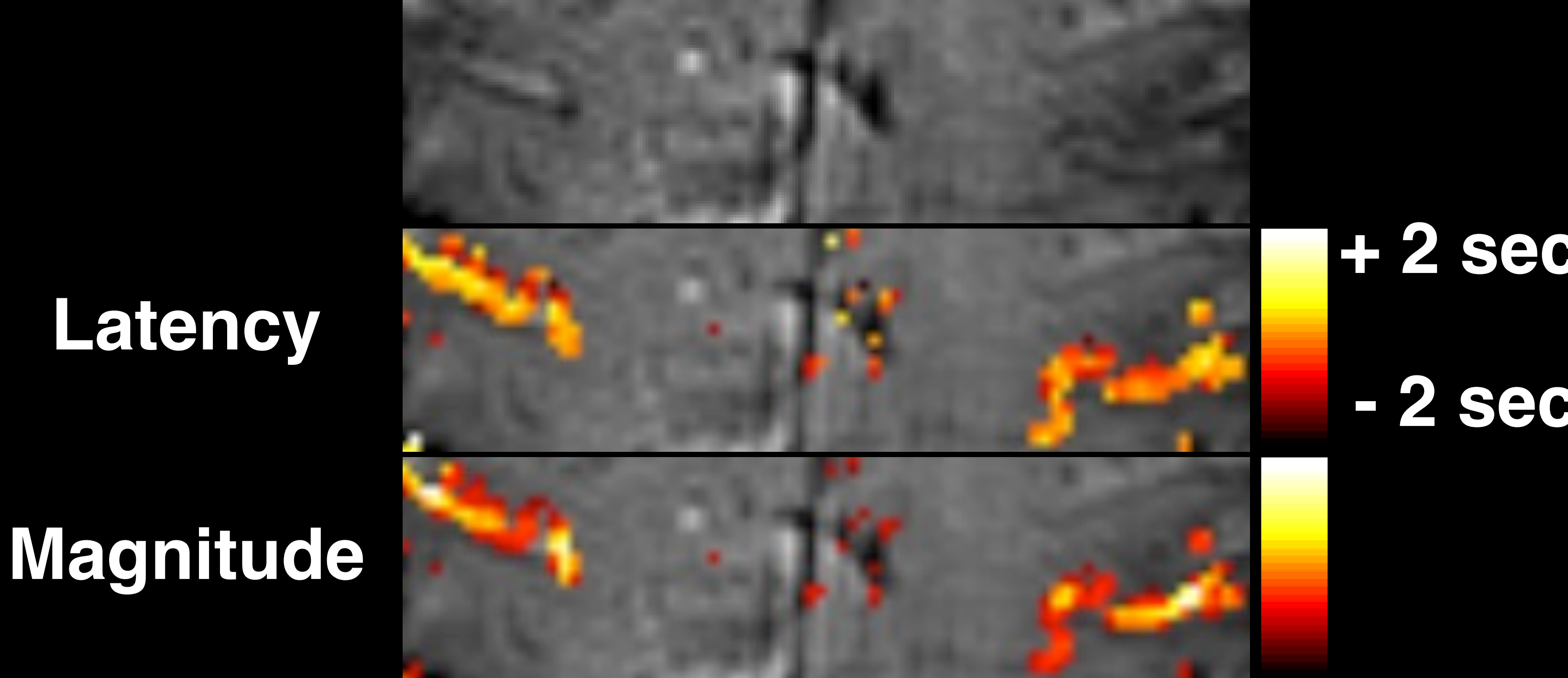
Latency
Magnitude
+ 2 sec
- 2 sec

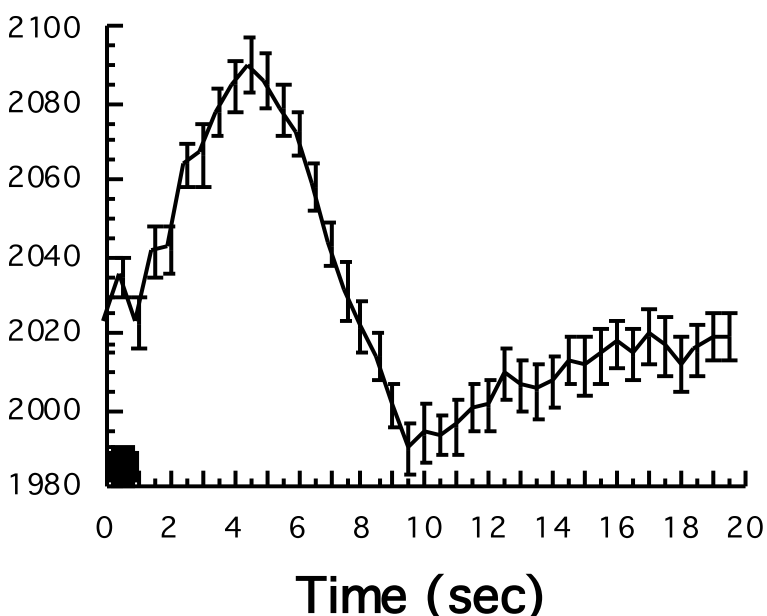
2100
2080
2060
2040
2020
2000
1980
0 2 4 6 8 10 12 14 16 18 20
Time (sec)

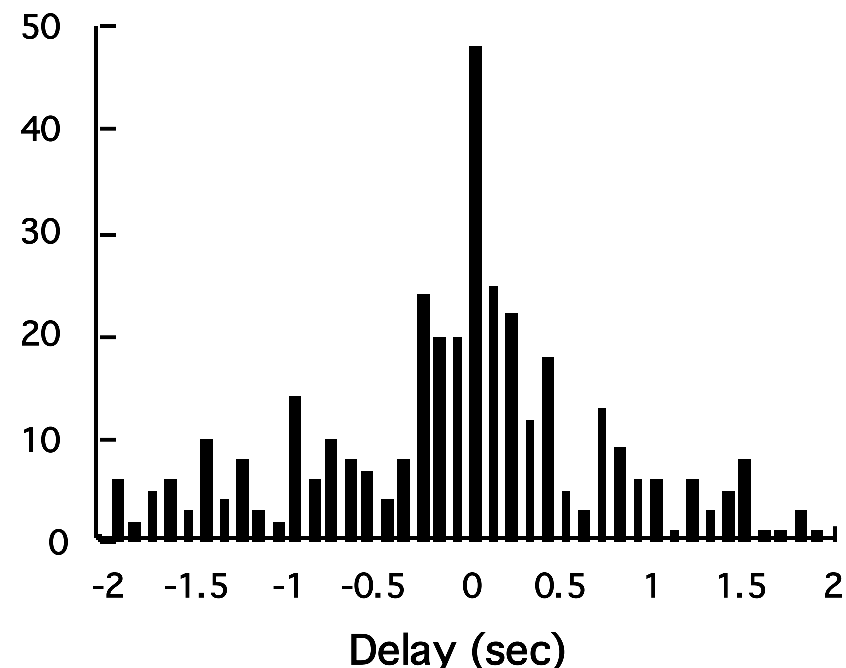
50
40
30
20
10
0
-2 -1.5 -1 -0.5 0 0.5 1 1.5 2
Delay (sec)

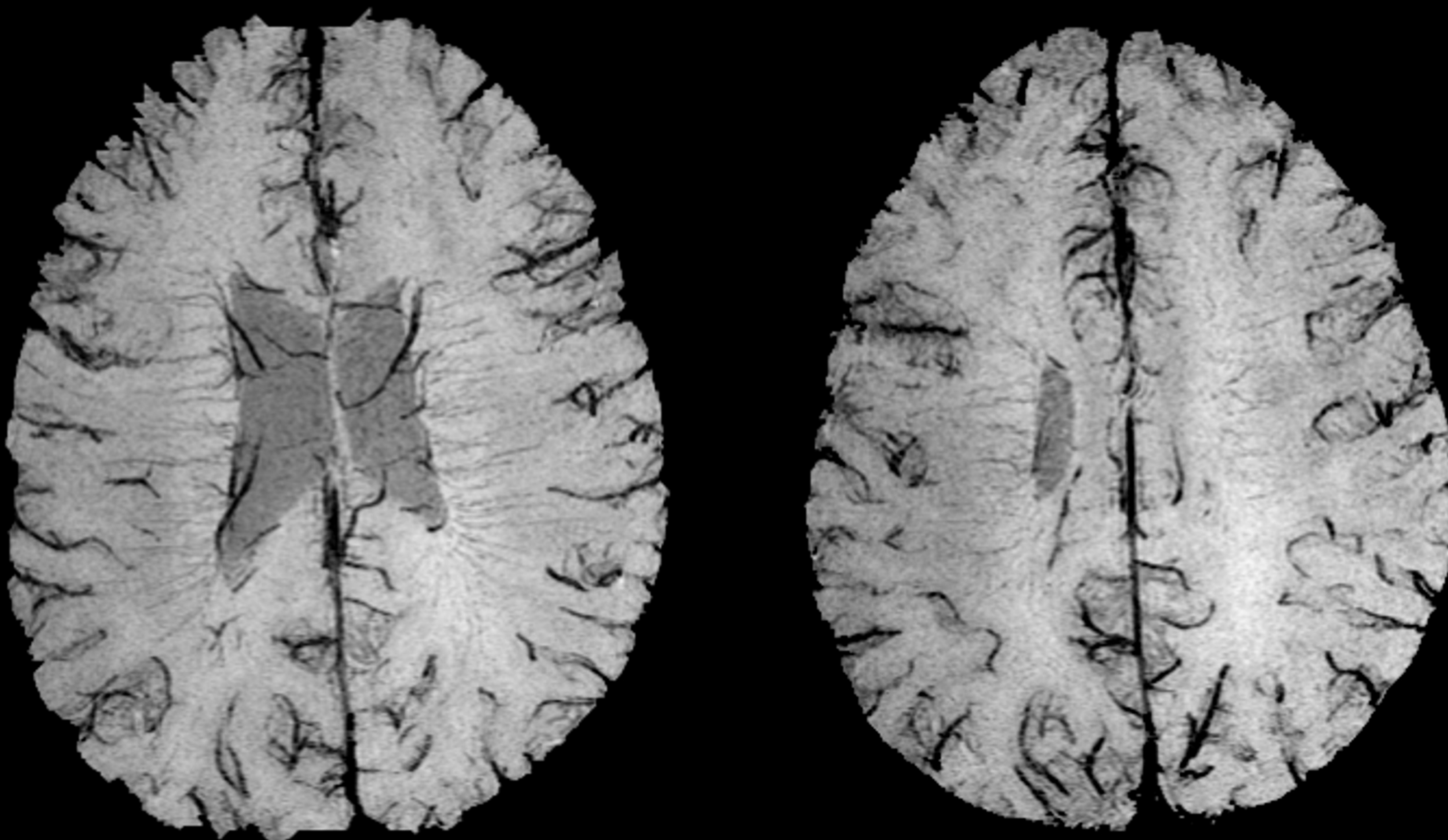

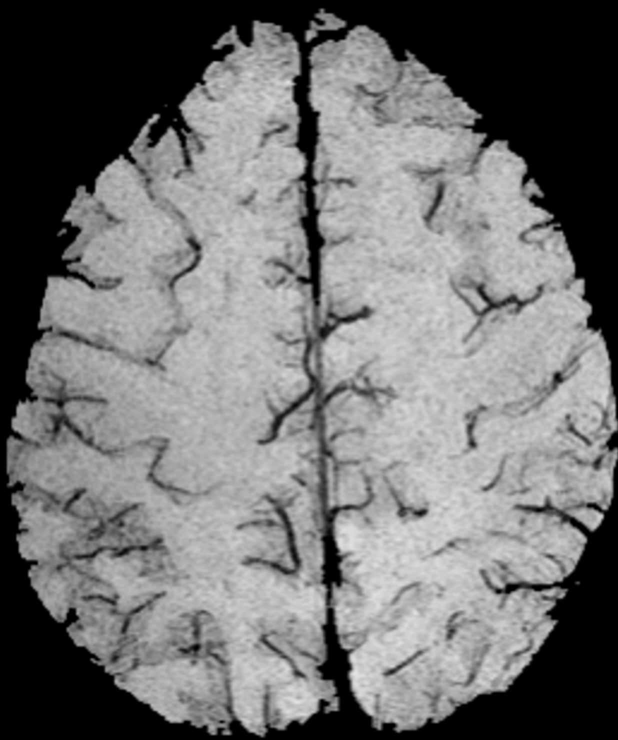

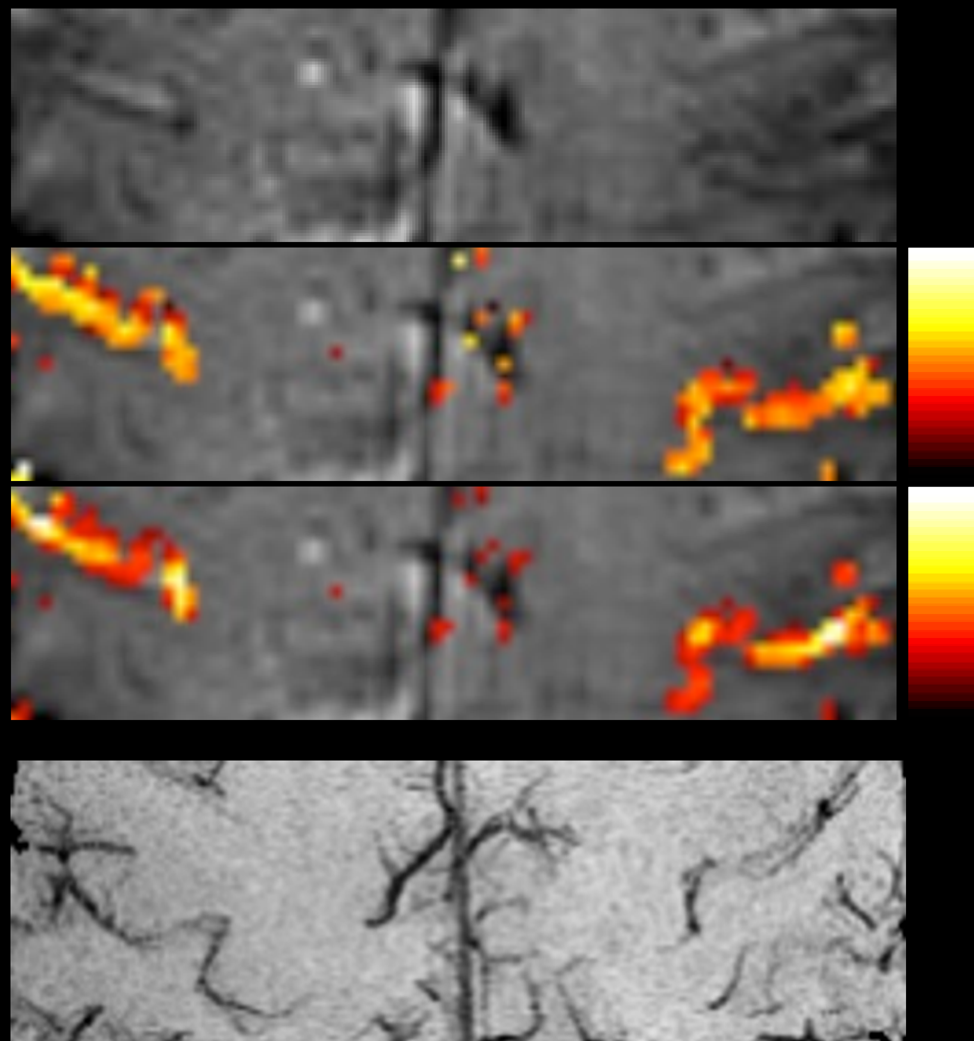

Regions of Interest Used for Hemi-Field Experiment

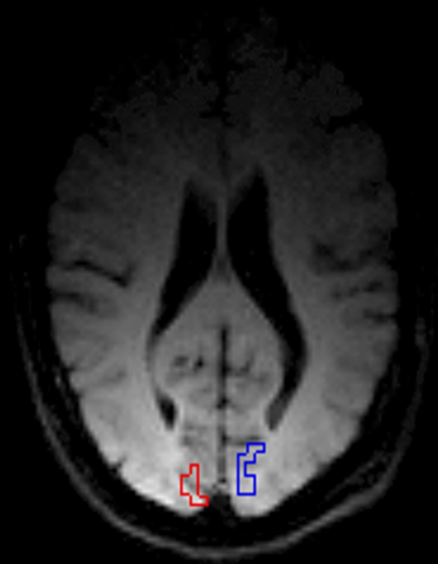

Right Hemisphere

Left Hemisphere

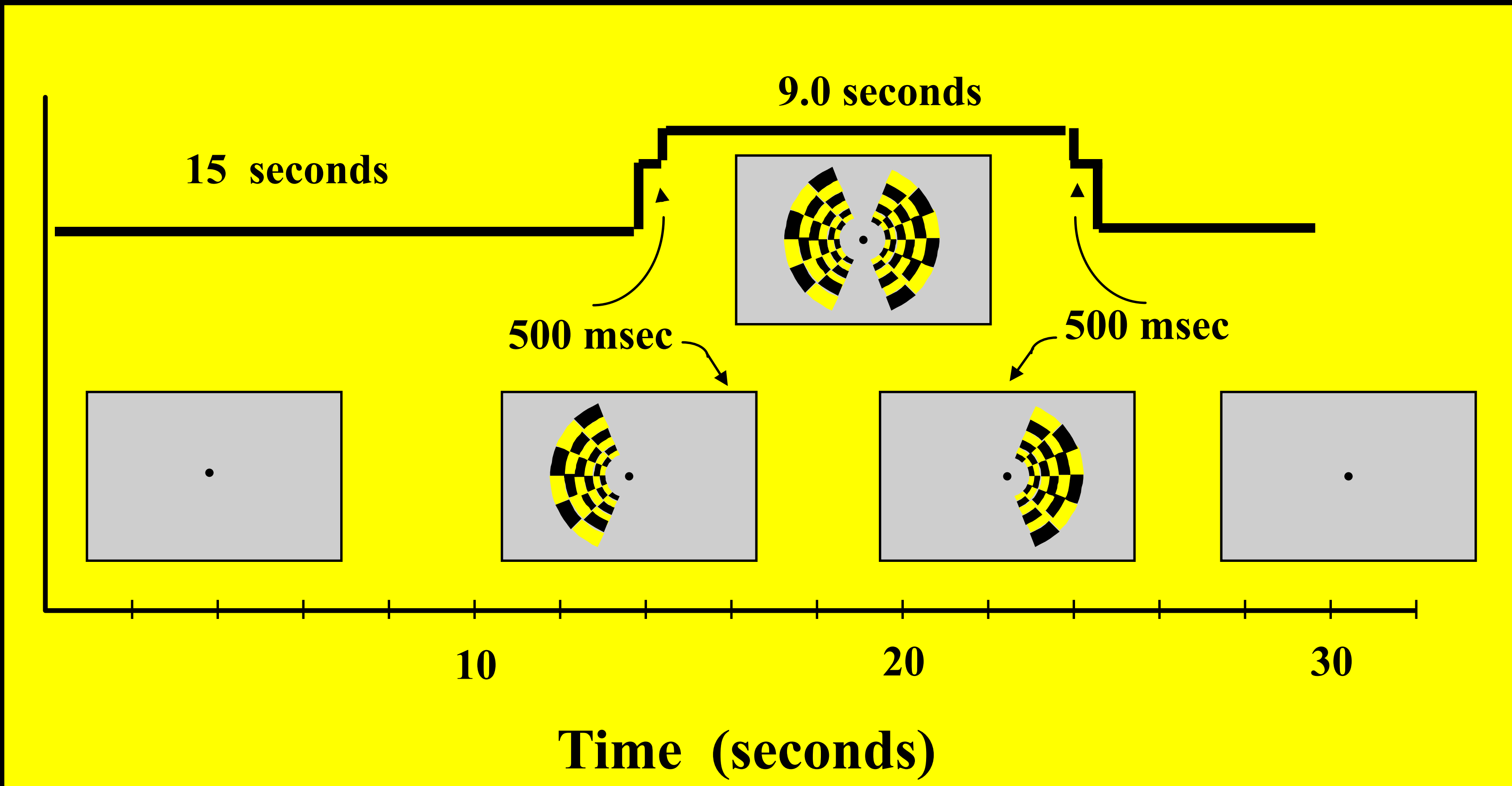
9.0 seconds
15 seconds
500 msec
500 msec
10
20
30
Time (seconds)

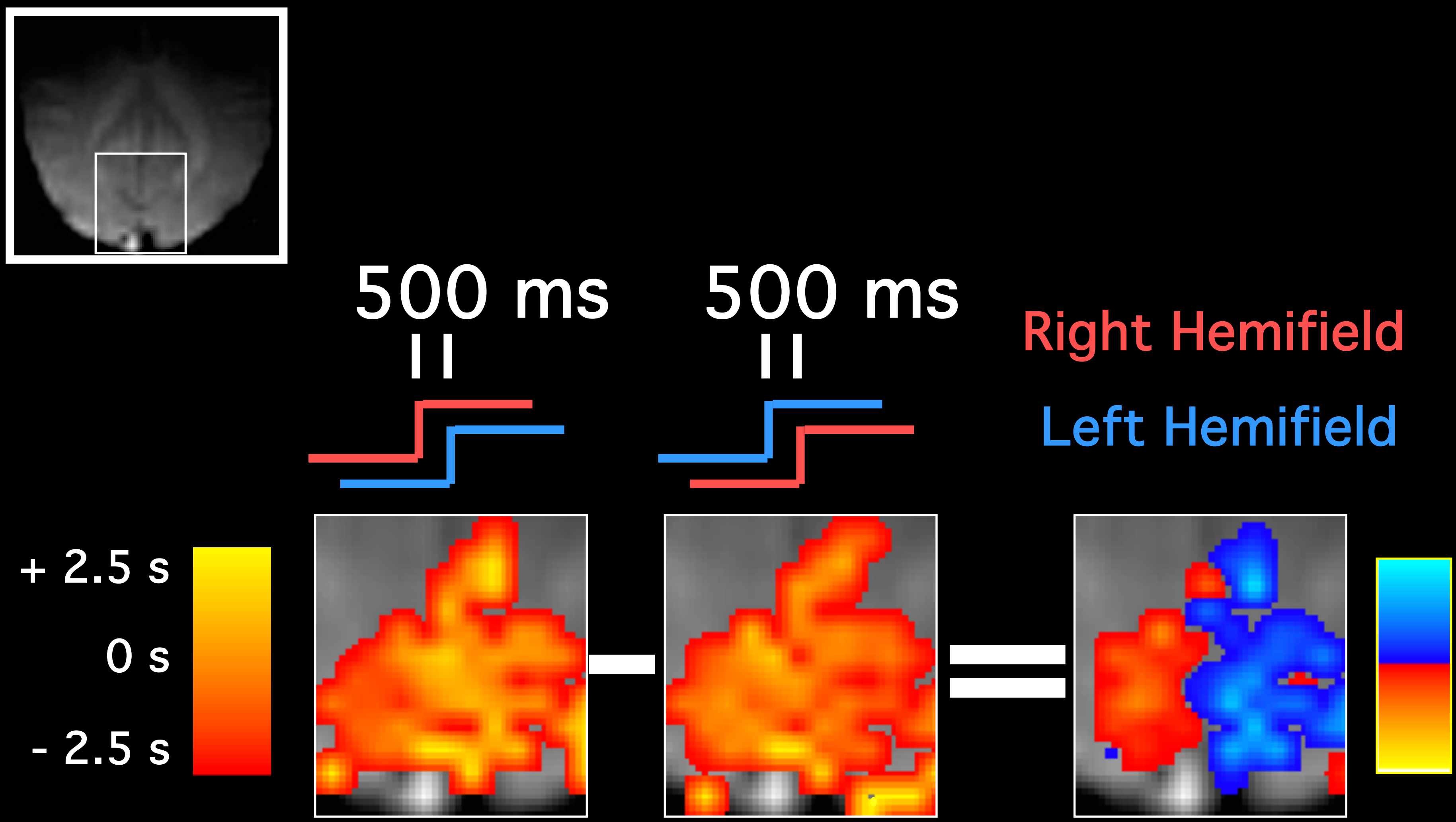

500 ms
500 ms
Right Hemifield
Left Hemifield
+ 2.5 s
0 s
- 2.5 s

Latency Modulation Application

Imaging Method: Scanner – 3T TR - 1000 ms TE - 30 ms

Behavioral Method:

Stimuli – Six-letter English words and pronounceable non-words.
Each word or non-word was rotated either 0, 60,or 120 degrees

Task – Lexical Decision (word / non-word).

Dependent Measures – Percent Correct and Reaction Time.

Hypotheses :

1) Stimulus rotation of 120 degrees will result in:
   a) Longer Reaction Times
   b) Wider IRF in Parietal Lobe
   c) Delayed IRF onset in Left Inferior Frontal cortex

2) Lexical discrimination will result in :
   a) Longer Reaction Times for non-words
   b) Wider IRF in Inferior Frontal cortex for non-words
   c) Delayed IRF onset in Left Middle Frontal Cortex

Lexical Delay

Rotational Delay

	Words	Non-Words	Mean Reaction Time
0^{0}	smudge	dierts	823 ms
60^{0}	frolic	cuhlos	891 ms
120^{0}	slouch	gedmus	1446 ms
Mean Reaction Time	986 ms	1219 ms	

Mean Impulse Response Functions for Activated Voxels

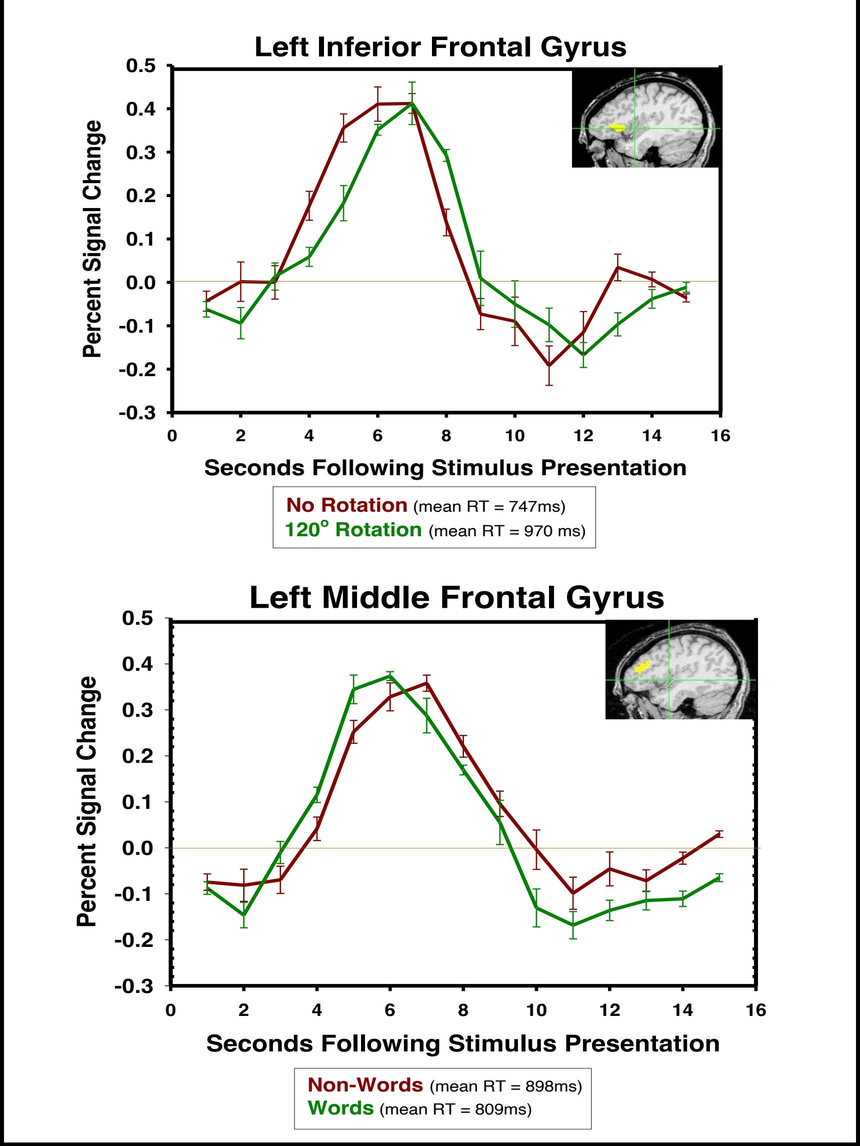

Rotation Effect

Lexical Effect

Delay Differences from Indivdual Voxels within the Above ROI's

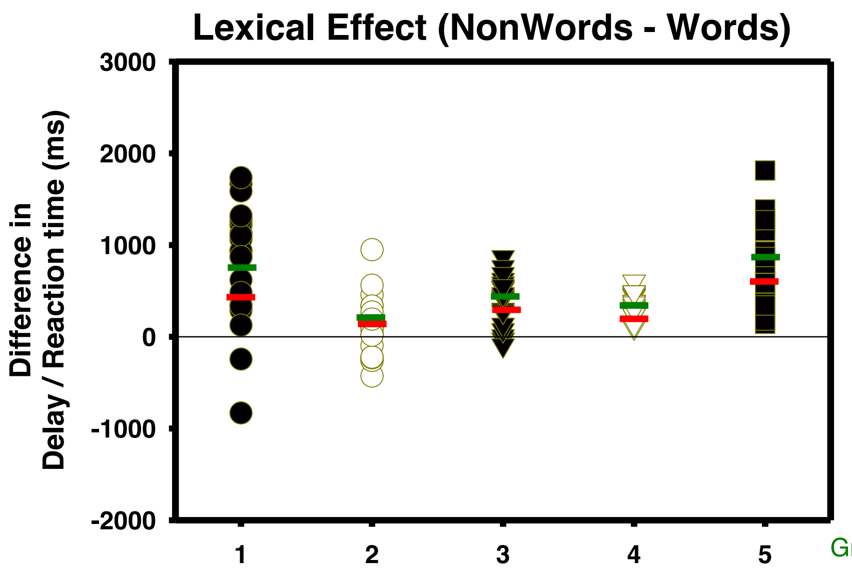

Green lines depict the median Voxel Delay estimate

Red lines depict the mean RT difference

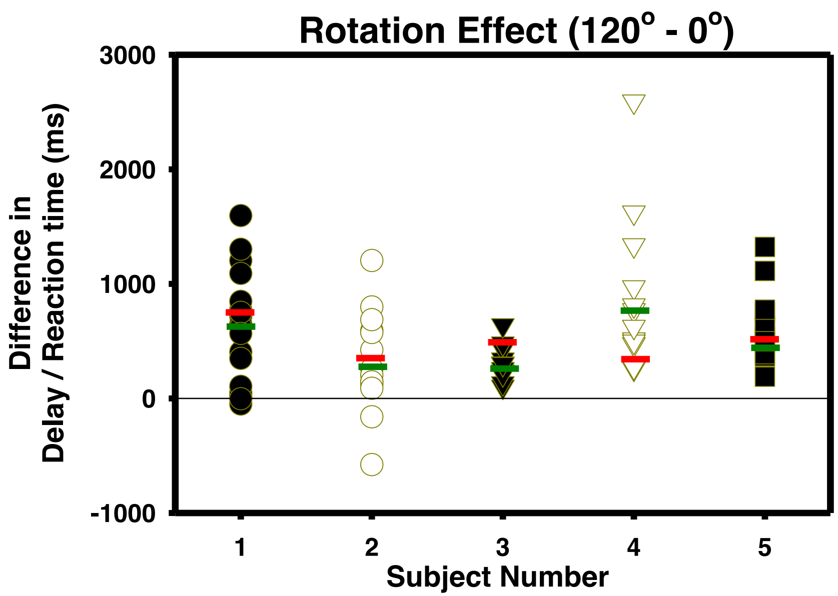

Linearity

Latency

Fluctuations and Sensitivity

“Current” Imaging

Temporal S/N vs. Image S/N

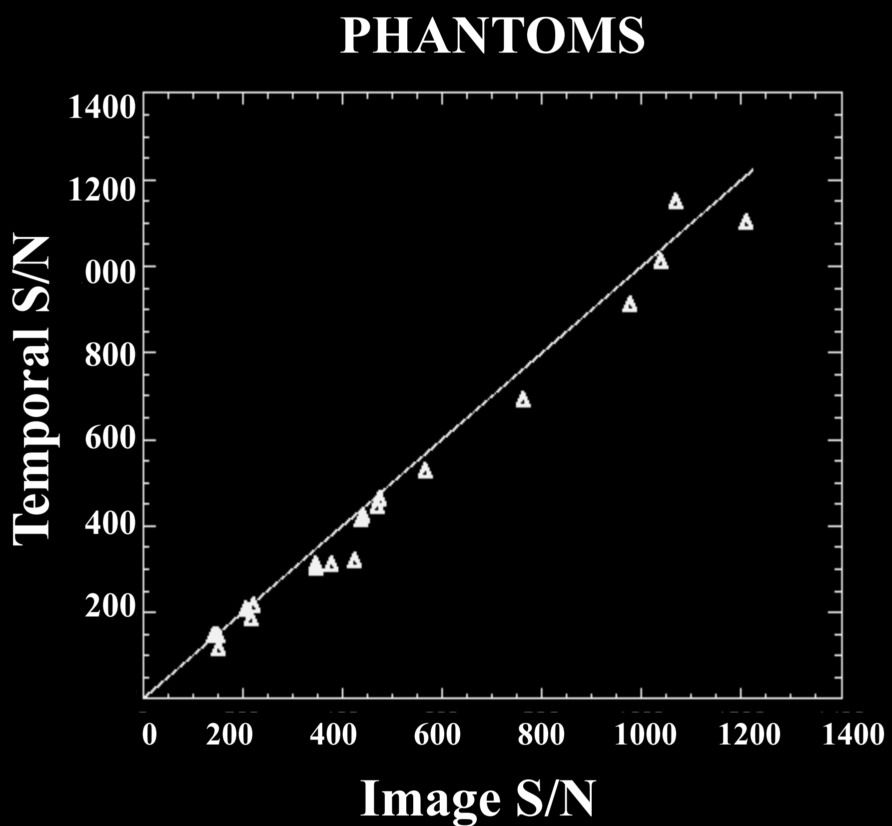

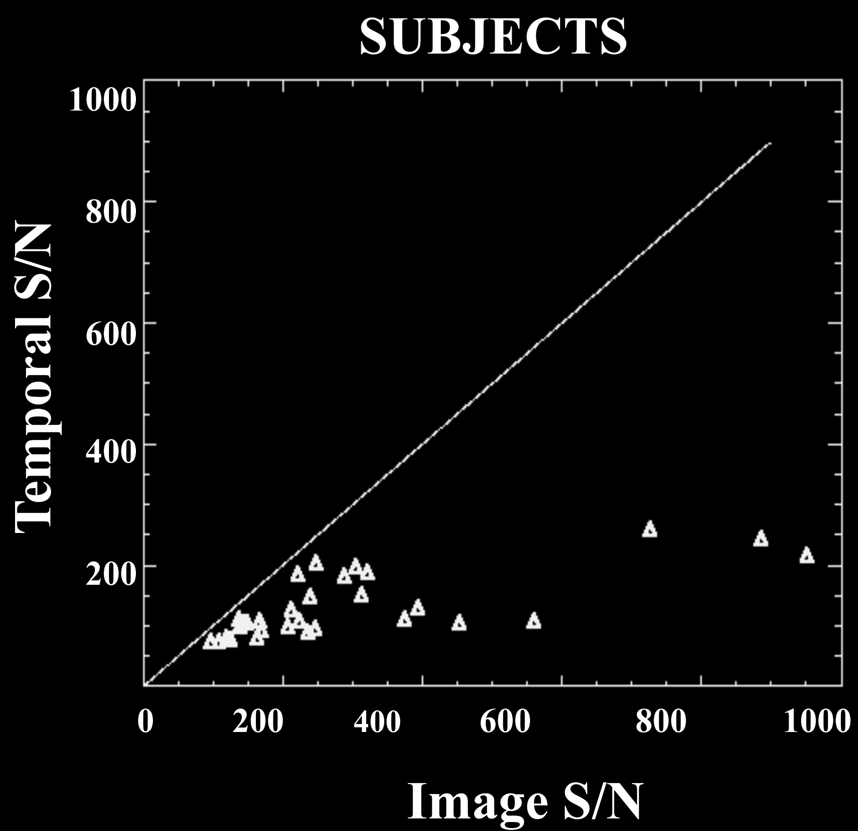

N. Petridou

Temporal vs. Image S/N
Optimal Resolution Study

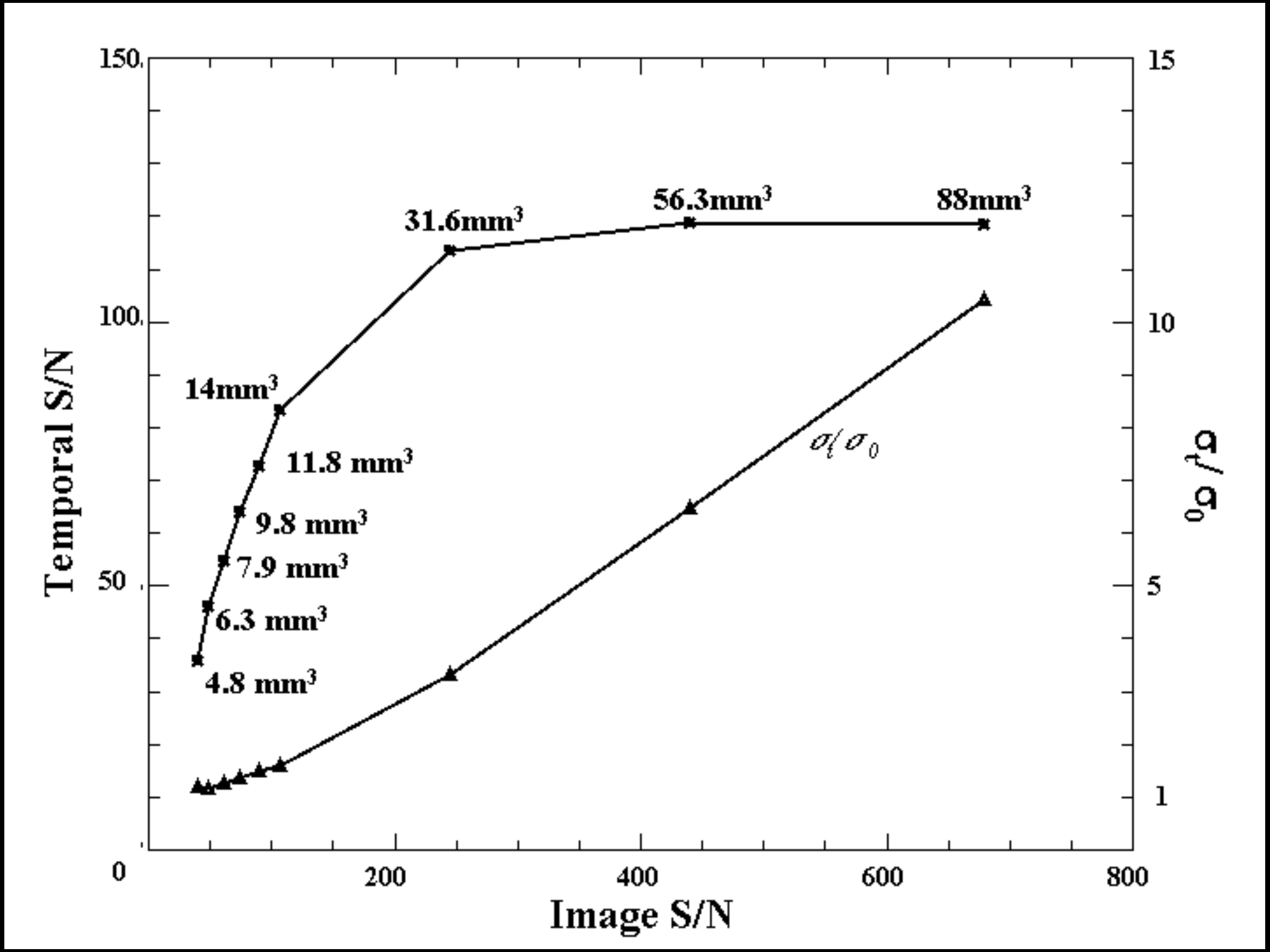

Human data

Petridou et al

Temporal vs. Image S/N
Optimal Resolution Study

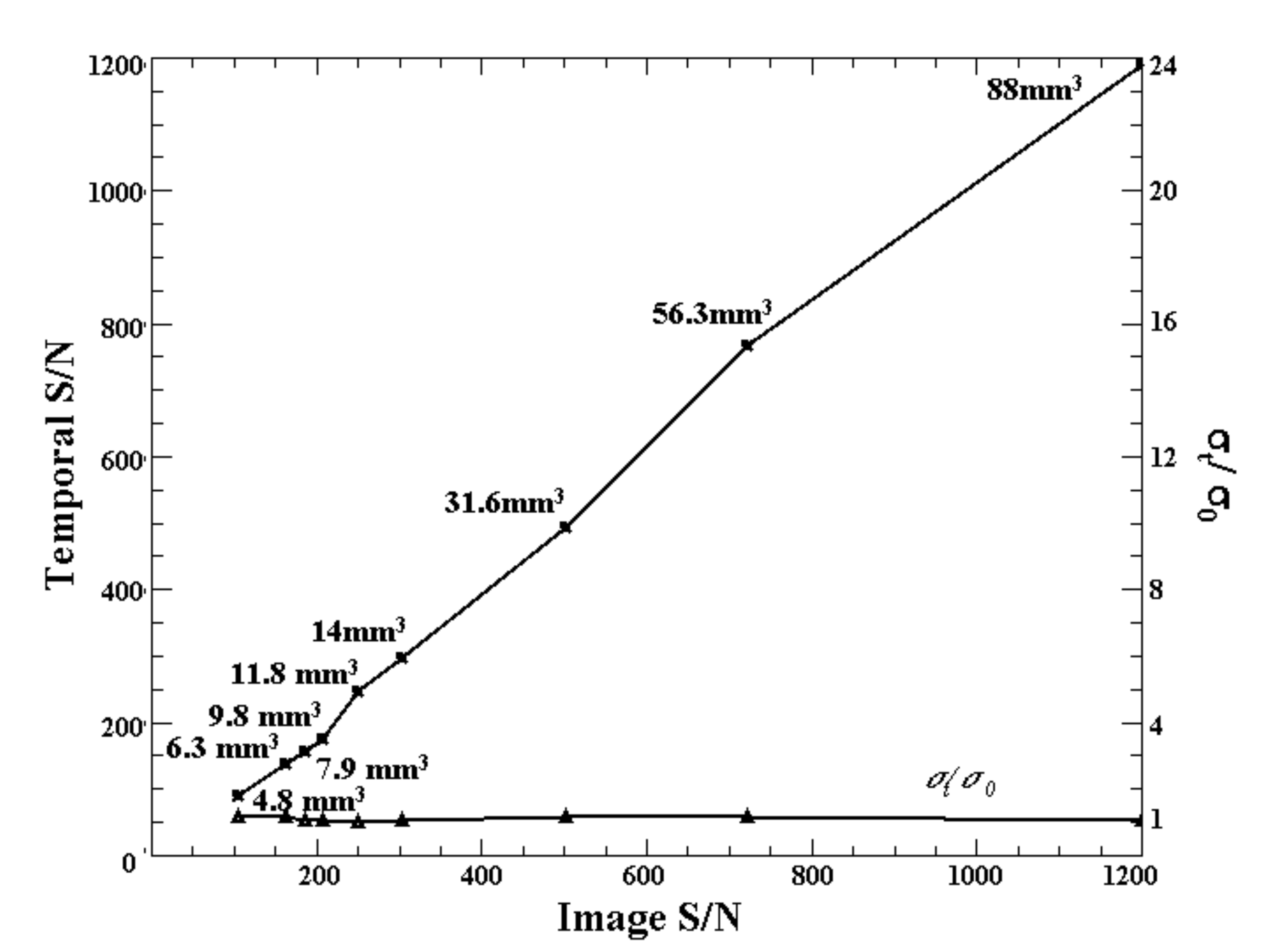

Phantom data

Petridou et al

Continuously Growing Activation Area

CC Histogram

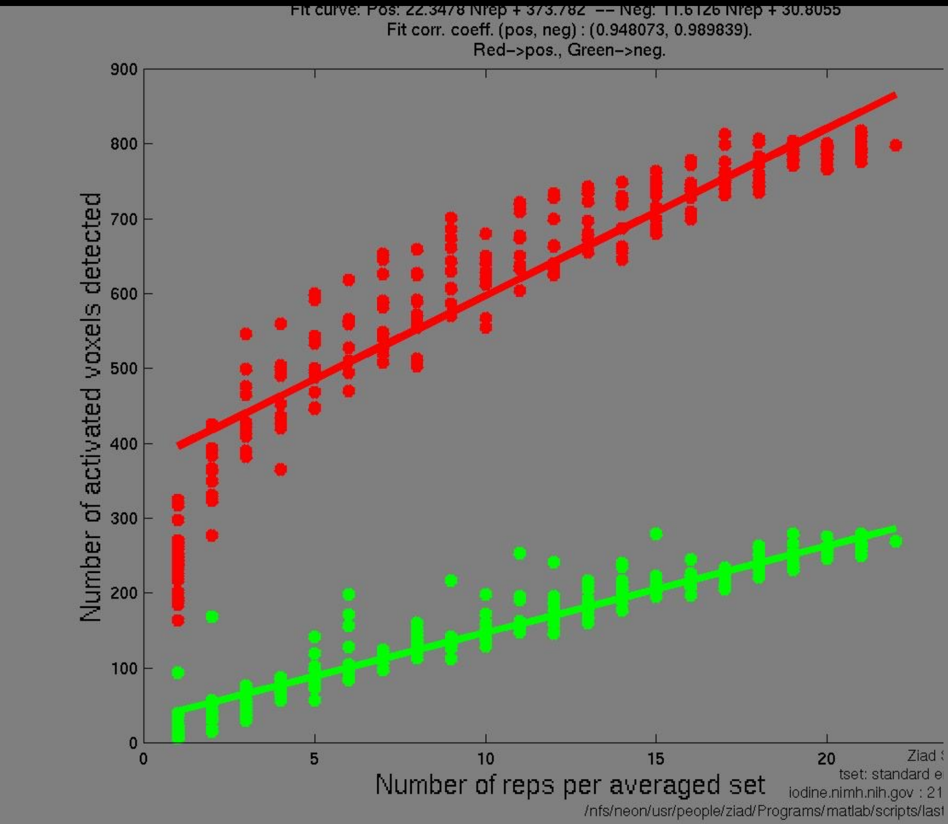

Inflection Point

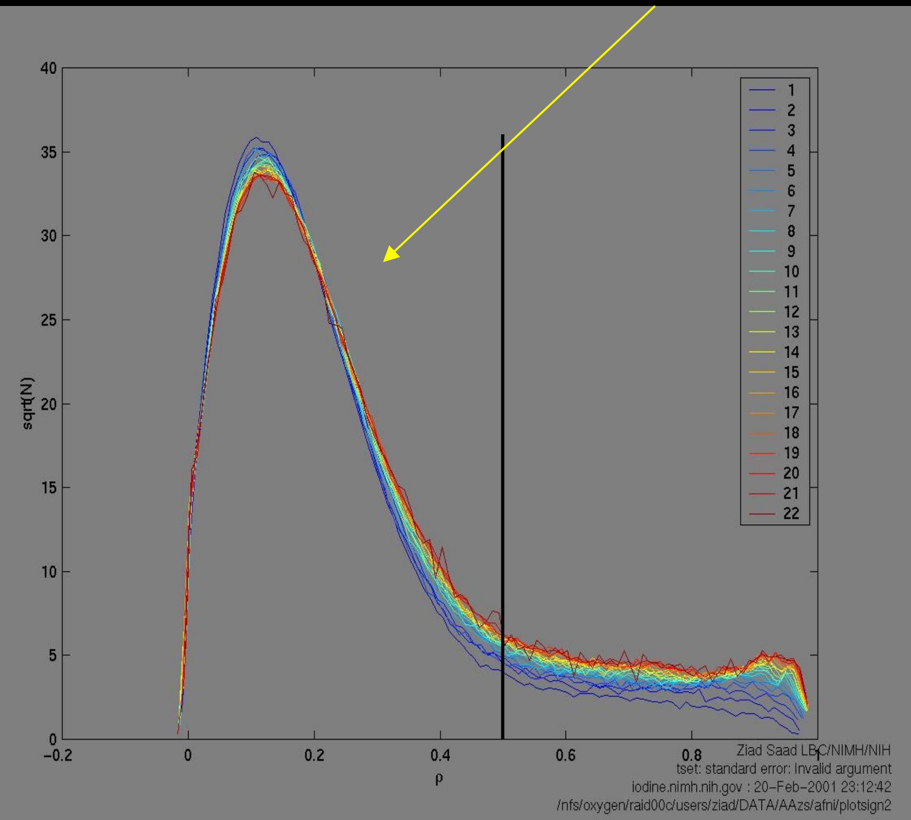

Ziad Saad, et al

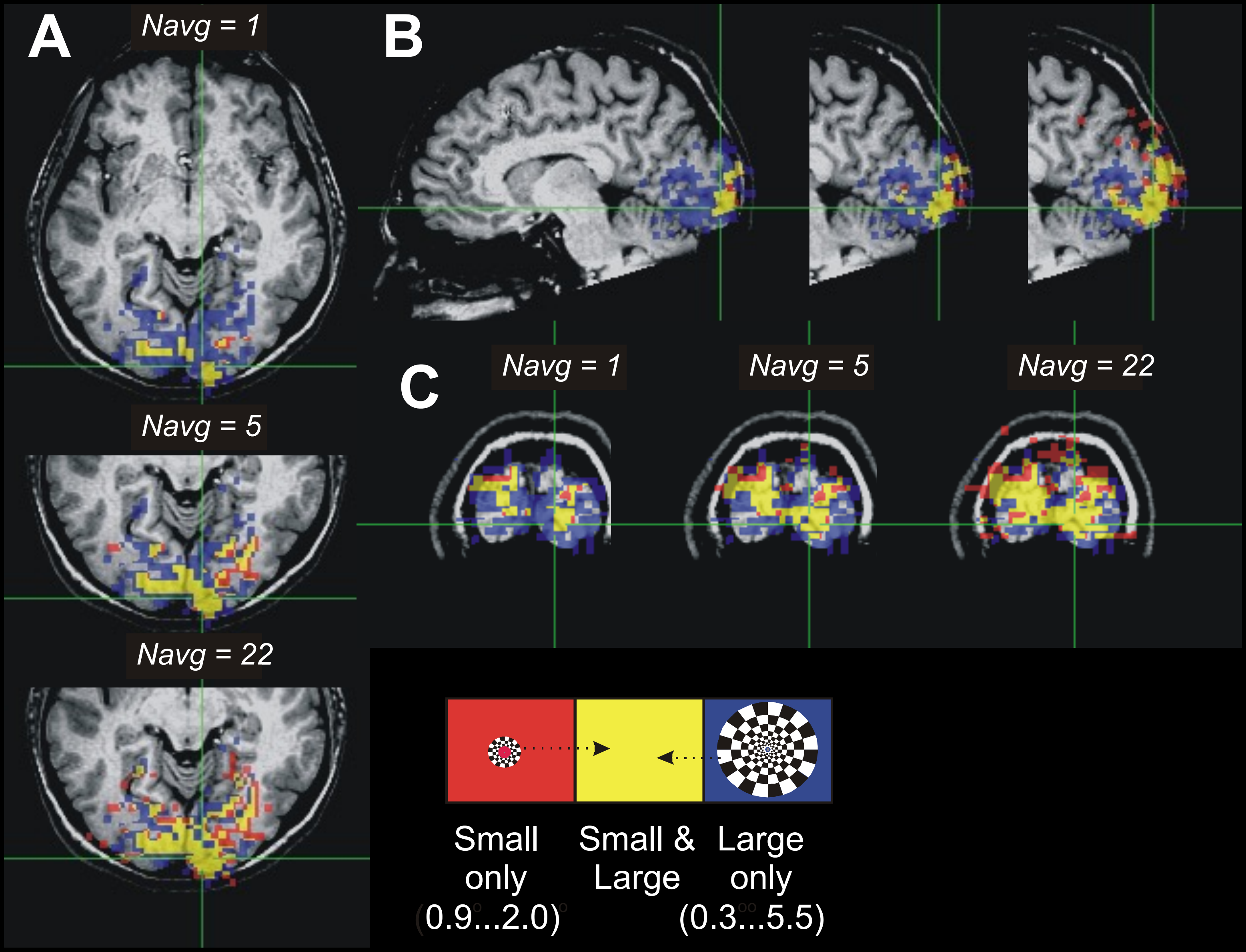
A
Navg = 1
Navg = 5
Navg = 22
B
C
Navg = 1
Navg = 5
Navg = 22
Small only (0.9...2.0)°
Small & Large
Large only (0.3...5.5)°

Resting ASL Signal

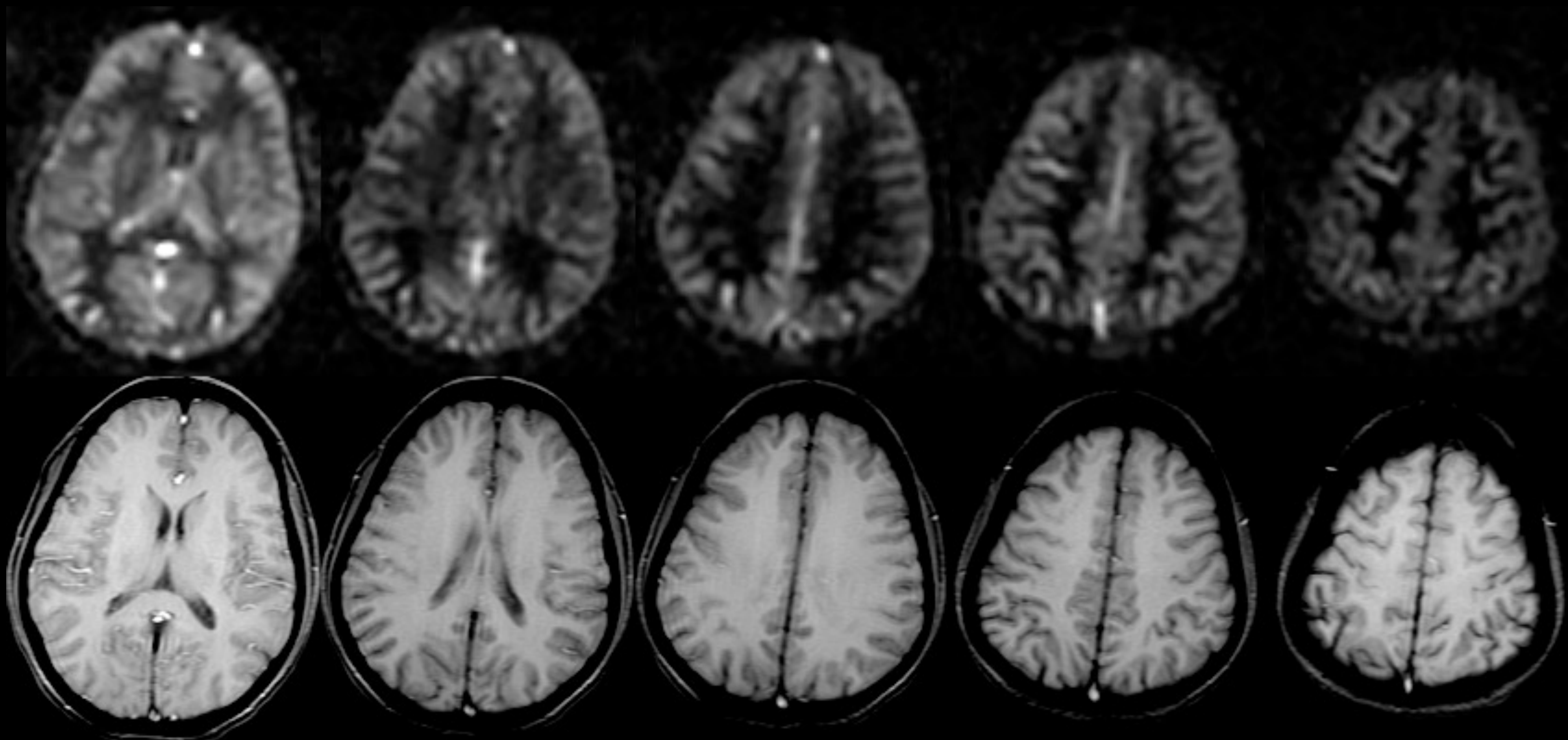

Comparison with Positron Emission Tomography

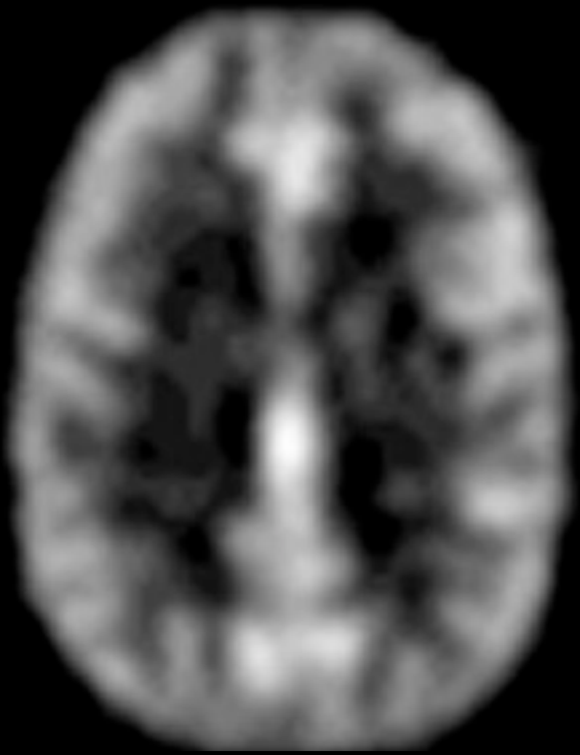

PET: $H_2{}^{15}O$

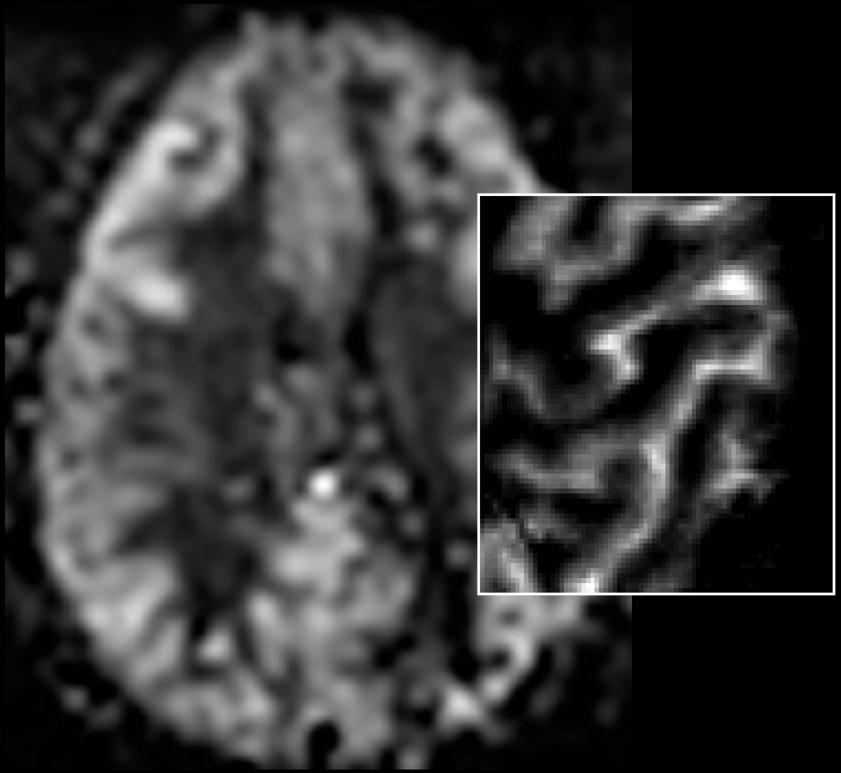

MRI: ASL

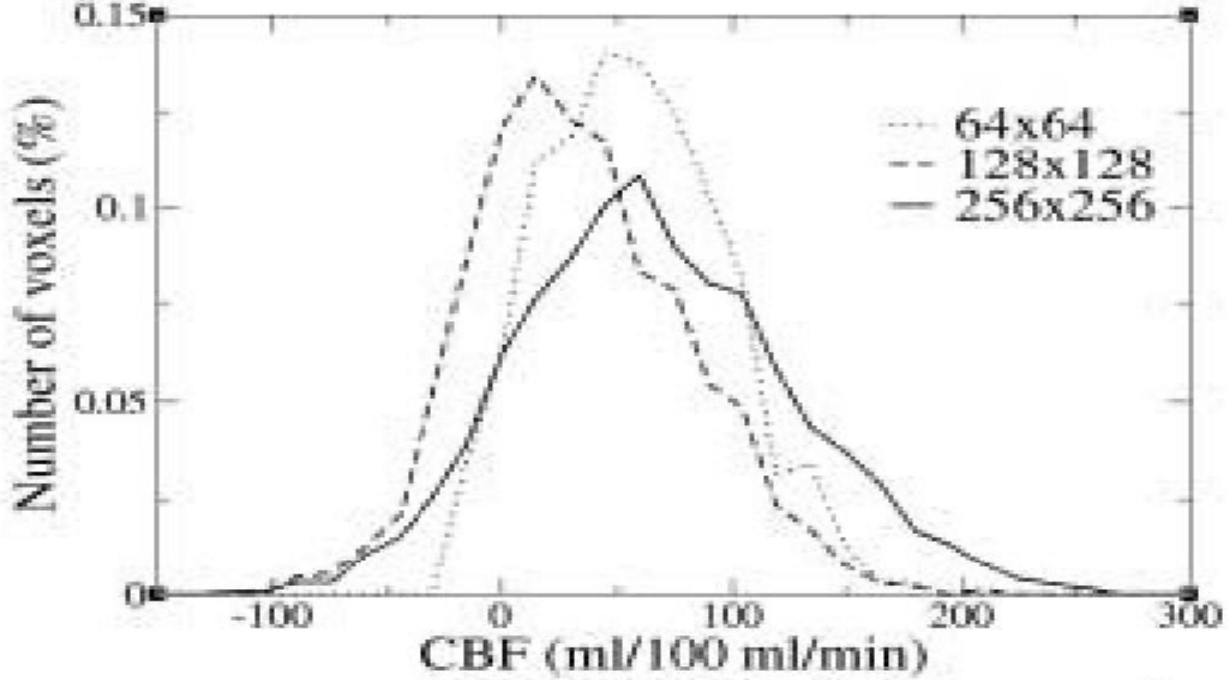

Figure 1. Histograms of absolute CBF values from 64^2, 128^2, and 256^2 images, respectively.

Resting Hemodynamic Autocorrelations

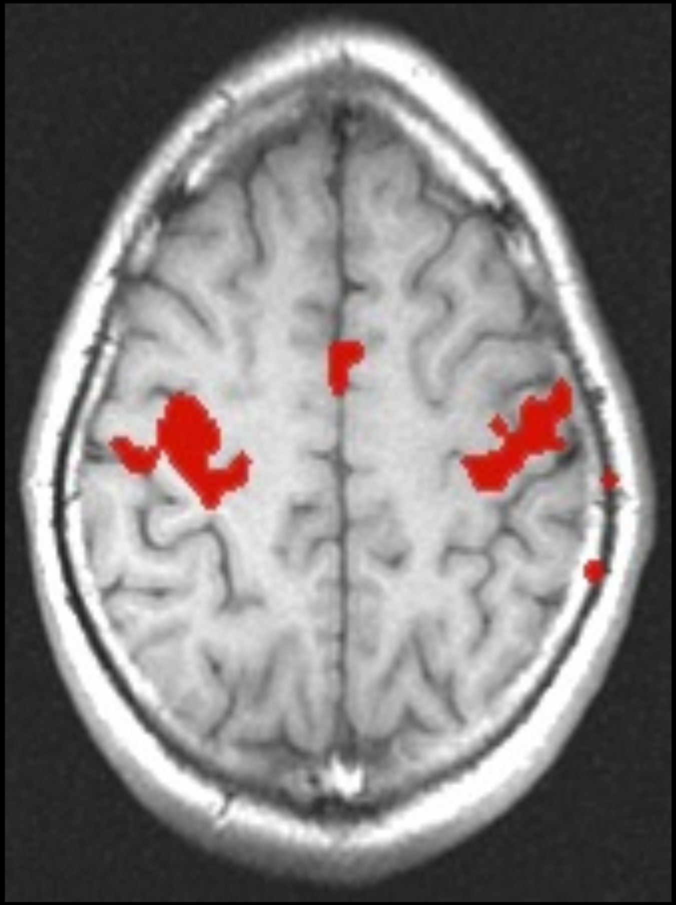

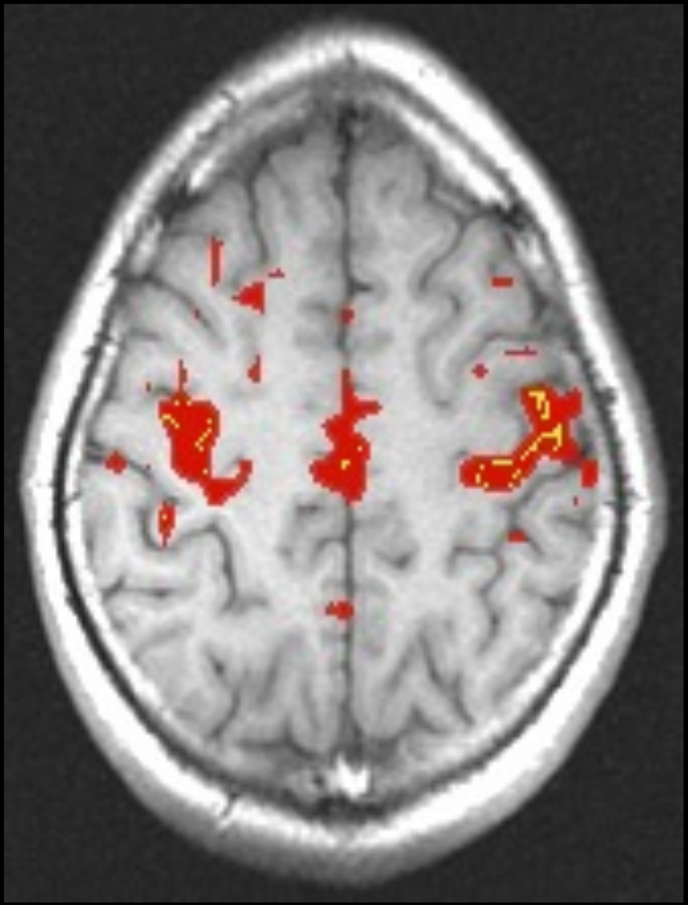

The Skin Conductance Response (SCR)

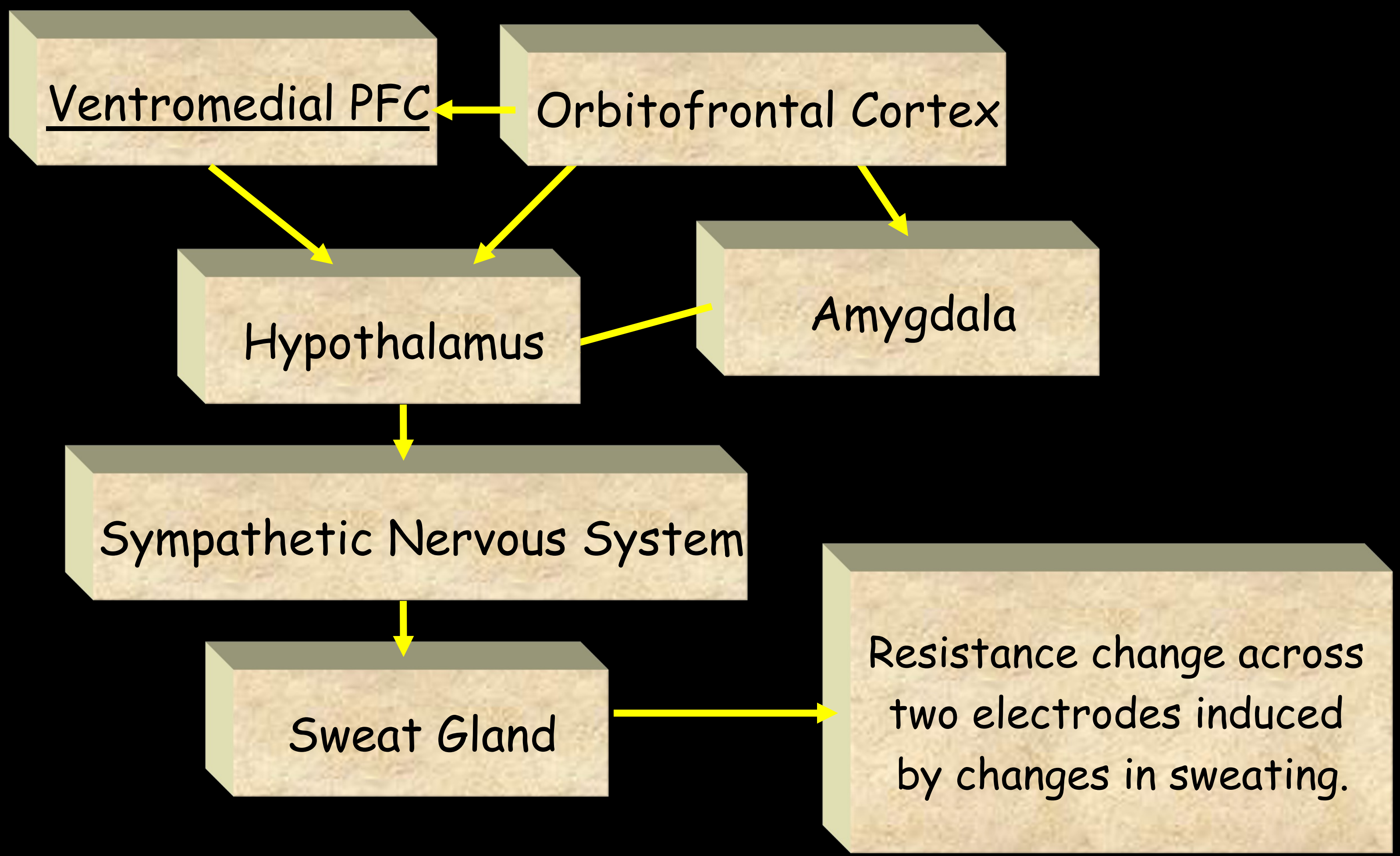

Skin Conductance Dynamics

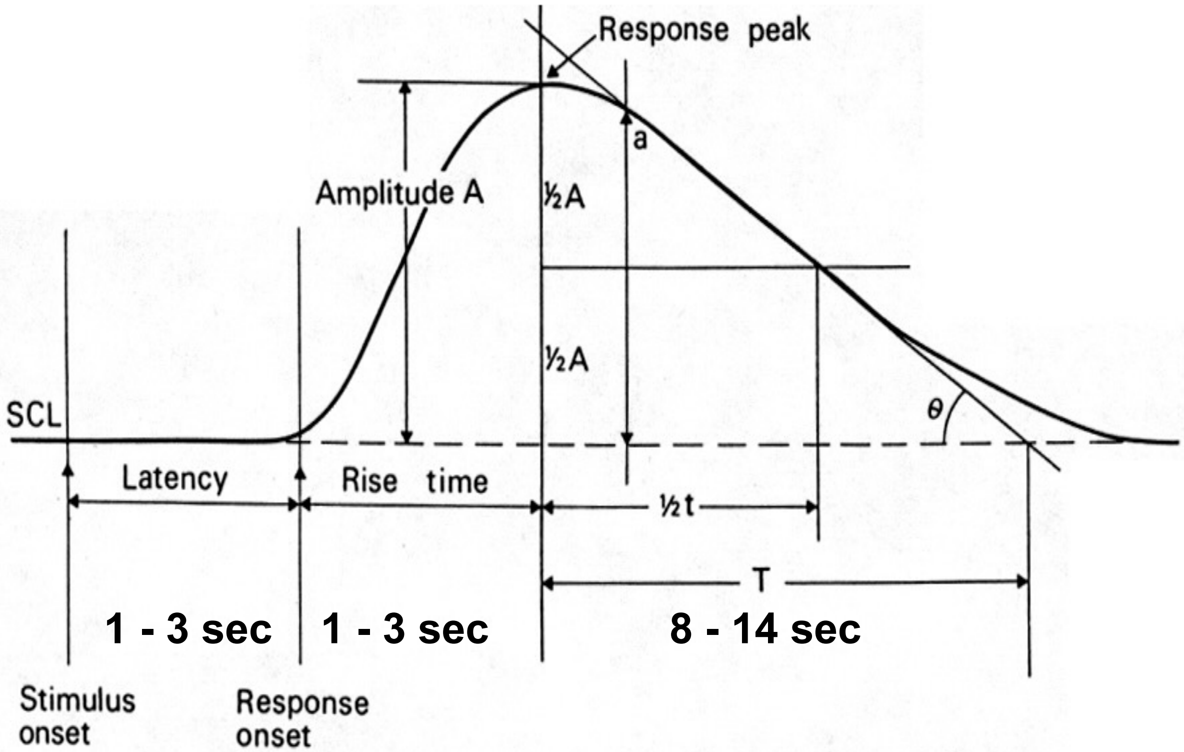

FIGURE 1. Diagrammatic skin conductance response.

- Boucsein, Wolfram (1992). Electrodermal Activity. Plenum Press, NY
- Venables, Peter, (1991). Autonomic Activity ANYAS 620:191-207.

Brain activity correlated with SCR during "Rest"

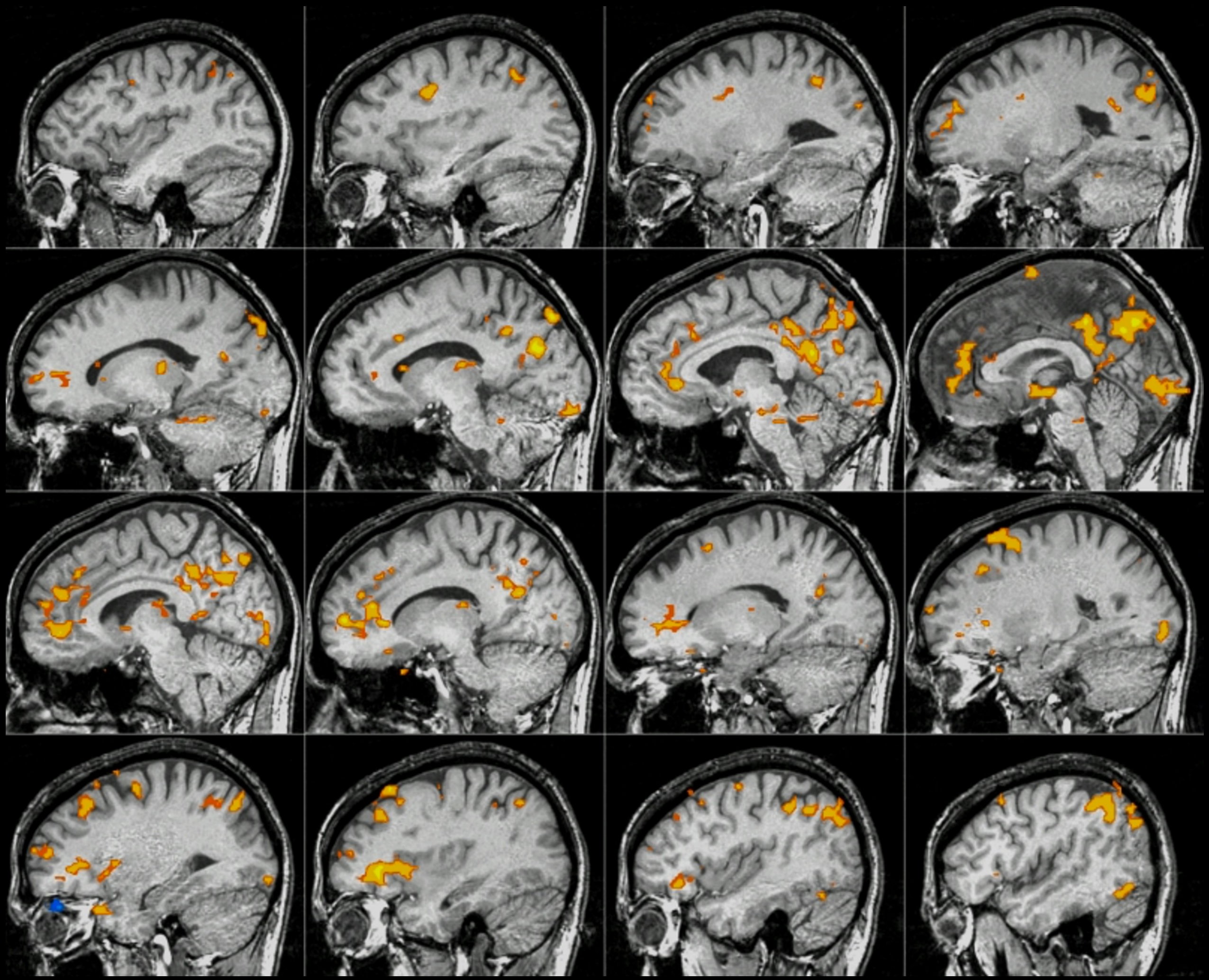

Brain activity correlated with SCR during "Rest"

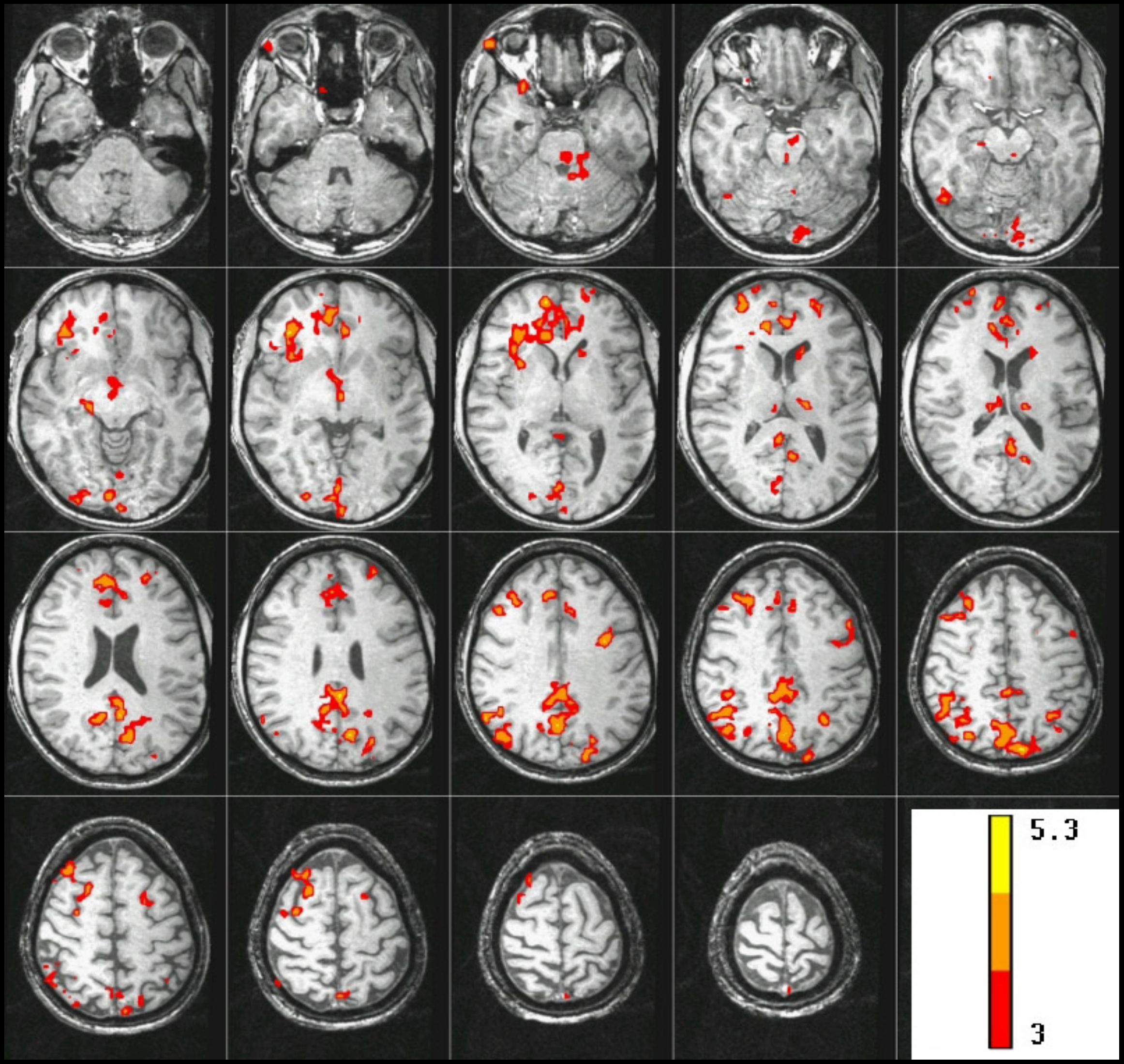

Linearity

Latency

Fluctuations and Sensitivity

“Current” Imaging

Neuronal Current Imaging

•Neuronal activity is directly associated with ionic currents.

•These bio-currents induce **spatially distributed and transient** magnetic flux density (B) changes and magnetic field gradients (dB/dr).

•In the context of MRI, these currents therefore alter the frequency, and therefore phase ,ϕ, of surrounding water protons.

Synchronous activity among large neuronal populations produce **small transient** magnetic field changes which are typically detected on the scalp with Magnetoencephalography (MEG).

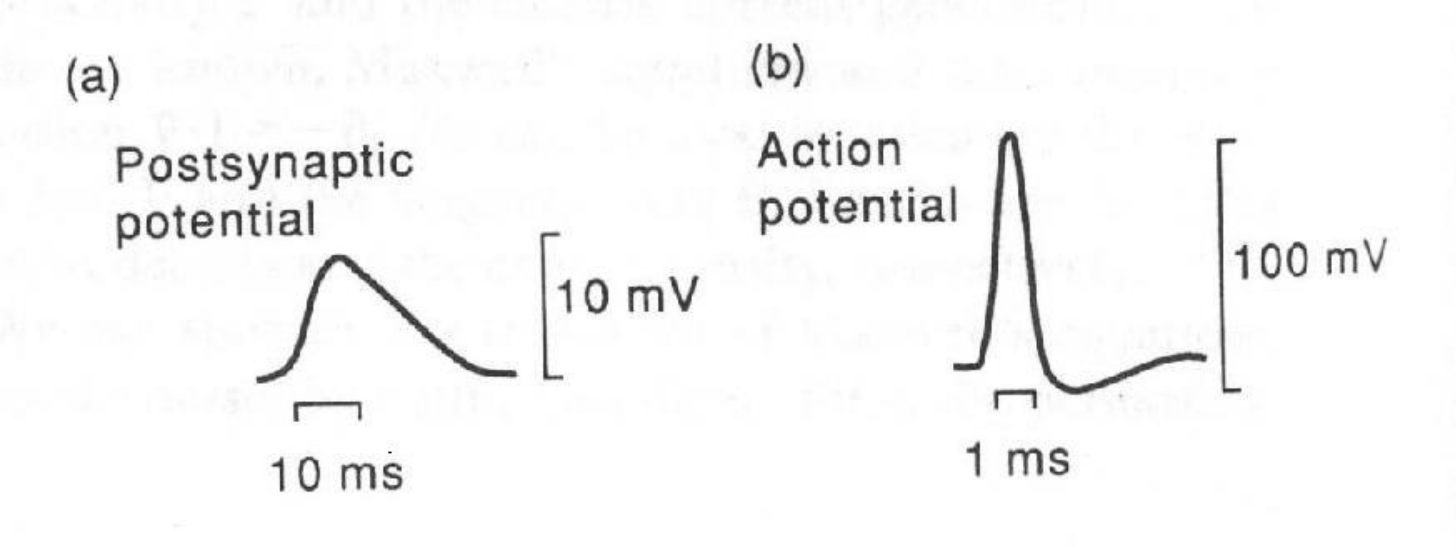

Schematic representation of (a) a postsynaptic potential and (b) an action potential as a function of time.

The post synaptic potential lasts for about 10ms, allowing integration of individual fields to create

MEG detectable > 100 fT field on surface of skull

Derivation of B field generated in an MRI voxel by a current dipole

Single dendritic tree having a diameter d, and length L behaves like a conductor with conductivity σ. Resistance is R=V/I, where $R=4L/(\pi d^2 \sigma)$. From Biot-Savart:

$$B = \frac{\mu_0}{4\pi}\frac{Q}{r^2} = \frac{\mu_0}{16}\frac{d^2 \sigma V}{r^2}$$

by substituting $d = 4\mu m$, $\sigma \approx 0.25\ \Omega^{-1}\ m^{-1}$, V = 10mV, r = 4cm

the resulting B field is: **B≈0.002 fT**

Because **B_{MEG}=100fT** (or more) is measured by MEG on the scalp, a large number of neurons**,** (0.002 fT x 50,000 = 100 fT), must coherently act to generate such field. These bundles of neurons produce, within a typical voxel, 1 mm x 1 mm x 1 mm, a field of order:

$$B_{MRI} = B_{MEG}\left(\frac{r_{MEG}}{r_{MRI}}\right)^2 = B_{MEG}\left(\frac{4\ cm}{0.1\ cm}\right)^2 = 1600\ B_{MEG}$$

B_{MRI} ≈0.2nT

Dipole Field in a 1 mm voxe

Can MRI Detect transient B_0 changes

On the order of 0.2 nT?

Current Phantom Experiment

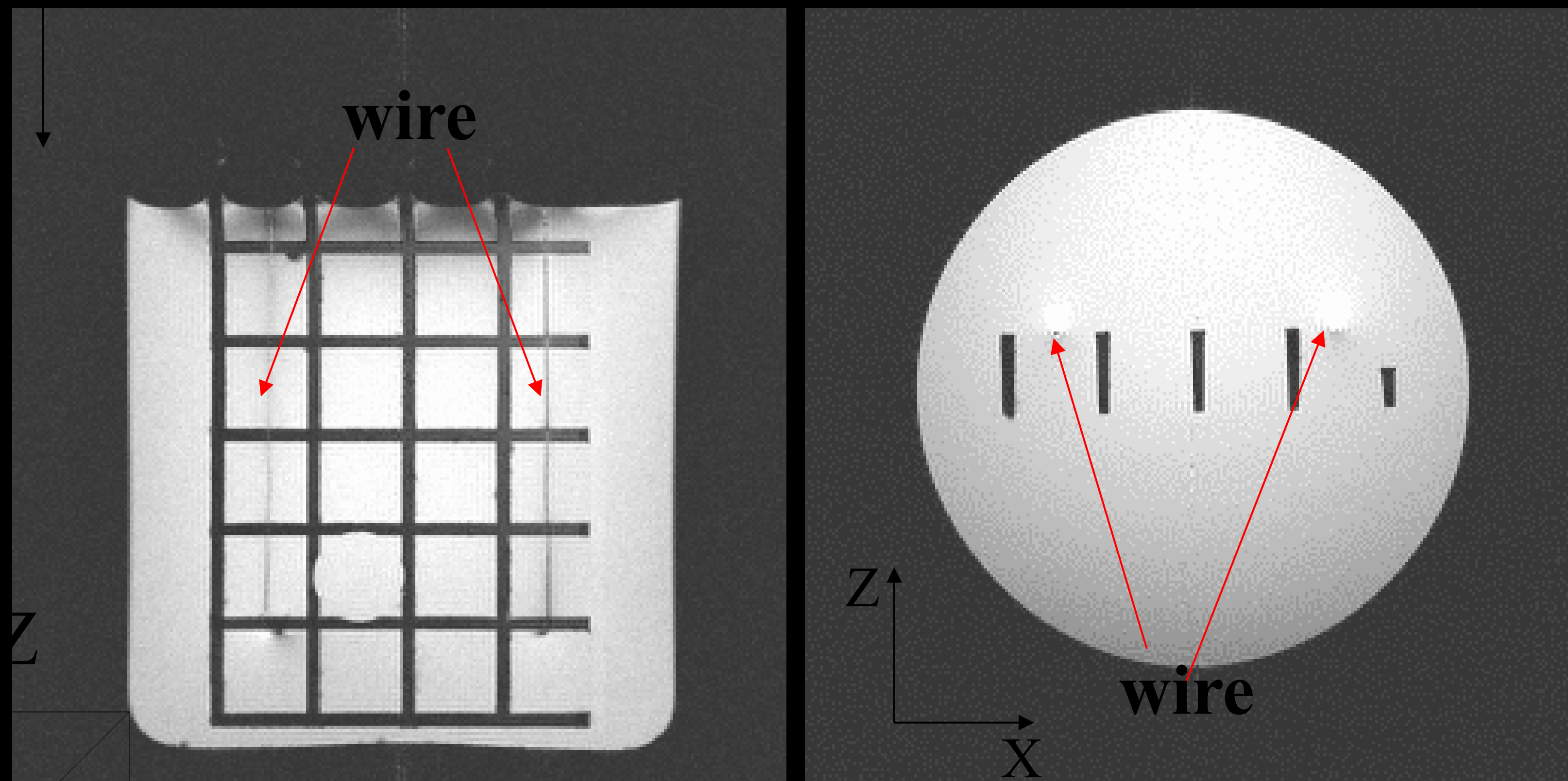

MRI phase:

$\Delta\phi \cong \gamma \Delta B_C TE$

Simulation

calculated $B_c \parallel B_0$

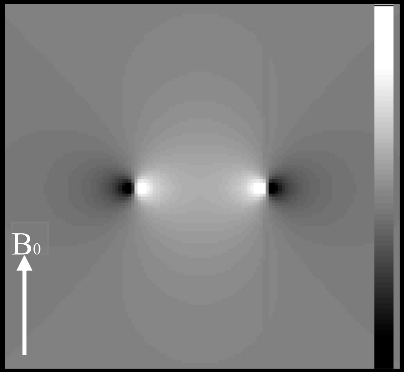

calculated $|\Delta B_c| \parallel B_0$

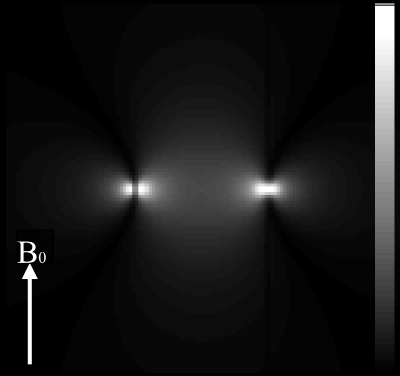

Measurement

Correlation image

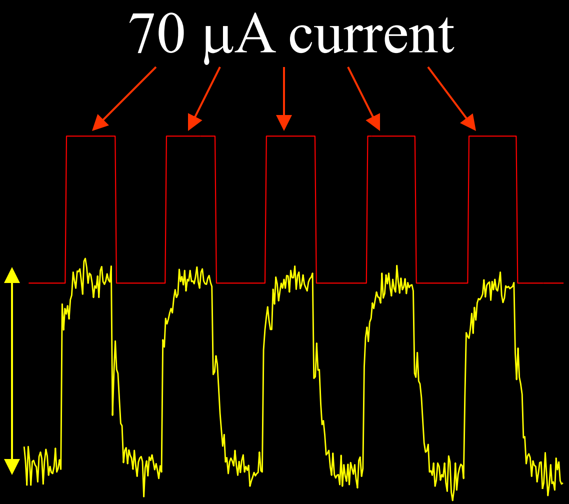

Single shot GE EPI

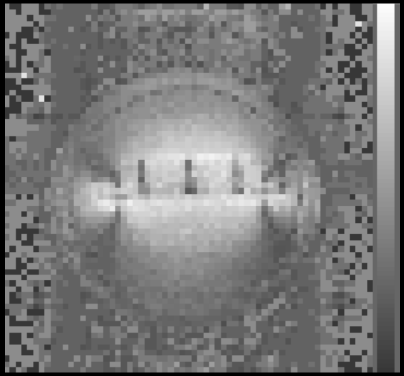

Spectral density image

$\Delta\phi \cong 20^0$

Experiment (human respiration)

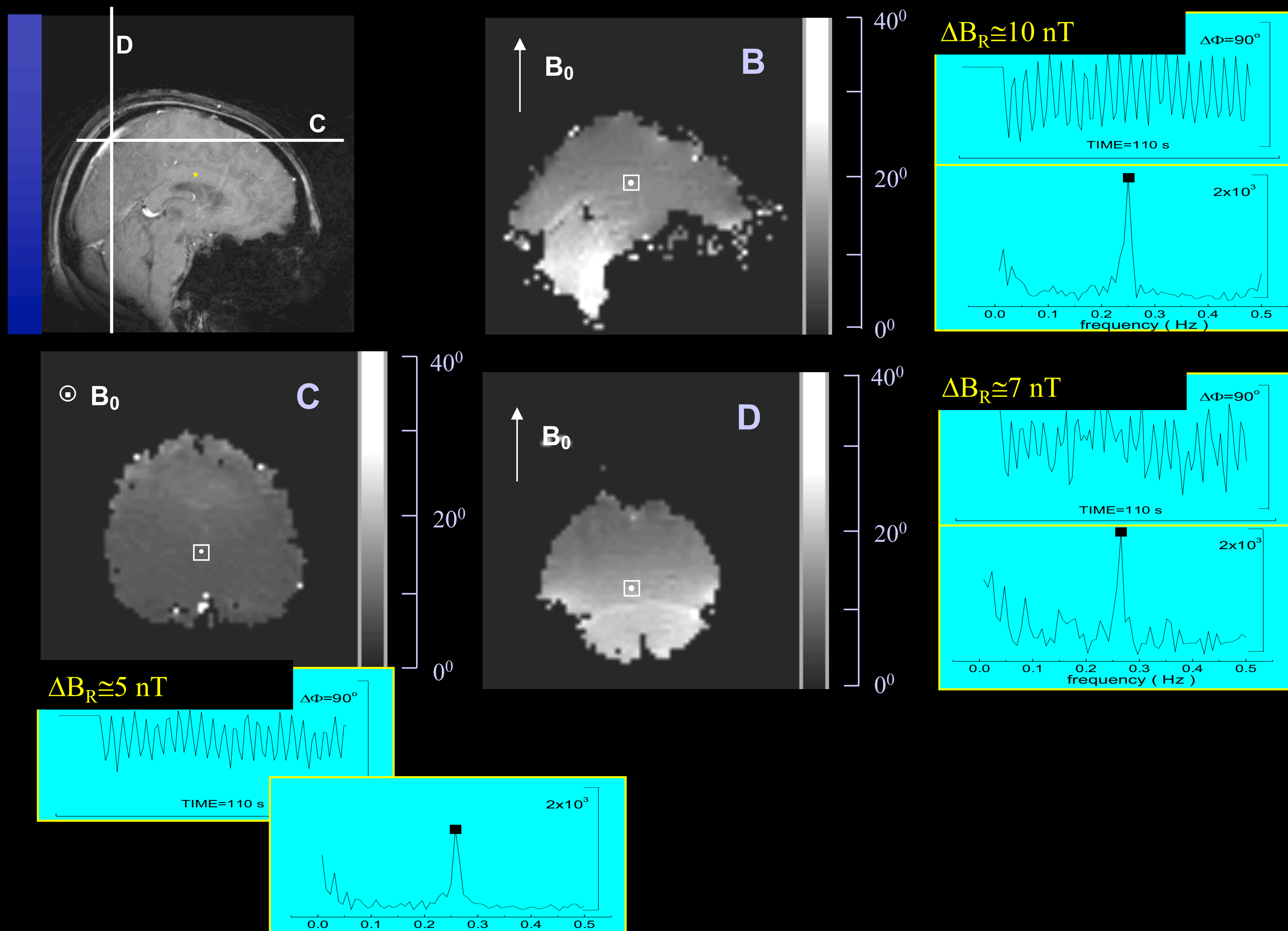

Sources of Phase Noise

- Respiration (chest wall movement)

- cardiac pulsation

- eye movement

-system instabilities (including eddy currents)

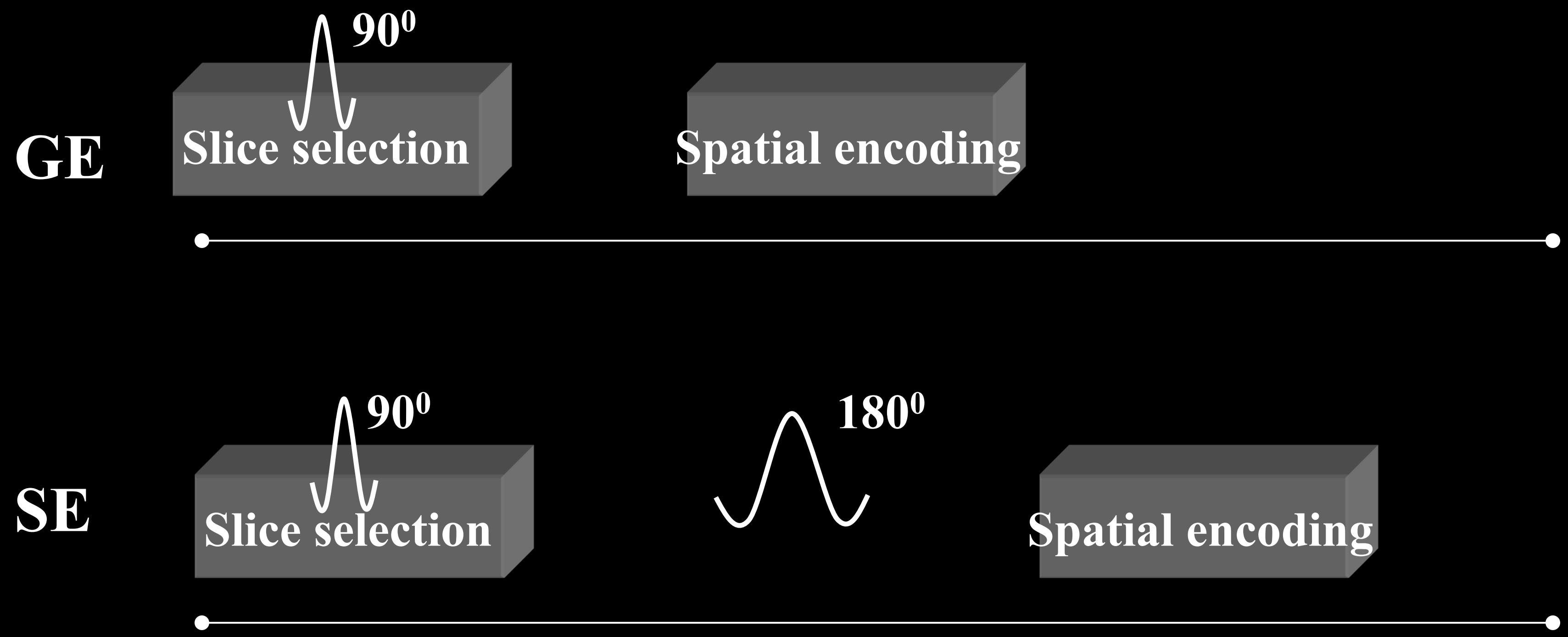
GE
90⁰
Slice selection
Spatial encoding
SE
90⁰
Slice selection
180⁰
Spatial encoding

Experiment (human respiration)

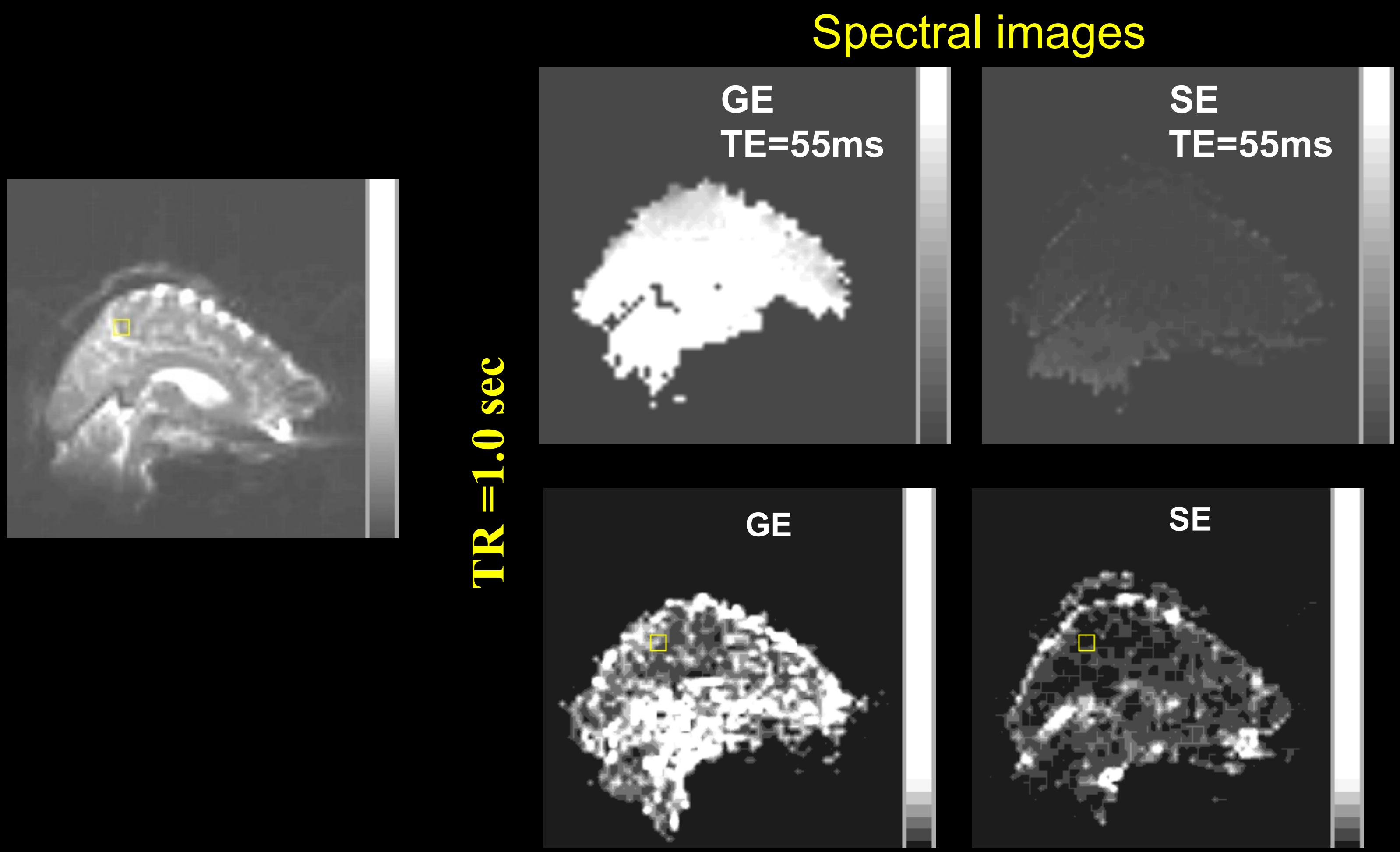

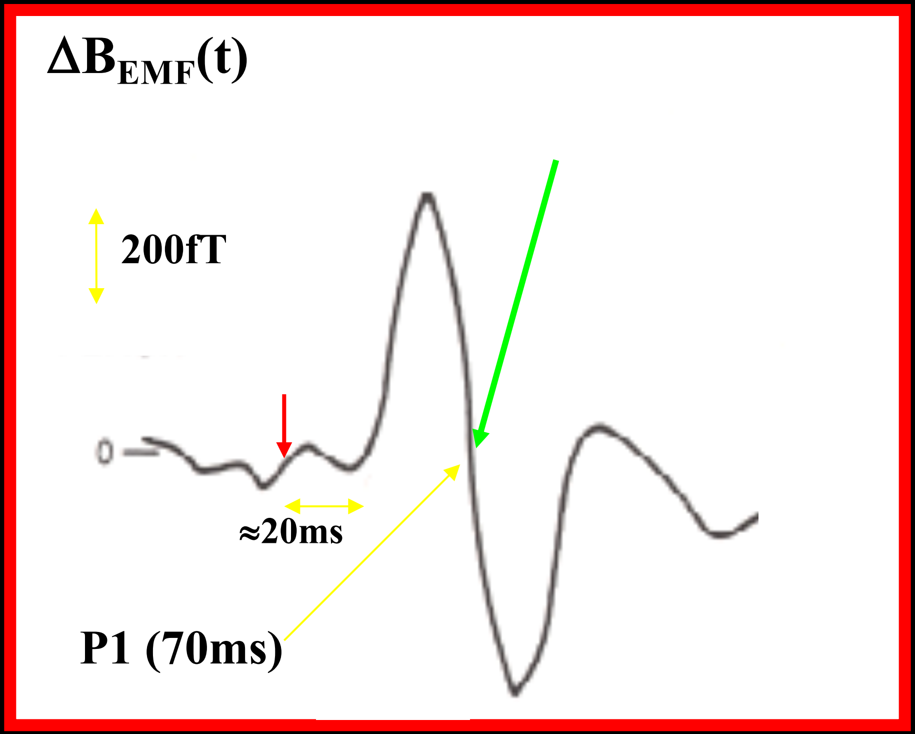

Optimal temporal position for 180 pulse

Spin-echo sequence advantages:

SE sequence improve sensitivity to small and transient $\Delta B(t)$ changes and simultaneously reduces unwanted low-frequency field shift.

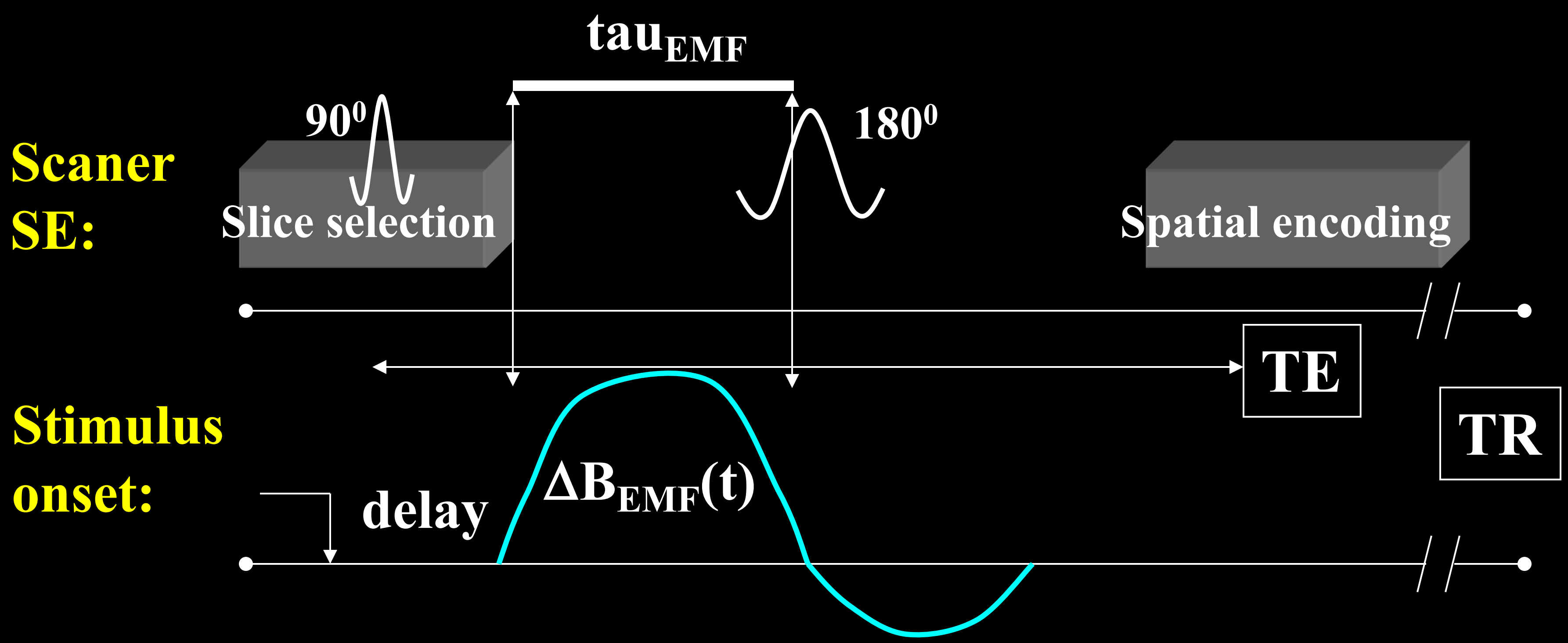

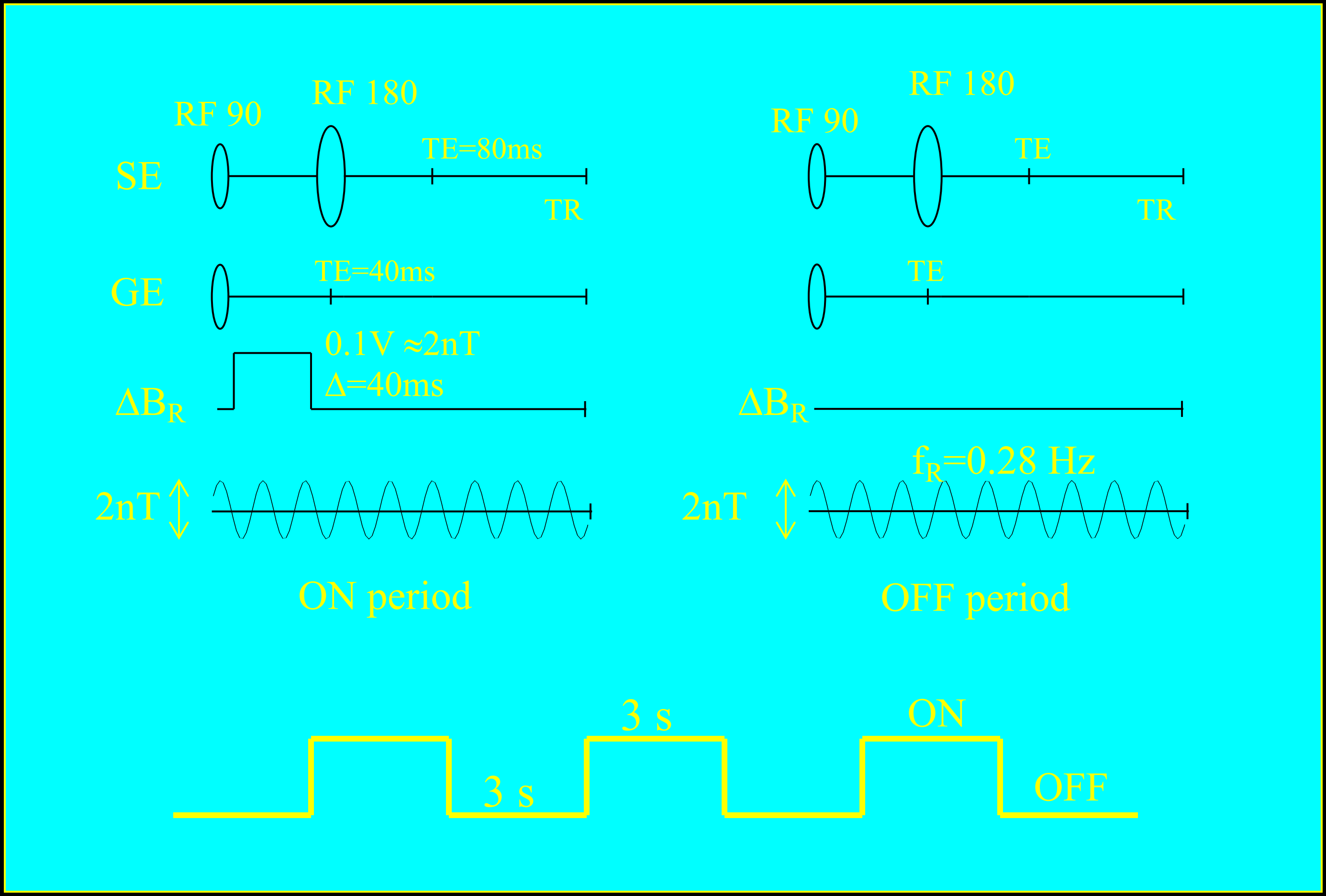

RF 90
RF 180
SE
TE=80ms
TR
GE
TE=40ms
0.1V ≈2nT
Δ=40ms
ΔB$_R$
2nT
ON period
RF 90
RF 180
TE
TR
TE
ΔB$_R$
f$_R$=0.28 Hz
2nT
OFF period
3 s
3 s
ON
OFF

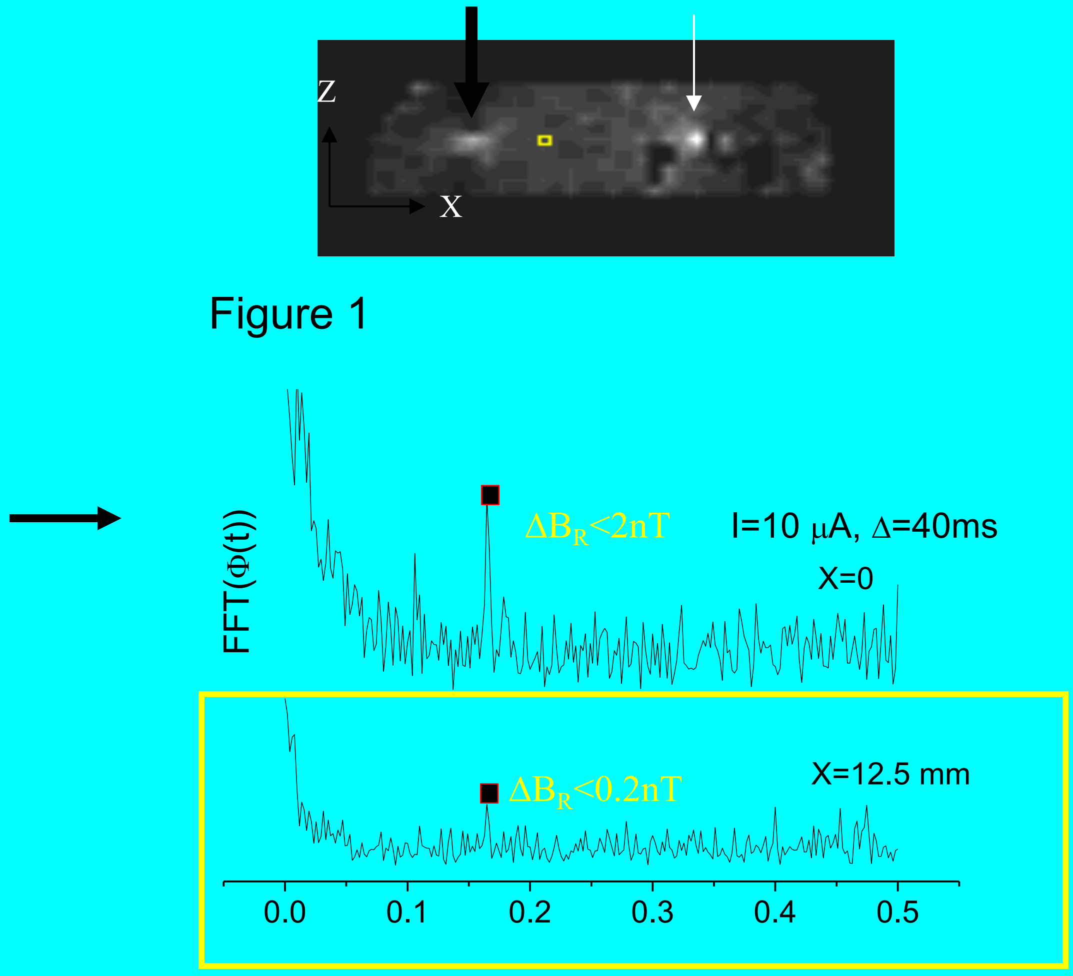
Z
X
FFT(Φ(t))
ΔB_R<2nT
I=10 μA, Δ=40ms
X=0
ΔB_R<0.2nT
X=12.5 mm
0.0
0.1
0.2
0.3
0.4
0.5

Figure 1

Conclusions:

While many unknowns about neuronal-induced current magnitudes and spatial scales remain, the combination of a SE EPI sequence with precisely synchronized stimulation protocol optimizes the ability to detect small and transient magnetic field changes.

Transient or periodic flux density changes as small as 200 pT (0.2 nT) can be detected using MRI.

Linearity

Latency

Fluctuations and Sensitivity

“Current” Imaging